

VITAMIN B₁₂ DERIVATIVES WITH PEPTIDE BACKBONES

Dissertation

zur

Erlangung der naturwissenschaftlichen Doktorwürde

(Dr. sc. nat.)

vorgelegt der

Mathematisch-naturwissenschaftlichen Fakultät

der

Universität Zürich

von

Kai Zhou

Promotionskomitee

Prof. Dr. Roger Alberto (Vorsitz)

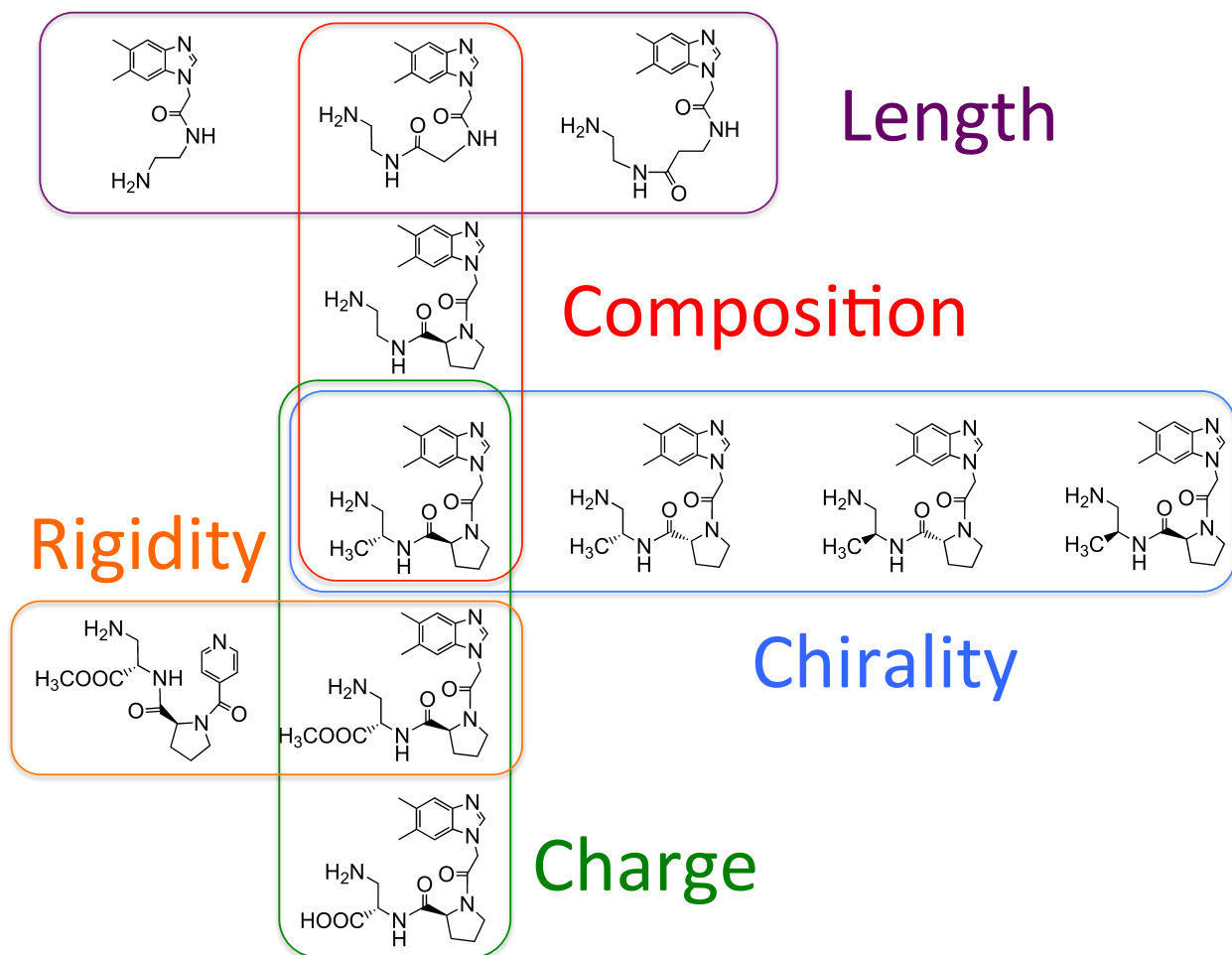
Dr. Felix Zelder (Leitung)

Prof. Dr. Roland Sigel

Zürich 2012

Vitamin B12 is an essential biomolecule for humans and it is only produced by certain microorganisms. Its elegant, yet complex structure combined with its fascinating properties attracted research of some of the most extraordinary scientists in the past, which opened new horizons in medicine, crystallography and organic synthesis.

Studies on the mechanism of B12 dependent enzymes suggest that the coordination and electrochemical properties at the cobalt centre of cobalamins are essential for its biological activity. The crucial role of cobalamins for cell replication is also attractive for developing inhibitors of B12 dependent enzymes as novel anti-proliferating drugs.



In this project, we developed modified B12 derivatives for fundamental and biological studies. We started with the conformational analysis of the sugar-phosphodiester backbone of B12, which was initially introduced by Eschenmoser and Kreppelt. Based on the understanding of the conformation of the loop structure at the f-side chain of B12 and considering the successful modeling of sugar-phosphodiester with peptide bonds in

other natural products than B12, we developed a new class of modified B12 derivatives with peptide loops of different length, composition, chirality, charge and rigidity.

The modifications of the loop structure influenced the stability of the intramolecular coordination (base on stability), which resulted in a change of the electrochemical properties at the cobalt ion. Cyclic voltammetry experiments of the peptide B12 derivatives showed that the Co(III)/Co(II) reduction potential and the strength of intramolecular coordination are linearly correlated. These results suggest that the coordination and electrochemical properties of peptide B12 can be simultaneously controlled.

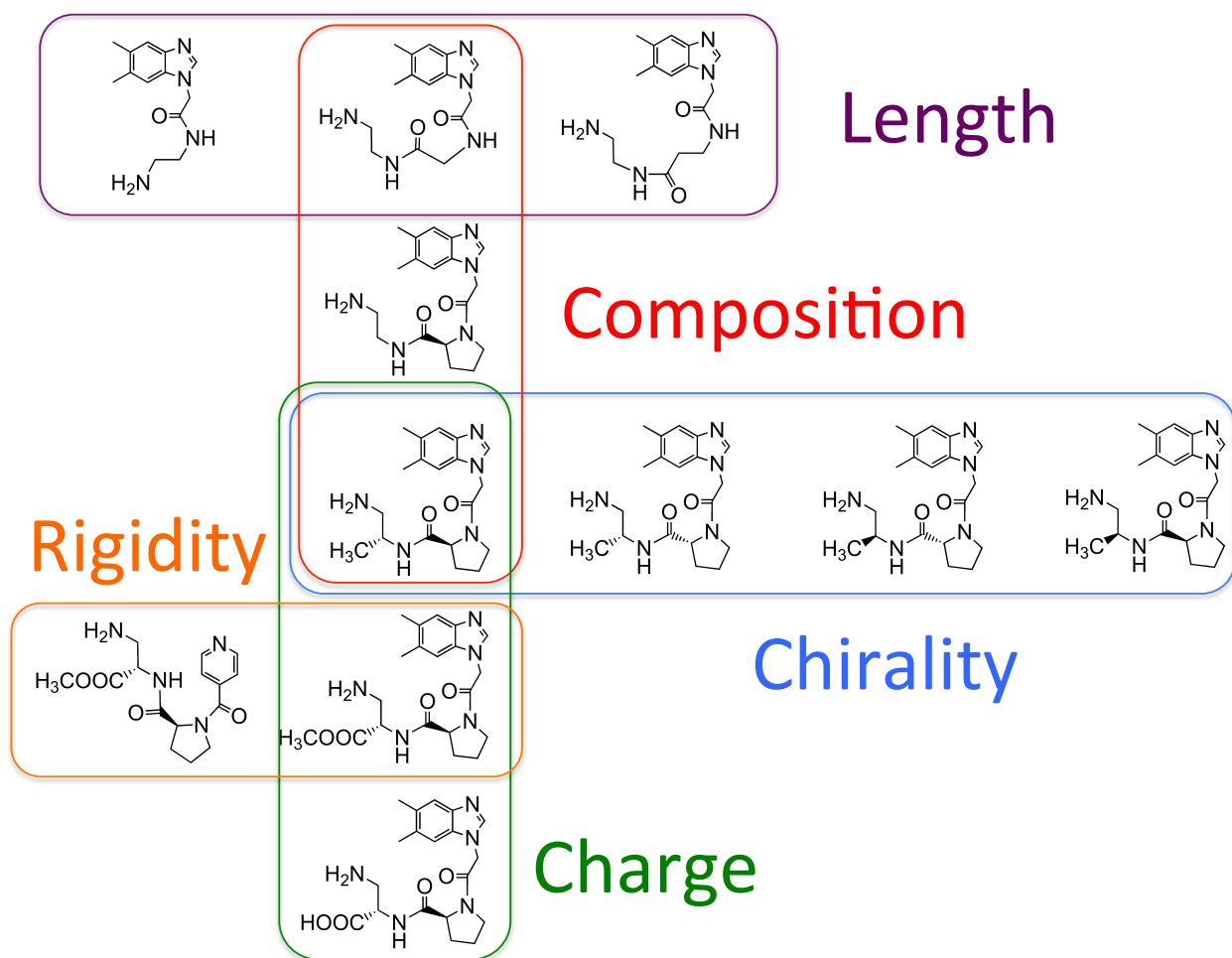
We cooperated with Fredrick Lyatuu and Prof. Wolfgang Buckel from the University of Marburg and PD Helmut Brandl from the University of Zurich in biological studies. Biological activity of peptide B12 derivatives has been tested with the microorganism *Lactobacillus delbrueckii* and the enzyme glutamate mutase showing (reduced) bioactivity in both, “base on” as well as “base off/ histidine on” enzymes. This behavior is promising for the design of peptide B12s with therapeutic effects.

Peptide B12 derivatives were also shown to exhibit interesting coordination chemistry. Derivatives with a tuned “base on” stability, can be used as a probe to identify the coordination structures of other “incomplete” corrinoids with ^1H NMR spectroscopy. This method is useful for applications in kinetic ligand exchange studies of corrinoids.

Another highlight of this Ph.D. thesis is the discovery of a B12 derivative having an unprecedented intermolecular coordination fashion. By controlling the coordination sites at the cobalt center and by implementation of a more flexible deamino histidine backbone, we developed the first example of a self-assembled dimeric cobalamin in solution. Of note, cobalamins have been considered until now to be “notoriously monomeric”. Multi-intermolecular interactions offer the opportunity to develop even more complex structures that could be of interest for mimicking B12 related enzymes.

Vitamin B12 ist essentiell für Menschen, kann aber nur von bestimmten Mikroorganismen produziert werden. Aufgrund seiner eleganten und komplexen Struktur sowie seiner einzigartigen Eigenschaften hat es einige der aussergewöhnlichsten Wissenschaftler fasziniert und ihre Arbeiten haben neue Horizonte in der Medizin, Kristallographie und Chemie eröffnet. Mechanismen B12-abhängiger Enzyme lassen auf eine Abhängigkeit der biologischen Aktivität von den koordinativen-, und elektrochemischen Eigenschaften der Corrinnoide schliessen.

Cobalamine spielen auch eine entscheidende Rolle bei der Zellteilung und sind somit attraktiv für die Entwicklung neuer Krebstherapeutika.



In diesem Projekt haben wir B12 Derivate für fundamentale und biologische Fragestellungen entwickelt. Wir sind dabei von Eschenmosers und Kreppelts Konformationsanalyse des Zuckerphosphatrückgrates von B12 ausgegangen. Basierend auf unserem Verständnis der Konformation der f-Seitenkette von B12 und

unter Berücksichtigung der Modellierung von Zucker-Phosphodiesterbindungen in anderen Naturstoffen, haben wir eine neue Klasse von modifizierten B12-Derivaten mit einem Peptidrückgrat hergestellt, die sich in der Länge, Konfiguration, Ladung und Rigidität unterscheiden.

Die unterschiedlichen Modifikationen haben die intramolekulare Koordination und die Redox Eigenschaften am Kobaltzentrum beeinflusst. Durch elektrochemische Studien wurde eine lineare Abhängigkeit der Co(III)/ Co(II) Reduktionspotentiale von der Stärke der intramolekularen Koordination festgestellt. Diese Resultate zeigen, dass die Koordinations- und Elektrochemie der Peptid-B12 Derivate simultan kontrolliert werden kann.

Die biologische Aktivität der Peptid-B12 Derivate wurde mit dem Mikroorganismus *Lactobacillus delbrueckii* und dem Enzym Glutamat Mutase in Kooperation mit Fredrick Lyatuu und Prof. W. Buckel (Universität Marburg) und PD H. Brandl (Universität Zürich) untersucht. Es wurde eine (verminderte) biologische Aktivität für sowohl base on als auch base off/ histidine on abhängige Enzyme festgestellt. Dieses Verhalten ist vielversprechend für die Entwicklung von Peptid-B12 Derivaten mit therapeutischen Eigenschaften.

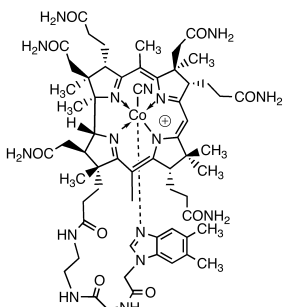
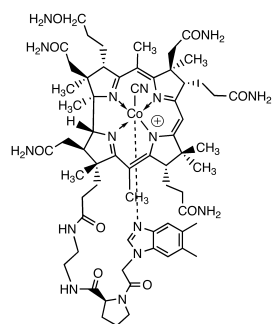
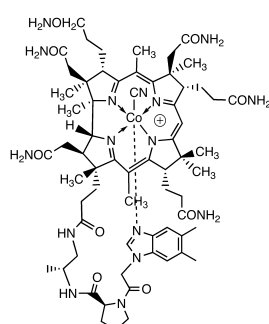
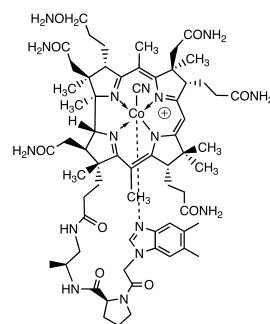
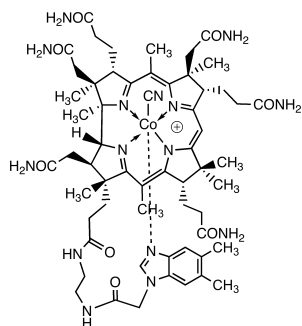
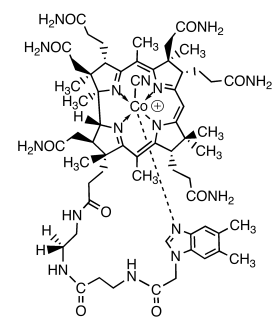
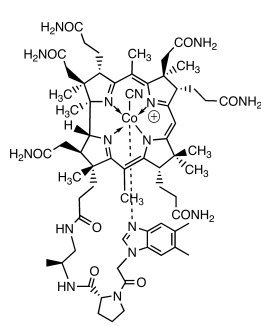
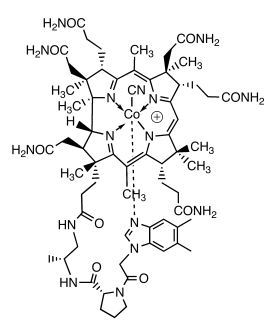
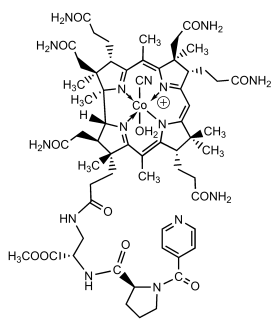
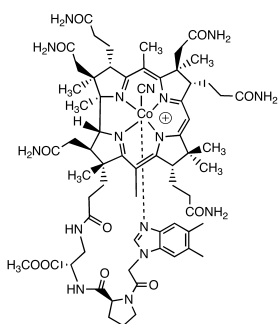
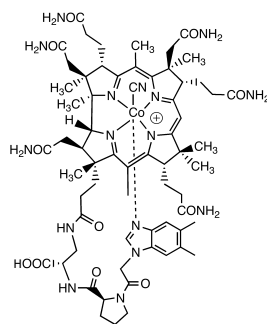
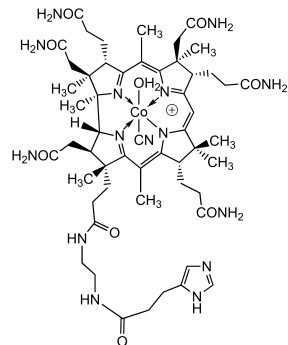
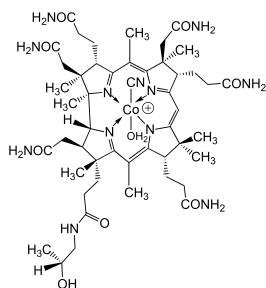
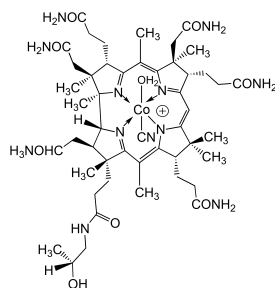
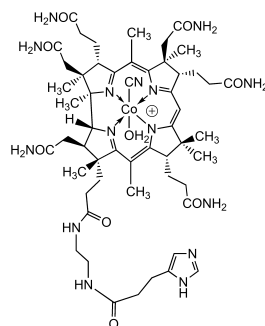
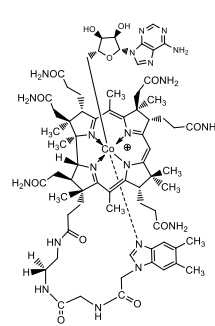
Peptid-B12 Derivate mit einem flexiblen Rückgrat sind jedoch noch viel vielseitiger und zeigen eine sehr interessante Koordinationschemie. Derivate mit einer veränderten base-on Stabilität wurden erfolgreich für die Identifizierung der Koordinationsgeometrie am Metallzentrum verwandter Corrinoiden mittels ^1H NMR Spektroskopie eingesetzt. Diese Methode ist ein wichtiges Werkzeug für die Untersuchung kinetischer Ligandaustauschreaktionen am Metallzentrum von Corrinoiden.

Einen weiteren Höhepunkt der Doktorarbeit stellt die Synthese des ersten intermolekular verbrückten Cbl-Dimers in Lösung dar. Dies wurde durch Kontrolle der Koordinationsgeometrie am Metallzentrum bei gleichzeitiger Einführung eines flexiblen Deaminohistidin-Rückgrates ermöglicht. Bis heute wurden Cobalamine als „notorisch monomere“ Verbindungen angesehen. Multiple intermolekulare Interaktionen eröffnen nun auch die Möglichkeit noch komplexere Strukturen zu entwickeln, die B12 abhängige Enzyme nachahmen könnten.

LIST OF ABBREVIATIONS

AdoCbl	Adenosylcobalamin
B12	Vitamin B12
Boc	tert-Butyl carbamate
CV	Cyclic Voltammetry
Cbl	Cobalamin
Cbi	Cobinamide
Cbz	Carboxybenzyl
DCC	N,N'-Dicyclohexylcarbodiimide
DCM	Dichloromethane
DIPEA	N-Ethyldiisopropylamine
DMAP	4-Dimethylaminopyridine
DMF	N,N'-Dimethyl formamide
Dmbz	Dimethylbenzimidazole
DMSO	Dimethyl sulfoxide
EDC	1-Ethyl-3-(3-dimethylaminopropyl) carbodiimide
ESI	Electron Spray Ionisation
Et	Ethyl
EA	Ethyl acetate
EtOH	Ethanol
Fmoc	9-Fluorenylmethyloxycarbonyl
HOBt	Hydroxybenzotriazole
HPLC	High Performance Liquid Chromatography
ROESY	Rotating Frame Overhauser Effect Spectroscopy
R _f	Retention factor
<i>s</i>	singlet
SPE	Solid Phase Extraction
<i>d</i>	doublet
<i>t</i>	triplet
T	Temperature

TLC	Thin Layer Chromatography
TCA	Tricarboxylic acid cycle
THF	Tetrahydrofolate

**2****3****4****5****12****13****14****15****16****17****18****26****19_β****19_β****29****30**

Summary.....	iii
Zusammenfassung.....	v
Abbreviations.....	vii
List of Key Compounds.....	ix
Table of Contents	xi
1 INTRODUCTION	1
1.1 Story of B12 – Past, present and future	1
1.2 Traveling of B12 – Origin, transportation and destination.....	6
1.3 Function of B12 – Coenzyme, thymine and cell division.....	7
1.4 Properties of B12 – Structure, derivatives and constitutions.....	9
1.5 Topics of B12 – Recent progress.....	12
1.6 Projects of B12 – Peptide backbone.....	16
1.6.1 Concept of peptide B12 – Simulation, correlation and suppression.....	16
1.6.2 Coordination Chemistry of B12 derivatives.....	19
2 RESULTS AND DISCUSSION	22
2.1 Peptide B12 - Derivatization of the backbone of B12.....	22
2.1.1 Conformational analysis – Guideline for the design of the loop.....	22
2.1.2 Peptide B12 derivatives – Coordination- and redox chemistry.....	27
2.1.3 Other B12 derivatives.....	31
2.2 Diastereomeric aquacyano cobinamide.....	36
2.2.1 Synthesis and characterization of Cbi.....	37
2.2.2 Some unexpected byproducts.....	41
2.3 Self-assembly of a B12 derivative with a flexible loop.....	43
2.3.1 Synthesis and design of loop-modified B12.....	43
2.3.2 Thermodynamic investigations.....	45
2.4 Biological studies of peptide B12 and B12 coenzyme derivatives.....	54
2.4.1 <i>Lactobacillus delbrueckii</i>	55
2.4.2 Glutamate mutase.....	58
3 CONCLUSION AND OUTLOOK	61
3.1 Peptide B12.....	61

3.2 Diastereomers of aquacyanocobinamides and intercoordinated Cbls.....	62
4 EXPERIMENTAL PROCEDURES.....	63
4.1 Experimental procedures.....	65
4.3 NMR tables.....	91
5 LITERATURE	101
Acknowledgments.....	I
Curriculum Vitae	III
Conference Contributions	IV
Publication List	V
Appendix I	VI
Appendix II	IX
Appendix III	XIV
Appendix IV	XIX

1. Introduction

1.1 Story of B12 – Past, present and future

The legendary story of vitamin B12 (B12), this most beautiful and unique biomolecule^[1] ^[2,3] started about a century ago in the 1920s, when George Whipple (1878-1976) discovered that liver was the most effective diet to treat anemic dogs due to blood loss^[4]. At that time he was not aware of this beautiful and complicated vitamin, but the result was exciting and inspiring. George Richards Minot (1885-1950) and William Perry Murphy (1892-1987) immediately sensed the application of this discovery to defeat a fatal human disease - pernicious anemia. They indeed succeeded to control the deadly anemia in 1926 with a daily diet of about half a kilogram of liver for the patients.^[4] Their remarkable discoveries were honored with the Nobel Prize in medicine and physiology in 1934.



Figure 1: (left) George Hoyt Whipple (middle) George Richards Minot (right) William Parry Murphy.^[4]

In the 1930s and 1940s, scientists were trying desperately to isolate this “magic drug” from liver, but without success. Mary Shaw Shorb, Karl Folkers and Alexander Todd creatively used the indication of bacterial assays to guide the isolation and finally crystalized B12 in 1948.^[5] This fundamental success paved the way for future structural studies.

After successful isolation of B12, researchers continued with the next challenging project that was the structural elucidation of this molecule. The complexity of the structure of B12 was beyond the limit of technologies in the 1940s, without “decent”

NMR and X-ray crystallography. Nevertheless scientists still devoted great efforts to obtain structural insights with various methods like pyrolysis and hydrolysis. Finally, chemists combined all the results and got a general idea about the composition of this molecule: a macrocycle ring, pyrole units, a six-coordinated trivalent cobalt ion with a cyanide ligand, a dimethylbenzimidazole base, an α -ribazole phosphate and a 2-amino-1-propanol unit. [6-11] (Figure 2)

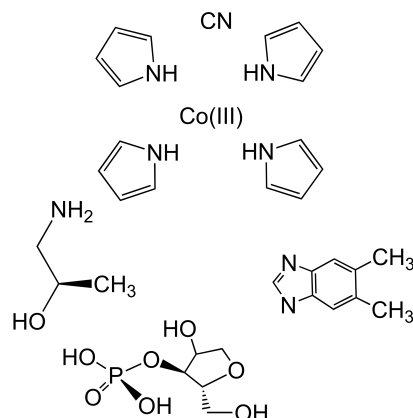


Figure 2: Proposed composition of B12 from pyrolysis and hydrolysis experiments.

The composition of B12 was revealed fragment by fragment, meanwhile X-ray crystallography was maturing fast.[12] This technology opened a new era of structure determination. In 1956, Dorothy Crowfoot Hodgkin (1910-1994), one of the pioneers in the field, determined the structure of the most complicated biomolecule at that time, and had drawn a successful closure to a three decades' exploration.[13-15] A Nobel Prize was granted to Dorothy Hodgkin for this marvelous work.

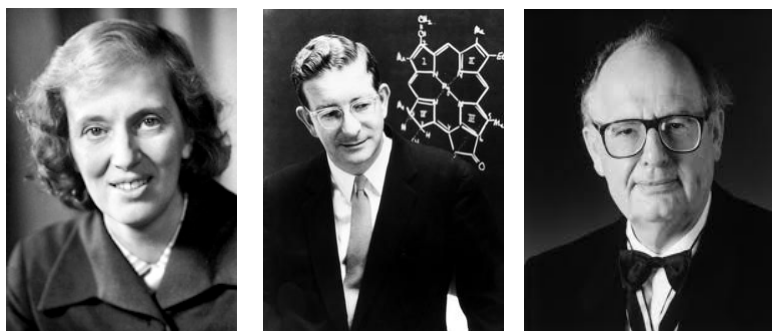
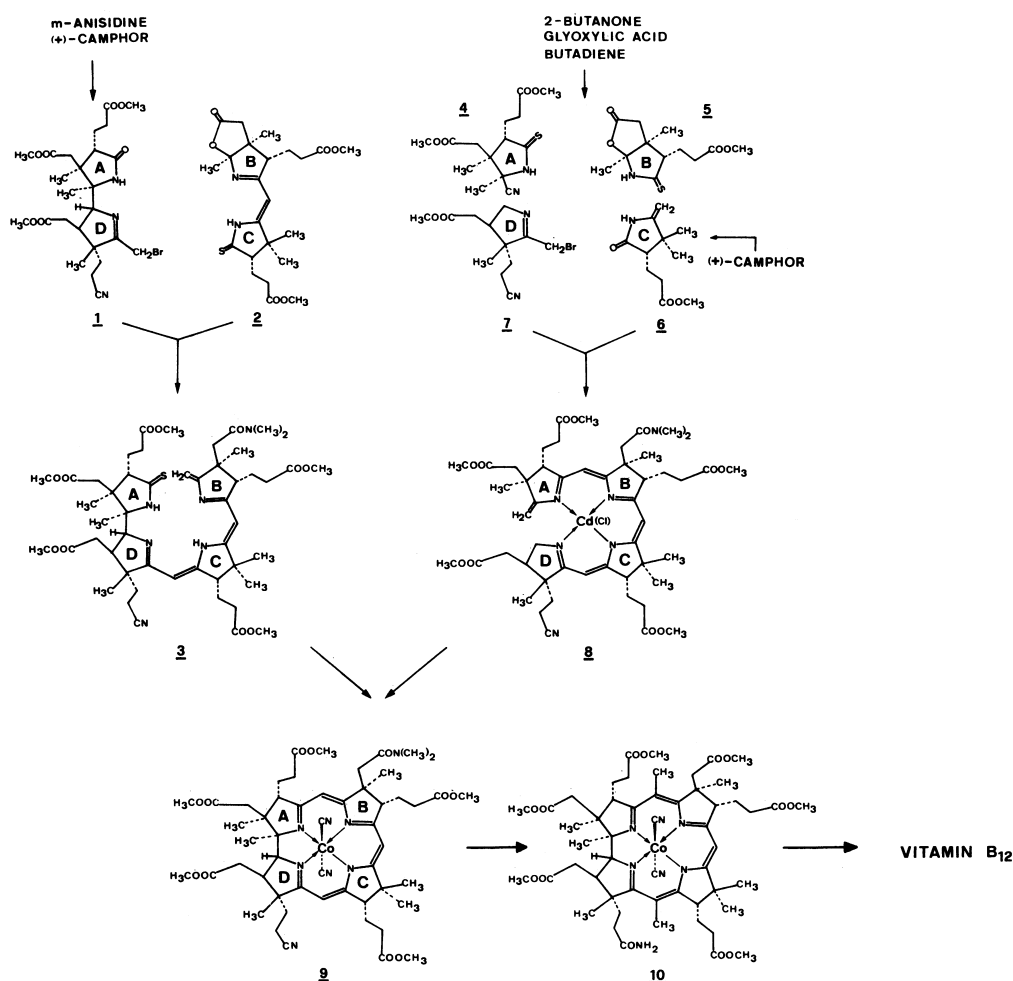


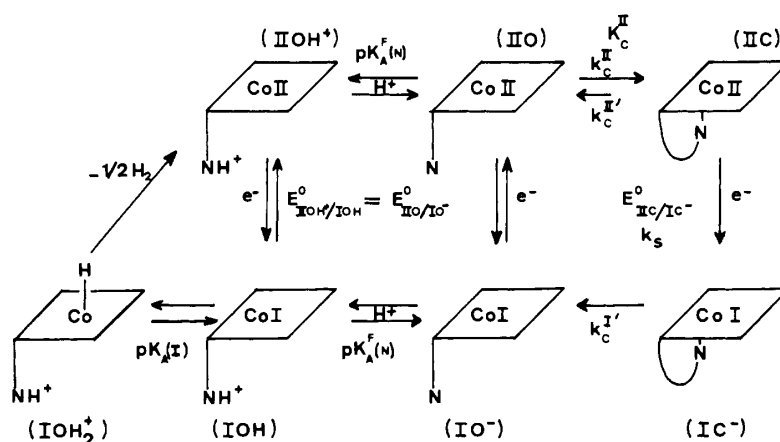
Figure 3: (left) Dorothy Crowfoot Hodgkin (middle) Robert Burns Woodward (right) Albert Eschenmoser.

After this scientific breakthrough, another ambitious project was emerging, which was the total synthesis of this molecule (Scheme 1),^[16-18] by a combined effort of the groups of Robert B. Woodward (1917-1979) of Harvard University and Albert Eschenmoser of the ETH Zürich. This unprecedentedly complicated project took over 90 steps and was finally accomplished in 1971 after 11 years with the anticipation of more than 100 coworkers. The meaning of this monumental achievement was far beyond B12 chemistry, and “rarely before has a synthetic project yielded so much knowledge, including “novel bond-forming reactions and strategies, ingenious solutions to formidable synthetic problems, biogenetic considerations and hypotheses, and the seeds of the principles of orbital symmetry conservation known as the Woodward and Hoffmann rules”.^[19]



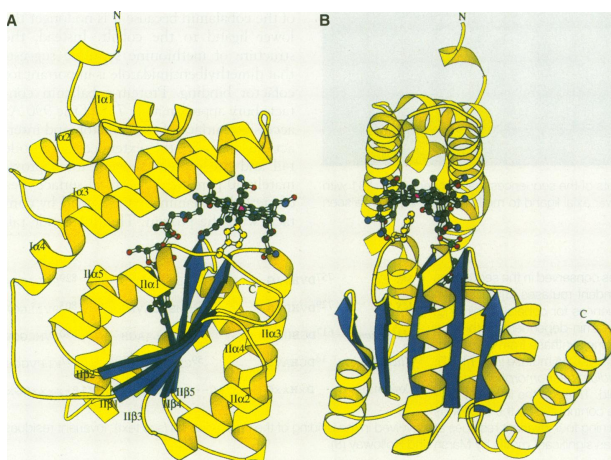
Scheme 1: Synthetic strategy of B12 (more details see reference^[16]).

Besides the structural studies, the properties and functions of cobalamins (Cbl) were intriguing as well. The inorganic chemistry at the cobalt center is the basis for the understanding of Cbls in biological systems. Especially the electrochemistry of cobalt is critical to understand the B12 dependent enzymatic reactions, e.g. methyl transfer^[20] and carbon rearrangement reactions^[21]. Doris Lexa and colleagues investigated the redox chemistry of different B12 derivatives such as cyanocobalamin^[22] and aquacobalamin^[23]. Diagrams of redox potential versus the environmental parameters (pH, cyanide concentration, solvent etc.) are extremely useful to understand the processes of cobalt reduction (Scheme 2).^[24,25]



Scheme 2: Redox equilibria of B12 derivatives (more details see reference^[23])

Important insights into a catalytic mechanism of a B12 dependent enzyme was achieved by Martha Ludwig's group in 1994. Her group solved the structure of a B12-binding domain of methionine synthase (Figure 4), showing that the cofactor is bound in a "base off/his on" constitution. Based on this result they elegantly explained the methyl transfer process with a proton assisted base on/base off switch.^[26] As the protein crystallization techniques and X-ray crystallography advanced rapidly, more and more B12 dependent enzyme structures were disclosed such as methylmalonyl-coenzyme A mutase^[27] in 1996, Glutamate mutase^[21] in 1999, diol-dehydratase^[28] in 2000, class II ribonucleotide reductase^[29] in 2002, transcobalamin II^[30] in 2006 and intrinsic factor^[31] in 2007. With these structural data in hand, a deep understanding of the B12 function to an unprecedented molecular level has been achieved, but detailed mechanisms are still



1.2 Traveling of B12 - Origin, transportation and destination

Neither plants nor animals are capable of producing B12 independently.^[32] Only about two dozens of microorganisms such as *Acetobacterium*, *Aerobacter*, *Bacillus* are known to produce this important class of cofactors.^[33,34]

Humans can obtain B12 through the daily diet, mainly from fish, shellfish, meat, liver, eggs and milk or taking vitamin pills as an alternative.^[35] After uptake, B12 is delivered with the assistance of haptocorrin, intrinsic factor, transcobalamin II^[36] and transcobalamin receptor into the cells.^[37] This sophisticated delivery system has high binding constants to the selected Cbls and makes sure that only “complete” corrinoids are passed to the enzymes (Scheme 3).^[3,38]

• haptocorrin	broad specificity of B12 analog
• intrinsic factor	B12 derivatives with nucleotide tail
• transcobalamin II	‘base on’ constitution (TCII·B12)
• transcobalamin receptor	‘base on’ , TCR:TCII·B12
• LMBD1	free lysosomal B12
• MMACHC	decyanation, Co(II), Co(III), ‘base off’
• methionine synthase	Co(I), Co(II), Co(III), ‘base off’
• methylmalonyl-CoA mutase	Co(I), Co(II), Co(III), ‘base off’

Scheme 3: The transportation of B12 in human beings (left). The selectivities of the transporters and/or changes of conformation and valence values of B12 (right).

The final destinations of Cbls in humans are the enzymes methionine synthase and methylmalonyl-CoA mutase and only tiny daily doses of B12 (1 - 2 µg) are required. Excess B12 is either stored in the liver (2 - 3 mg) or excreted through the urine.^[34]

1.3 Function of B12 – Coenzyme, thymine and cell division

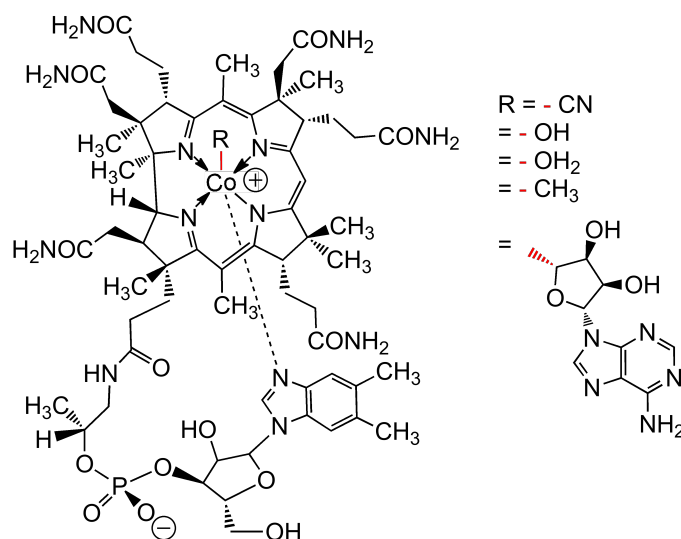
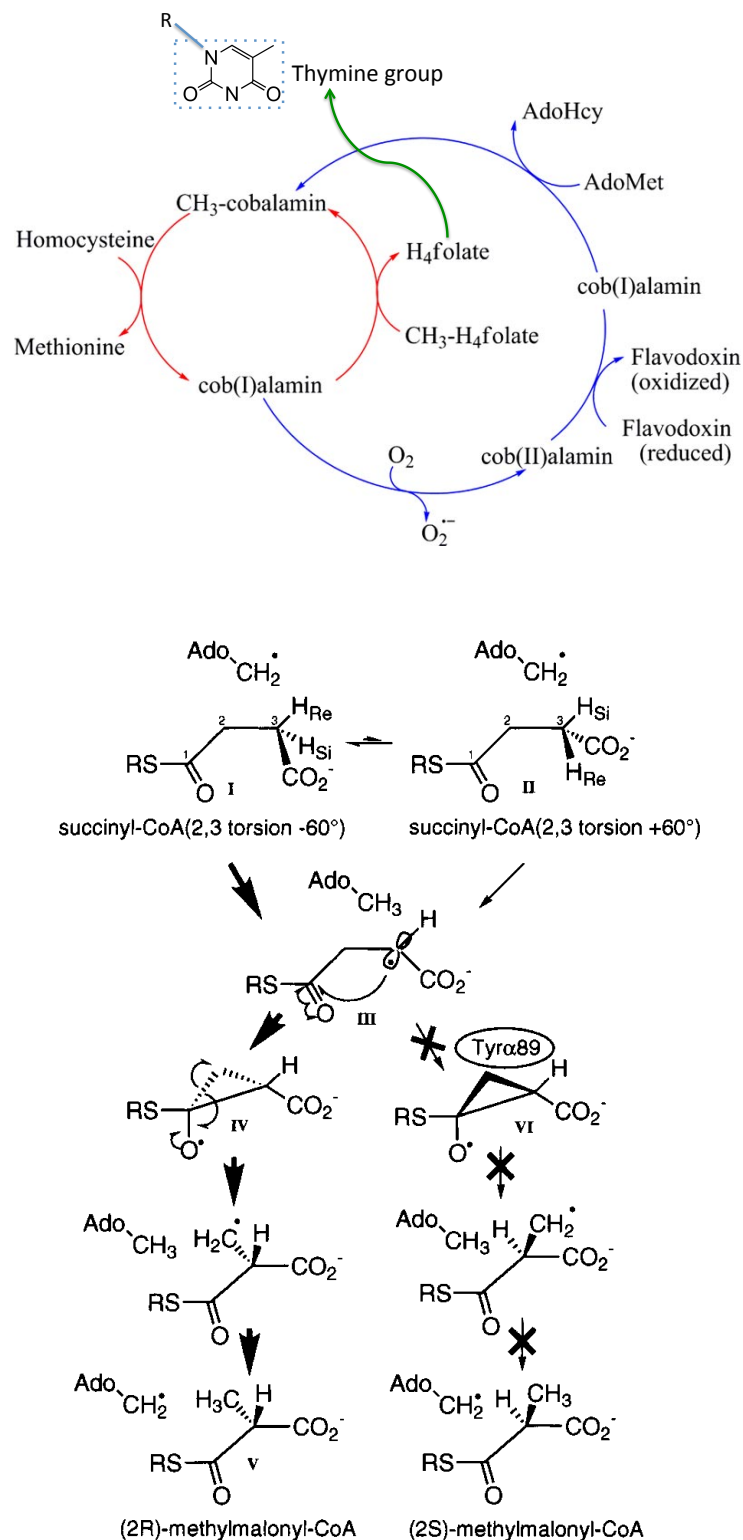


Figure 5: Structures of five B12 derivatives with different upper ligands (R = CN, cyanoCbl; R = OH, hydroxoCbl; R = OH₂, aquaCbl; R = adenosyl, AdoCbl).

Cbls participate in enzymatic reactions as their alkylated forms methylcobalamin and adenosylcobalamin, respectively (Fig 5).^[39]

Methylcobalamin is a cofactor of methionine synthase that regenerates methionine from homocysteine by a transfer of the methyl group from 5-methyl-folate.^[20,40-42] As a byproduct tetrahydrofolate (THF) is generated and converted by a B12-independent process to 5,10-methylene-THF, which is involved in the synthesis of thymine group (Scheme 4, up).^[43] As one of the four nucleobases of DNA, insufficiency of thymine obviously impedes the replication of DNA and therefore retards the cell division.^[44] This behavior causes failure of blood cell production and results in fatal pernicious anemia.^[45,46]



Scheme 4: (up) The catalytic (red) and reactivation (blue) cycles of *E. coli* MetH^[47]; (down) Proposed mechanism of the carbon skeleton rearrangement between (2R)-methylmalonyl CoA and succinyl-CoA^[48].

Adenosylcobalamin (AdoCbl) is the cofactor of methylmalonyl CoA mutase, which catalyses a reversible carbon skeleton rearrangement between methylmalonyl CoA and succinyl-CoA (Scheme 4, down).^[48] This is a crucial step in the extraction of energy from proteins and fats for humans.^[34] Succinyl-CoA participates in the tricarboxylic acid cycle (TCA), responsible for aerobic respiration in cells.^[49] AdoCbl also widely exists in other organisms than humans as a coenzyme for different apoenzymes such as glutamate mutase^[50,51], ribonucleotide reductase^[21] and diol-dehydratase^[28,52]. Although the apoenzymes are different in structure, they catalyze similar types of rearrangement reactions.

1.4 Properties of B12 – Structure, derivatives and constitutions

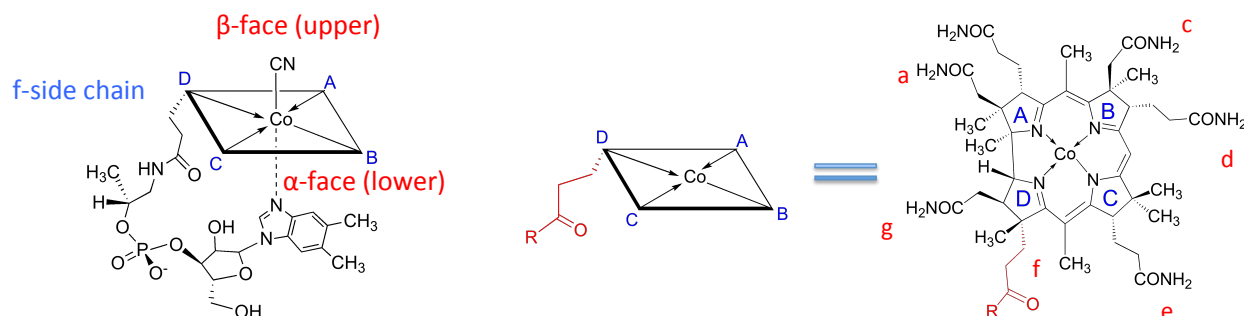


Figure 6: Structure of B12 (Charges on the corrin rings have been omitted).

B12, as a member of water-soluble vitamins, is the most complicated and also the only metal containing vitamin.^[53] The core of B12 is a trivalent cobalt ion, which is tetra-coordinated by a corrin ring in the equatorial positions. In the axial positions of the corrin are bound a cyano group on the top (β -face) and a nucleobase on the bottom (α -face) of the molecule. The seven amide side chains of the corrin ring are pointing to the β -face (a-, c-, and g-side chains) and the α -face (b-, d-, e- and f-side chains), respectively (Figure 6). The ligands on the upper and lower sides can be substituted in various ways, whereas coordination to the lower face is limited by strong coordination of the Dmbz base.

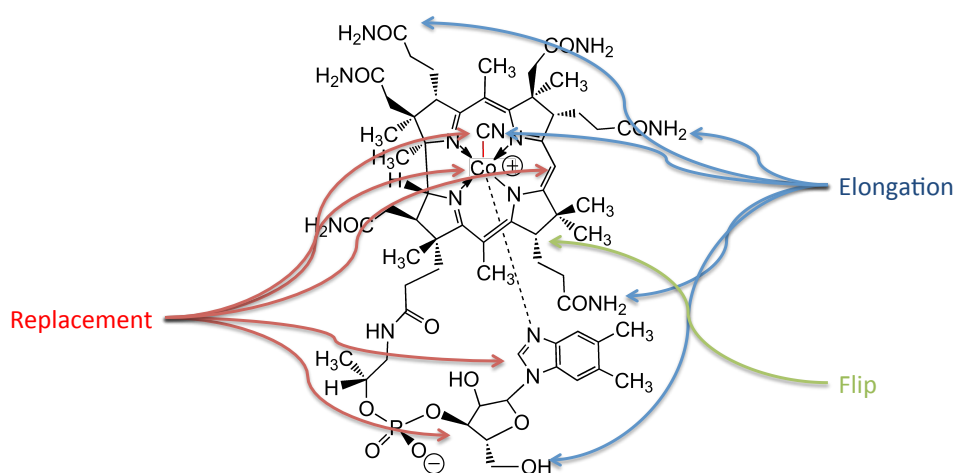


Figure 7: Possible modification sites of B12.

Most modifications of B12 focused on the upper ligands with either coordinative or

covalent bonds to the metal center. The former ones such as in cyano-B12 are relatively light stable. The latter organometallic ones are light sensitive due to the low activation energy of the Co-C bond.^[54]

Modifications of B12 extend almost every part of the molecule ranging from the upper ligands to the lower ones, from side chains of the corrin ring to the replacement of the central metal ion, from binuclear metal complex to extension at the ribose group (Figure 7).^[55,56] Most of these efforts are intended to study structural influence on the bioactivities.^[57-59] Nevertheless the difficulty of understanding interactions between cofactors and proteins are extremely challenging and more practical methods are required to control enzymatic activity.

Constitution represents another interesting topic in B12 chemistry. “Complete” corrinoids exist in the intramolecular “base on” constitutions unless the base is trapped by environmental parameters such as protonation^[60] (Figure 8, left) or encapsulation of the base^[61] (Figure 8, middle). Decoordination can also be caused by other strong competitive ligands like cyanide,^[62] which is the fundamental principle of cyanide detection with B12 derivatives.^[63]

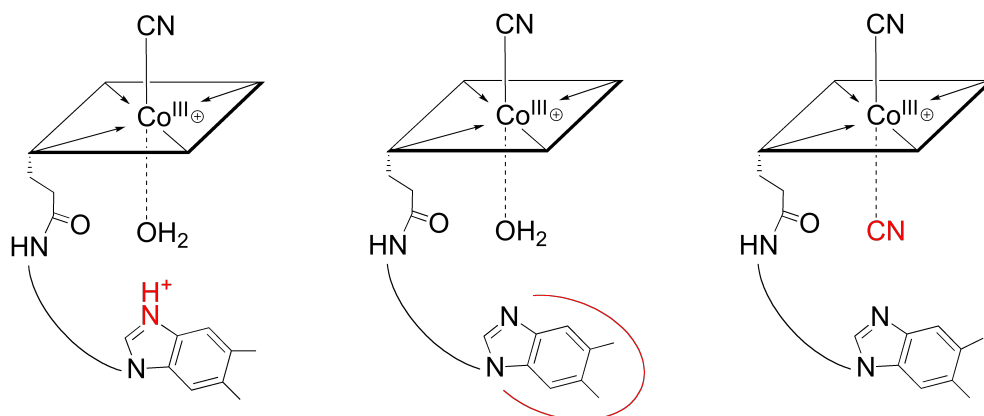


Figure 8: Three examples of “free” base off B12: (left) protonation of the Dmbz base; (middle) encapsulation of the bases; (right) substitution by cyanide ligand.

Compared to the B12 derivatives in non-biological environments, protein-bound cobalamins exhibit “base on”^[29], “base on/his on”^[30] and “base off/his on”^[26] constitutions (Figure 9).

“Base-on” cobalamins are generally buried inside the cavity of proteins by multiple hydrogen bonds between the protein and the amides-, the ribose-, and phosphodiester functionalities of the cofactor (Figure 9, top right).^[29] Of note, in transcobalamin II, an imidazole group of the protein coordinates to the upper face of the corrin ring to further fix its position (Figure 9, top left).^[30]

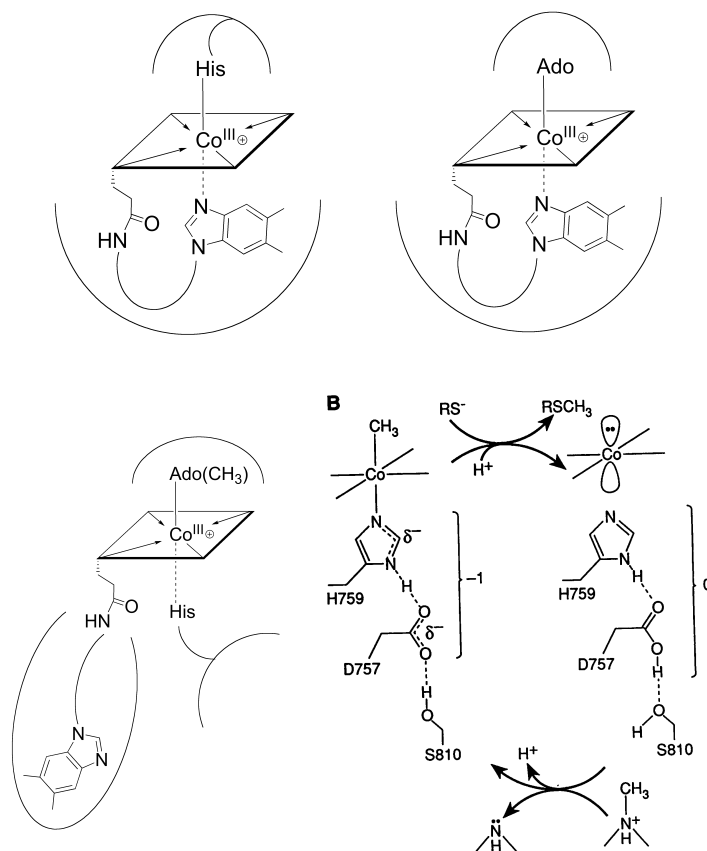


Figure 9: (top and bottom left) Three binding modes of coenzyme B12; (bottom right) Stabilization of the methylcobalamin in the methionine synthase reaction^[26] - the proton relay.

The “base off/his on” constitution is quite unique and fascinating.^[26] The dissociated Dmbz base of the cofactor is buried in a hydrophobic pocket of the protein, and a histidine group from the protein coordinates to the cobalt ion (Figure 9, bottom left). This critical constitutional change is the activation mechanism of methionine synthase.^[20,26,42] According to crystal structure analysis of methionine synthase, there is a protein relay

mechanism during the catalytic cycle, triggered by the NH functionality of the histidine group (Figure 9, bottom right).^[26] Matthews and coworkers showed that the pH value of the environment affects the redox properties of the cobalt center supporting the proton relay theory.^[64]

1.5 Topics of B12 – Recent progress

The first 50 years of B12 chemistry were mainly focused on the exploration of its structure. From the 1960s to the 1980s, fundamental studies yielded deep insights into the properties of natural as well as artificial corrinoids.

Thanks to rapid developments of NMR-^[65] and crystallographic techniques^[66] in the last 20 years, structural biology became more and more powerful for studying the mechanism of enzymatic reactions. Although crystal structures of protein-cofactor complexes may not reflect the real, biological situation, it yields the most convincing mechanistic insight, especially with the help of complimentary multi-dimensional NMR-, and computational studies. Benefiting from these advancements, a deep understanding of B12 dependent enzymes has been gained.

Using B12 as imaging materials or as drug delivery vehicles for medical application is an intriguing field. This method takes advantage of the natural high accumulation of B12 in fast proliferating cells like cancer cells in order to either track or deliver drugs to specific locations.^[67-69] One of the most sensitive methods to track B12 is radio labeling. Early attempts included direct labeling with radioactive cobalt^[70] (⁵⁶Co, ⁵⁷Co, ⁵⁸Co, ⁶⁰Co) or iodine^[71] (¹²⁵I, ¹³¹I), but none of them gained any practical use. Later, two new radioactive isotopes ^{99m}Tc and ¹¹¹In made a breakthrough in this field, and were not only tested in mice and pigs, but also in clinical studies.^[72,73]

The impact of modifications of the stereochemistry at position C13^[74,75] as well as the adenosyl ligand^[76] on the biological activities were tested. Changing the electronic properties of the corrin ring by replacing the proton at position C10 with electron withdrawing groups (-Cl or -NO₂) was another option.^[77,78] All of these derivatizations resulted in the deactivation of the enzymes.^[77]

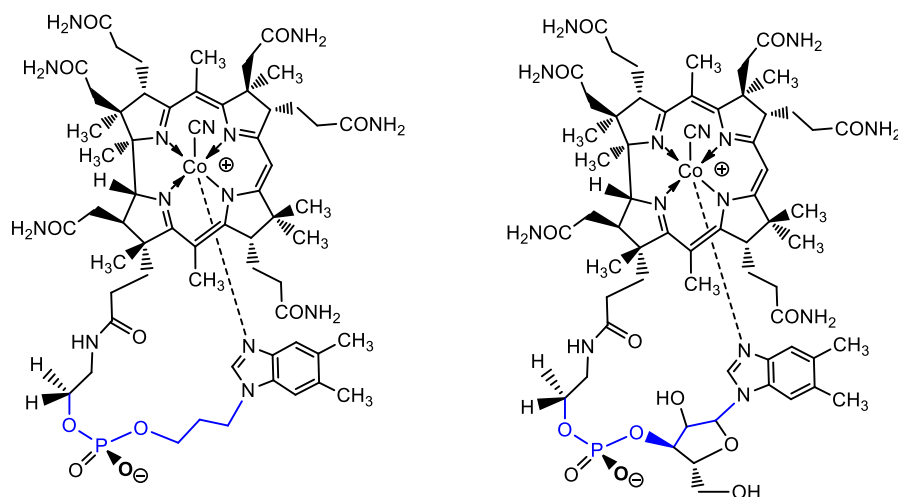


Figure 10: (left) Trimethylene B12 (right) norvitamin B12.

The modification of the loop structure or the coordinating base are expected to change the binding mode of the cofactor, thus decreasing the enzymes' activity. Two studies on the loop modification were particularly interesting for us. Toraya and coworkers replaced the ribose group with multi-methylene groups (Figure 10, left),^[58] which resulted in a decrease of the base on stability and low enzymatic activity in diol dehydratase. Kräutler and coworkers did a precise surgery on natural B12 by removing the methyl group at position C176 (Figure 10, right), and this remote methyl group far away from the coordination center surprisingly destabilized the base on constitution by a factor of 3.^[79,80] These two studies suggest that the modification on the loop part has impact to the intrinsic coordination properties as well as biological activities.

Other appealing perspectives of B12 chemistry include studies regarding the evolutionary origin of B12^[81,82], structural mimics of B12 coenzymes^[83,84], radical catalyst^[85-87], B12 labeling system^[69], cyanide sensors^[63,88-91], cobalamin regulated riboswitches^[92-94] and colorimetric detection^[68,95].

1.6 Projects of B12 – Peptide backbone

1.6.1 Concept of peptide B12 – Simulation, correlation and suppression

B12 is extremely high efficient for the metabolism of humans. It participates in cell division and only a very small amount of B12 is consumed per day (1 - 2 μg).^[37] B12 deficiency is rather uncommon and only known for either vegetarian or people with malfunction of B12 absorption. Up to 2 - 3 mg are stored in the liver enough for keeping metabolic functions running for 3 years.

Sufficient supply of B12 is critical for healthy people, but not advantageous for cancer patients. B12 participates in cell division and stimulates therefore the undesirable fast replication of cancer cells resulting in the progression of the disease.^[96,97] Taking advantage of the critical role of B12 in the metabolism, an alternative mechanism of cancer treatment can be envisaged based on the suppression of cell replication through manipulation of B12, either by reducing the amount or by decreasing the activity of B12.^[98] The former strategy is based on the control of dietary B12 absorption, but the normal cells will suffer starvation as well. A more promising solution is the latter one, replacing the highly active natural B12 with low-active artificial substitutes in order to suppress replication of fast proliferating cells, but the healthy cell can still survive.

The deactivation of B12 dependent enzymes can be realized by changing the structure of B12 cofactors in several ways. The upper ligands participate directly in the enzymatic reactions, and studies showed that hydrogen bond interactions between the upper ligands and the proteins are crucial to the catalytic efficiency.^[51] Therefore, the modification of upper ligands (methyl or adenosyl) can be one option for deactivation of B12 dependent enzymes. The lower base is also a potential candidate for this application. In “base off/his on” enzymes, the dmbz base and the tethering loop is not directly involved in the reaction and far away from the active center.^[26] However, the loop acts like an anchor to fix the bonding site of the cofactor. Modification of the structure of the loop influences the activity of B12 dependent enzymes, as demonstrated by replacing the ribose group of B12 with methylene fragments that either reduce or deactivate the activity of diol dehydratase.^[58] A third strategy is to exchange

either the metal center or modulate the redox properties at the cobalt ion. The former goal has already been achieved, but biological activity tests of these so called metbalamins are still lacking.^[99-102] For the latter strategy, it is possible to influence the properties at the cobalt ion by modifications of the conjugated π -system of the corrin ring through C10 substitution.^[77]

We focused on tuning of coordination- and electrochemical properties of the cobalt ion in B12 through modification of the lower face of the corrin. We assumed that changes of the “lower” base or the strength of intramolecular coordination can tune the electron density and thus influence the redox properties of the cobalt ion. Therefore, in enzymatic reaction with the cofactor bound in the base on constitution, homolysis of the Co-C bond as well as the activity of the enzyme might be tuned.

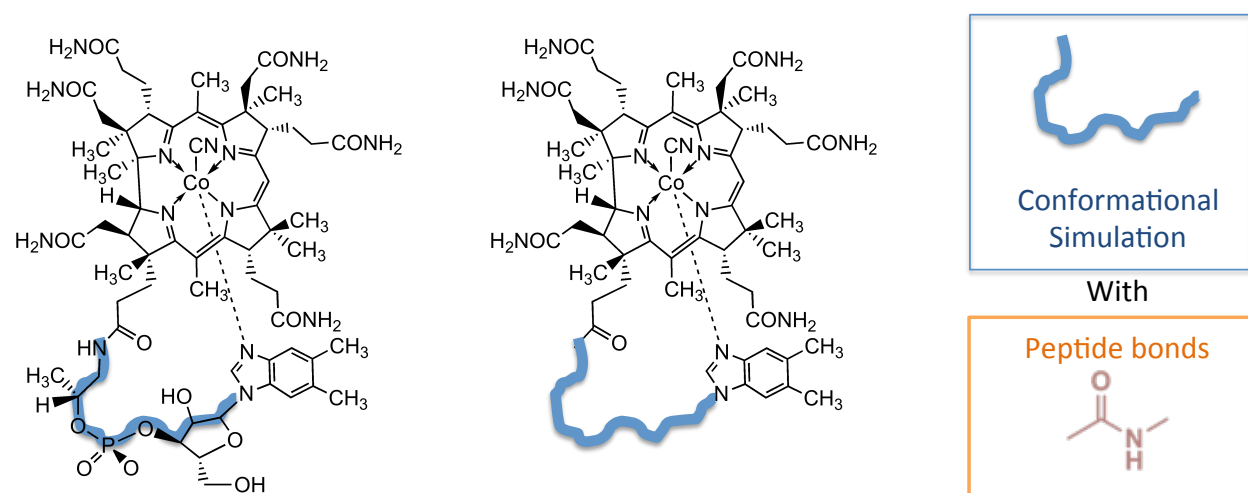


Figure 11: Conformational mimic of B12 in the ribose phosphodiester part with peptide structures (Charges on the corrin rings have been omitted).

Most important for the lower-face strategy is the selection of alternative structures for the replacement of the ribose phosphodiester loop. Toraya and coworkers have used methylene fragments for this purpose, but destabilization of intramolecular coordination was too dramatic and the implementation of structural alternatives seemed to be time consuming and challenging.^[58] Peptide bonds are resilient structures having a near planar conformation but still with some flexibility in folding. Prediction and design of different conformation of peptides is straightforward and we intended to mimic the

conformation of the linker of B12 (Figure 11).^[103-106] With a big pool of various amino acid “building blocks”, the design of loop structures with distinct properties is possible. The high affinity of peptide bond structures to proteins was another consideration in regard of biological activity tests. Thus a new class of vitamin B12 with embedded peptide structure was proposed, and we call these derivatives peptide B12 (Figure 12).

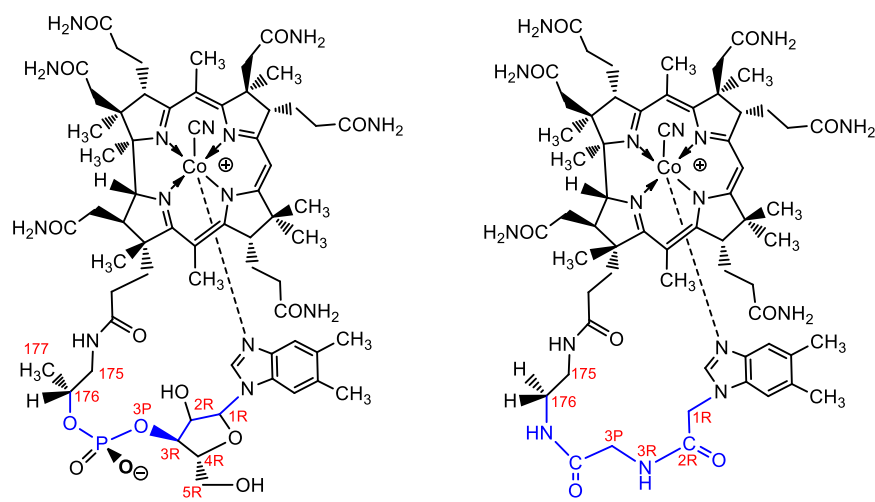


Figure 12: (left) B12; (right) prototype of peptide B12.

The consequence of the modifications of the loops on the coordination chemistry and electrochemistry of the cobalt has been investigated. Furthermore, the bioactivity of the modified cofactors is also intriguing.

1.6.2 Coordination Chemistry of B12 derivatives

Diastereomers of aquacyanocobinamides

“Incomplete” corrinoids have two stable isomeric coordination structures at the cobalt center,^[107-109] and they are usually synthesized by cleavage of the phosphodiester bond of B12.^[110] Friedrich and coworkers^[111,112] devoted enormous effort to characterize the axial diastereomers of aquacyano Cbi and finally Brown's group assigned the isomers in a mixture of chemically enriched aquacyano Cbi ¹³C NMR spectroscopy.^[113]

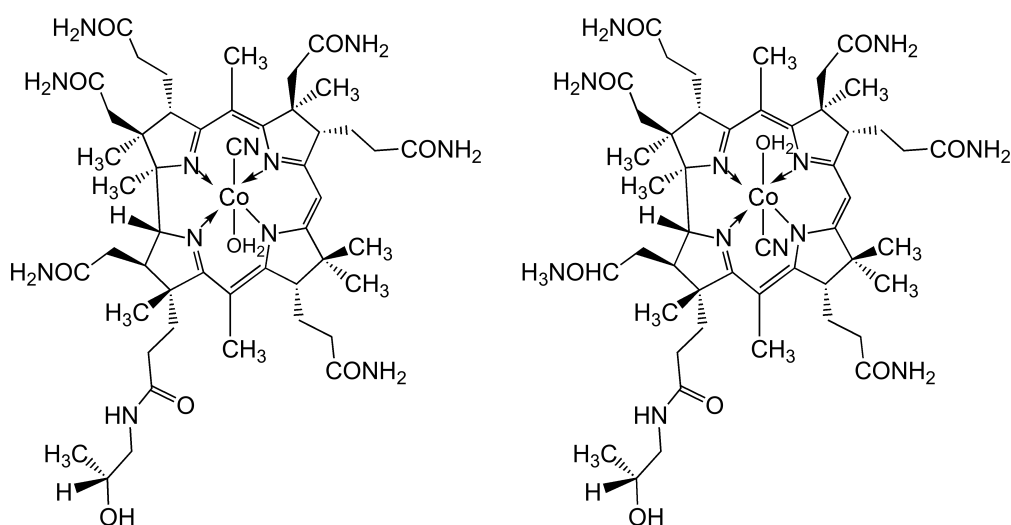


Figure 13: α-aqua,β-cyano cobinamide (left) and α-cyano,β-aqua cobinamide (right). Charges on the corrin rings have been omitted.

We intended to develop a convenient method for the synthesis, separation and identification of diastereomeric aquacyanocobinamides (Figure 13). This sub-project was important for mechanistic studies performed in our group concerning the application of incomplete corrinoids as optical sensors for cyanide.^[88]

Intermolecular coordination of “complete” corrinoids

Intermolecular interactions are important for the transportation, uptake, and enzymatic activities of cofactors in proteins,^[114-116] but outside of proteins, “complete” corrinoids rarely have multiple intermolecular interaction with other molecules.

In porphyrin chemistry, self-assembly is a common phenomenon, and many examples of supramolecular chemistry of heme derivatives have been reported.^[117-120] Corrinoids, on the other hand, have only been observed to dimerize in the solid-state^[121] or with covalent bond^[122,123]. We assumed that the relatively rigid ribose phosphodiester backbone and the strong intramolecular coordination of Dmbz to the cobalt ion impede the formation of complex structures (Figure 14, left).

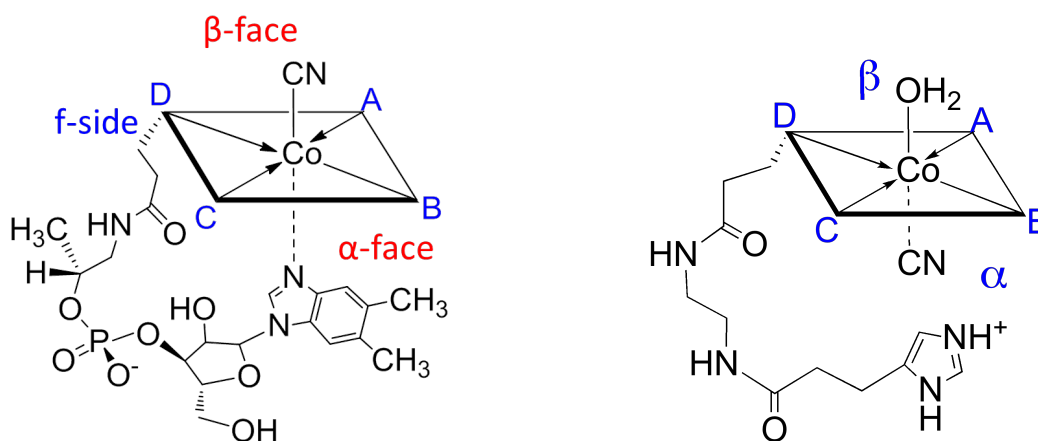
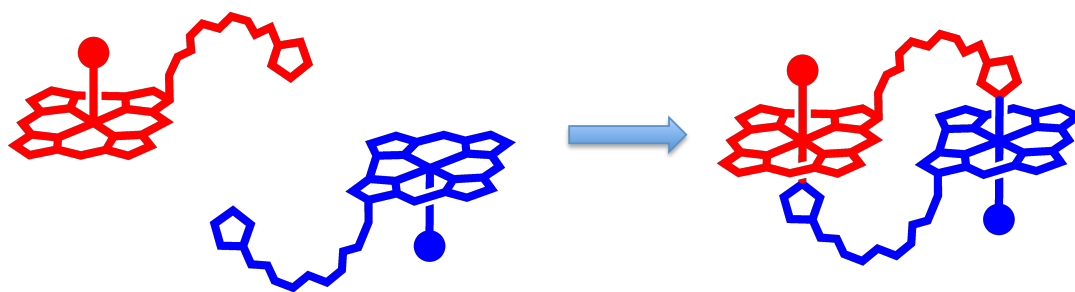


Figure 14: (left) B12 (right) base off “complete” corrinoid with α -cyano, β -aqua structure at the cobalt center. Charges on the corrin rings have been omitted.

To overcome this limitation and render self-assembly possible, we intended to replace the rigid ribose phosphodiester loop with a flexible structure and the bulky Dmbz with an imidazole (Figure 14, right). To avoid intramolecular coordination at the α -side of the corrin, we wanted to block this face with a strong ligand such as cyanide (Figure 14, right). We envisaged that realization of these two key elements would open the possibility for intermolecular coordination of “complete” corrinoids (Scheme 5).



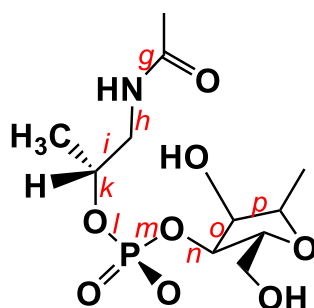
Scheme 5: Dimerization of “complete” corrinoids.

2 Results and Discussion

2.1 Peptide B12 - Derivatization of the backbone of B12

The loop structure of B12 is critical to the strength of intramolecular coordination of Cbls.^[81] We used peptide bond structures to simulate the conformation of the ribose phosphodiester part of B12, which result in the change of the electrochemistry of the cobalt ion. Furthermore, the impact of well-designed structural changes on the stability of intramolecular coordination is discussed.

2.1.1 Conformational analysis - Guideline for the design of the loop



B12 Loop

Figure 15: The bonds of the loop structure of B12 are labelled *g* to *p*.

Inspired by Eschenmoser and Kreppel's conformational analysis^[81,124] of the loop structure of B12, we decided to apply this method to mimic and design the structure of the backbone in artificial peptide B12 derivatives. We were particularly interested in effective substitutes for partial eclipse conformations, since we expected that low-energy conformations (e.g. anti-periplanar, synclinal) would adopt naturally.

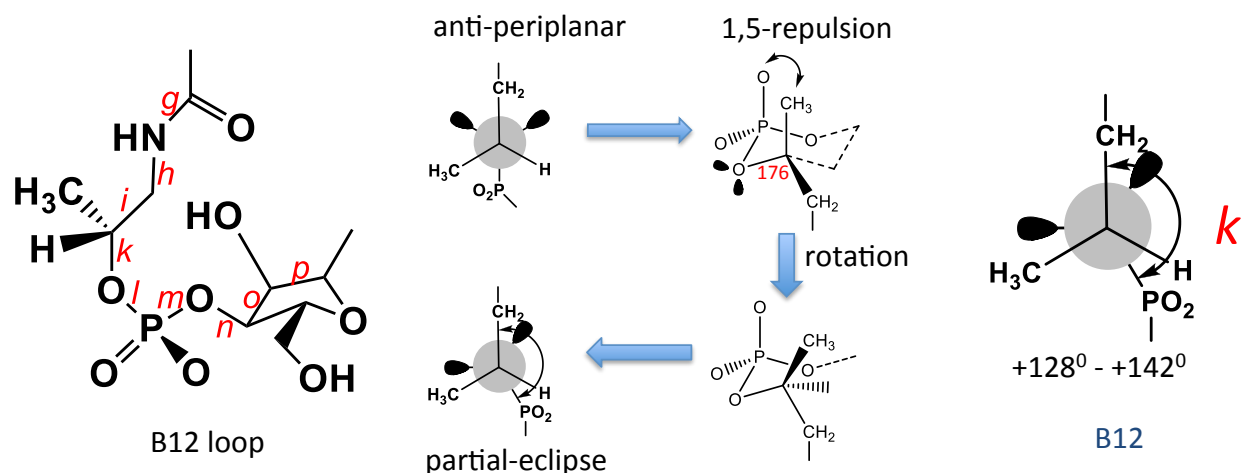


Figure 16: 1,5 repulsion in B12 results in a conformational change of the k -bond from anti-periplanar to partial-eclipse.

By comparing results from the “ideal” conformational analysis with crystal structure data of B12,^[124] partial-eclipse conformations have been proposed in order to avoid unfavorable 1,5 repulsion or ring constraints. In an “ideal” conformation as defined by Eschenmoser,^[124] 1,5 repulsion would be caused by the interactions between an oxygen of the phosphodiester moiety and the methyl group at C176, but it is circumvented by rotation of 38 to 52° around the k -bond to form the partial-eclipse conformation as shown in Figure 16. Partial-eclipse conformation is also caused by limited rotation around the o -bond in the ribose ring. We decided to replace the phosphodiester, and the ribose group in B12 with peptide bonds in order to mimic partial-eclipse conformations in bonds k and o (Figure 15).

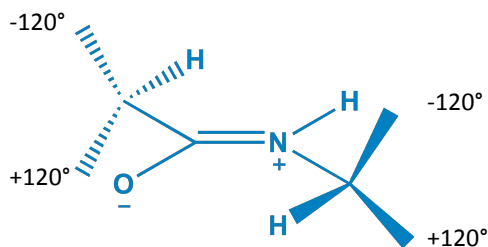


Figure 17: The “ideal” conformation of the iminiumoxide-form of a peptide bond.^[124]

The iminiumoxide-form of a peptide bond has a planar structure in the O-CR-NR'H region and a (theoretical) *anticlinal* angle of torsion of $\pm 120^\circ$ at the adjacent bonds

(Figure 17).^[124] According to investigations of amides with $-\text{CH}_2\text{-CON-}$ and $-\text{CONH-CH}_2\text{-}$ moieties, these values are actually in the region of $\pm 60^\circ\text{-}180^\circ$.^[125] The relatively well-defined conformational structural motif of the peptide bond provided us therefore the basic tools for mimicking partial-eclipsed structures in bonds *k* and *o* of B12 (Figure 15).

Replacing the phosphodiester group in the backbone of B12 with an amide bond leads to similar conformations in the region of the *i*, *k* and *l* bonds (Figure 18), but the “ideal” conformation of the *m*-bond in the “prototype” peptide B12 differs by 120° from that observed in B12 (Figure 18). We introduced therefore a flexible methylene group between the *m*-, and *n*-bonds of the loop to compensate for this conformational “error”.

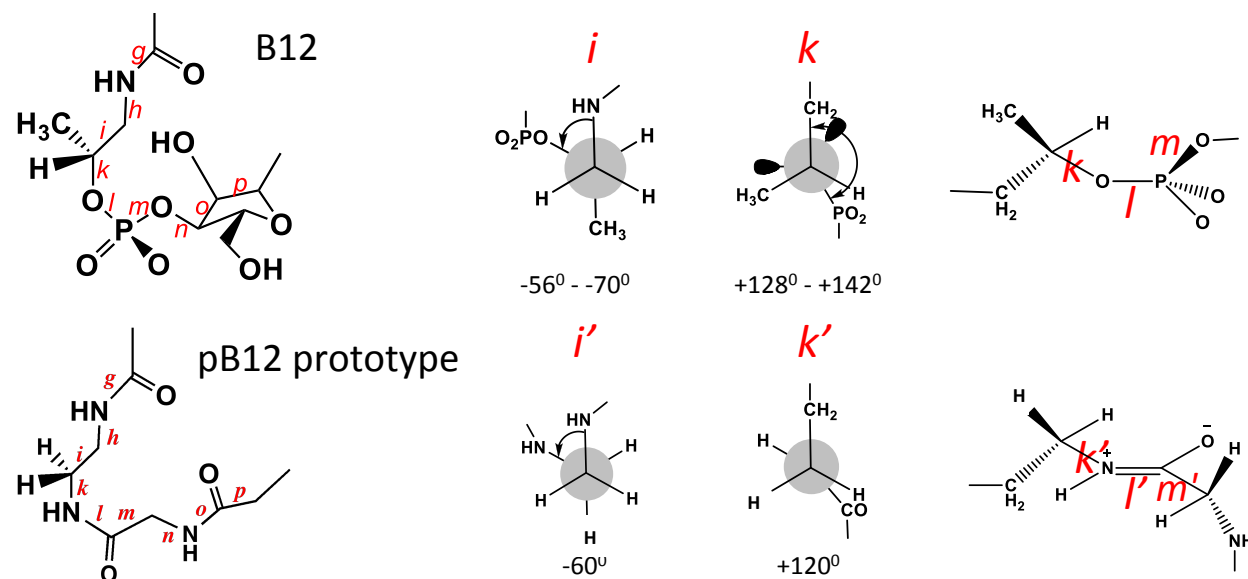


Figure 18: Simulation and comparison of the conformation of the natural and artificial backbone of B12 at bonds *i*, *k*, *l* and *m*.

Crystal data analysis of B12 revealed that the dihedral angle at the *o*-bond (Figure 19, right up) ranges from $+152^\circ$ to $+162^\circ$.^[124] This structural motif can therefore also been replaced with a peptide bond (Figure 19). Assuming an ideal conformation of the latter, this mimic will only cause slight deviations ($18^\circ\text{-}28^\circ$).

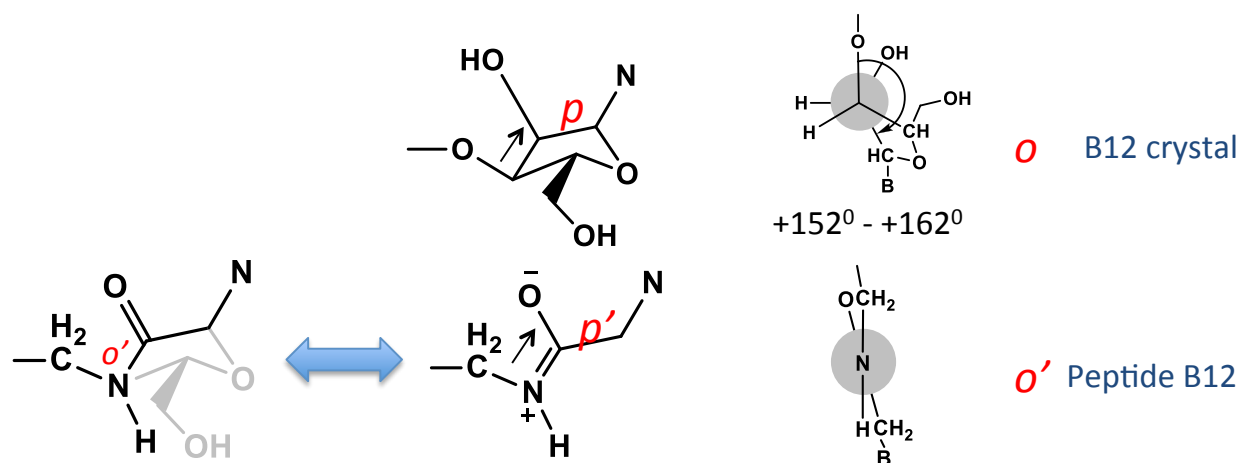


Figure 19: Simulation of the “ideal” structure of B12 at the o-bond.

The conformational analysis of the o-p-q bonds in the loop of the peptide B12 prototype is depicted in Figure 20 and compared to B12.

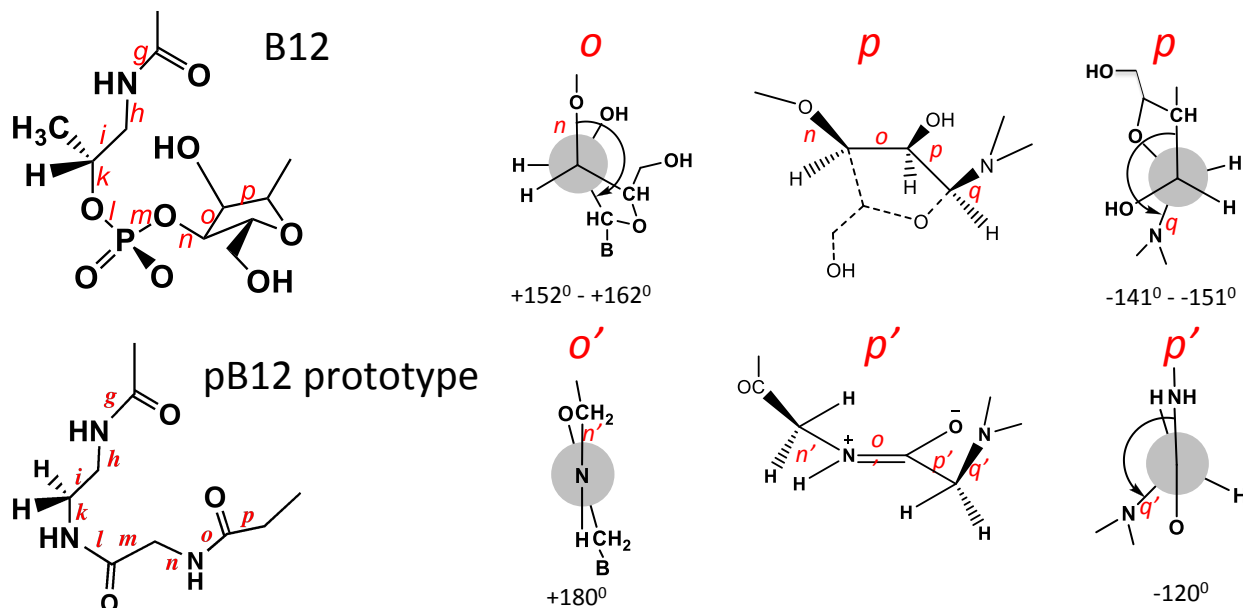


Figure 20: Simulation and comparison of the conformation of the natural and artificial backbone of B12 at bonds n, o, p, q.

As a complement to the conformational analysis, computational calculation of the lowest energy state was performed by Olivier Blacque (Table 1). These results suggest that the calculated or the ideal structure of the peptide backbone of the prototype differs only in two positions (*l* and *o*, or *i* and *l*) from that of B12. The conformation of the other bonds

fit well with those from the crystal structure of B12 (Table 1).

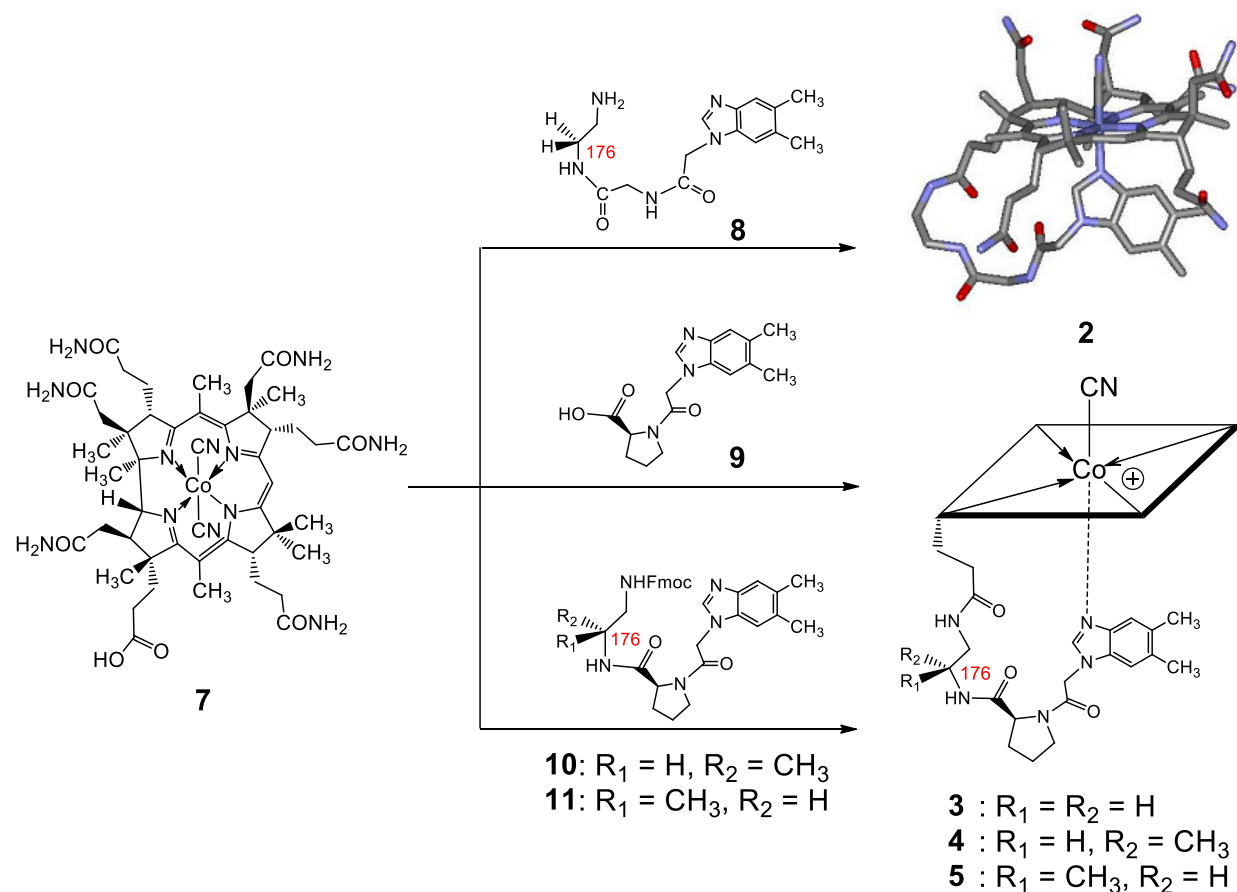
Table 1: Comparison of the conformation at i - q bonds (°) between peptide B12 prototype (computational calculation)^b, pB12 (ideal conformation)^c with B12 (crystal data)^a:

	i	k	l	m	o	p	q
B12 ^a	-63	134	-70	168	124	158	-148
pB12 ^b	-71	143	-173	151	-82	167	154
pB12 ^c	-180	120	-180	120	180	180	-120
B12 ^a - pB12 ^b	8	9	103	17	152	9	52
B12 ^a - pB12 ^c	117	14	110	60	56	22	28

Starting from the structure of the prototype, further adjustments of the structure as well as the conformation have been considered. To mimic the ribose group of B12, we introduced a proline group as a “U-turn” mimic to pre-organize the loop for better coordination to the cobalt center. Another interesting modification is the methyl group in different configurations at position C176 (Scheme 6). This modification will be discussed in the next part in more detail.

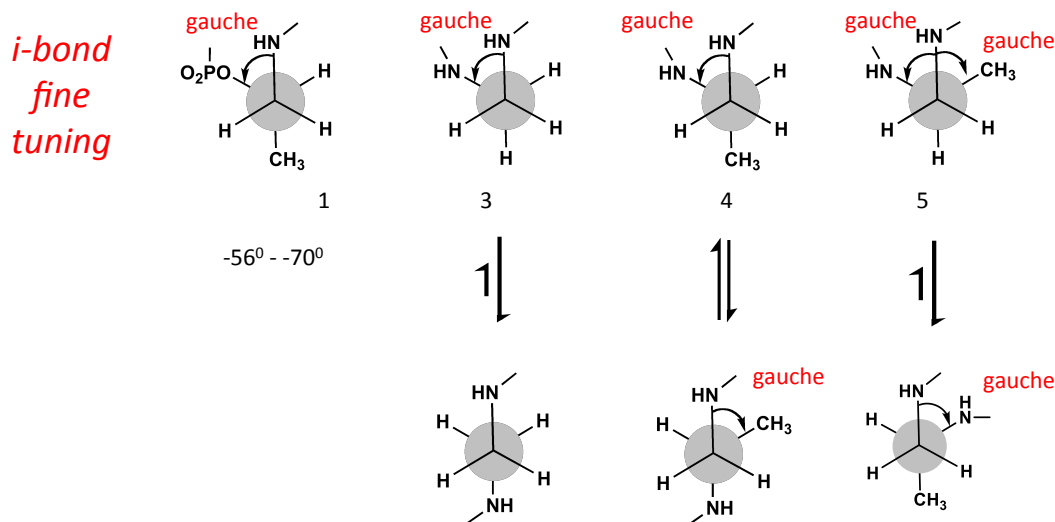
2.1.2 Peptide B12 derivatives - Coordination and redox chemistry

The peptide B12 derivatives (**2** - **5**, the counter ion TFA is omitted) were synthesized from dicyano-cobyric acid (**7**) and peptide loops as shown in Scheme 6. The cobyrinic acid (**7**) was synthesized from B12 (**1**) according to Müller's method^[126]. The peptide loops (**8** - **11**) were synthesized from dimethylbenzimidazole using standard peptide coupling reagents according to methods applied for the synthesis of building blocks of peptide nucleic acids (for details see experiment part).^[127] Cobyric acid was then coupled with the loop parts with EDC•HCl and DMAP in DMF (Scheme 6). The isolated yields differed between 42 % and 80 %. The UV/vis and NMR spectra suggested intramolecular coordination by comparison to base-on B12 as discussed in reference^[127] in more detail (Appendix I).



Scheme 6: Synthesis scheme of compound **2** - **5**.^[127]

Spectrophotometric pH titrations of compounds **2** - **5** revealed that their pK_a value varied between 0.62 and 1.64 (Figure 21). The methyl group of **4** at position C176 enhances its base on stability ($pK_{\text{base-off}} = 0.62$) compared to **3** ($pK_{\text{base-off}} = 0.97$), which is similar to the stabilizing effect observed for this functionality in B12. Kräutler et al. used conformational analysis of the i-bond in both B12 and norvitamin B12 to explain the stabilizing effect of the methyl group at C176 of (R)-configuration.^[79] The experimental results confirmed earlier prediction of Eschenmoser and Kreppelt.^{[81][124]} We suggest the same form of analysis to explain the methyl group effect at C176 in peptide B12 derivatives **4** and **5** compared to **3** (Scheme 7). In compound **3**, the (-) synclinal conformation at the i-bond is the same as in B12 (**1**). It is energetically disfavored compared to its anti-periplanar conformation because of a gauche interaction (Scheme 7). This behavior is disadvantageous for simulating the conformation of B12 with peptide B12 derivatives. In order to overcome this limitation, we introduced compound **4** with an additional methyl group in R-configuration at C176. In compound **4**, the (-) synclinal conformation is not anymore energetically disfavored compared to the anti-periplanar conformation, because of the same number of gauche interactions. It mimics therefore better the structure of B12 than compound **3** (Scheme 2). In contrast, the introduction of the methyl group in the opposite S-configuration (**5**, $pK_{\text{base-off}} = 1.64$) causes an additional gauche interaction in the (-) synclinal conformation and disfavors thereby the modeling of the conformation of B12 (Scheme 7). These considerations are experimentally supported by the base-on stabilities of the compounds (**4** > **3** > **5**) according to the spectrophotometric pH titrations (Figure 21).



Scheme 7: The gauche effect of the methyl group in different conformations of compound **1**, **3** - **5**. (Up) The peptide B12 derivatives (**3**, **4** and **5**) are in the same conformation (- synclinal) as B12 (**1**) at *i*-bond. (Down) The more or equally stable conformation at the *i*-bond of peptide B12 derivatives.

Cyclic voltammetry (CV) experiments of these derivatives showed that the reduction potential of the cobalt ion was influenced by the loop structure. (Figure 21)

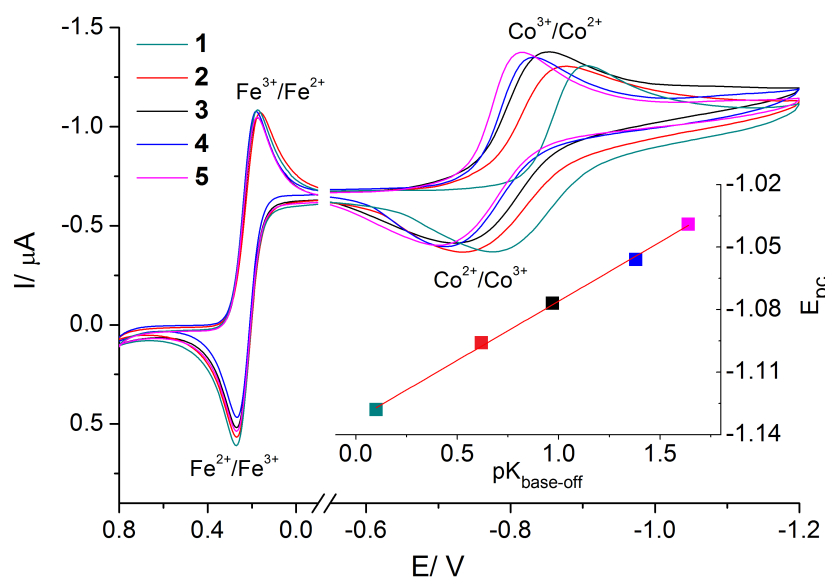


Figure 21: The CV spectra of compound **1** to **5** (**1**: B12; **2** - **5**: see Scheme 6). Inset: correlation of $\text{pK}_{\text{base-off}}$ values versus reduction potentials.^[127]

The stability of the “base on” constitution ($pK_{\text{base-off}}$) and the reduction potential of the cobalt(III)/Co(II) couple are linearly correlated (Figure 21: inset), that can be explained by the strength of intramolecular coordination of the Dmbz base to the metal center. The stronger intramolecular coordination the shorter the Co-N bond (Figure 22, right), which results in a higher electron density at the cobalt ion and therefore leads to a lower reduction potential of Co(III) (Figure 22, left).

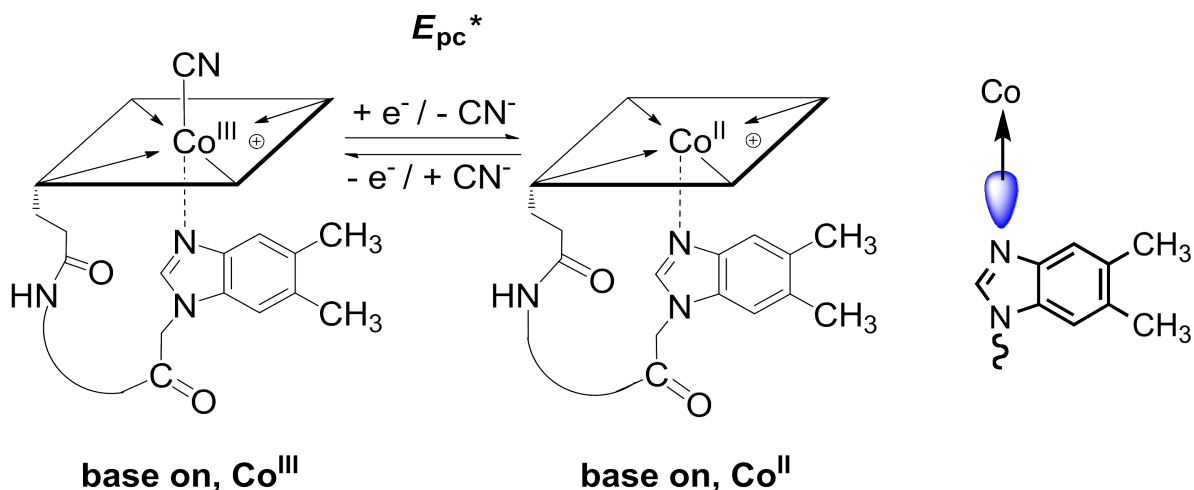


Figure 22: (Left) The Co(III)/Co(II) equilibrium of Cbl derivatives; (right) The coordination from Dmbz to the cobalt ion.

2.1.3 Other B12 derivatives

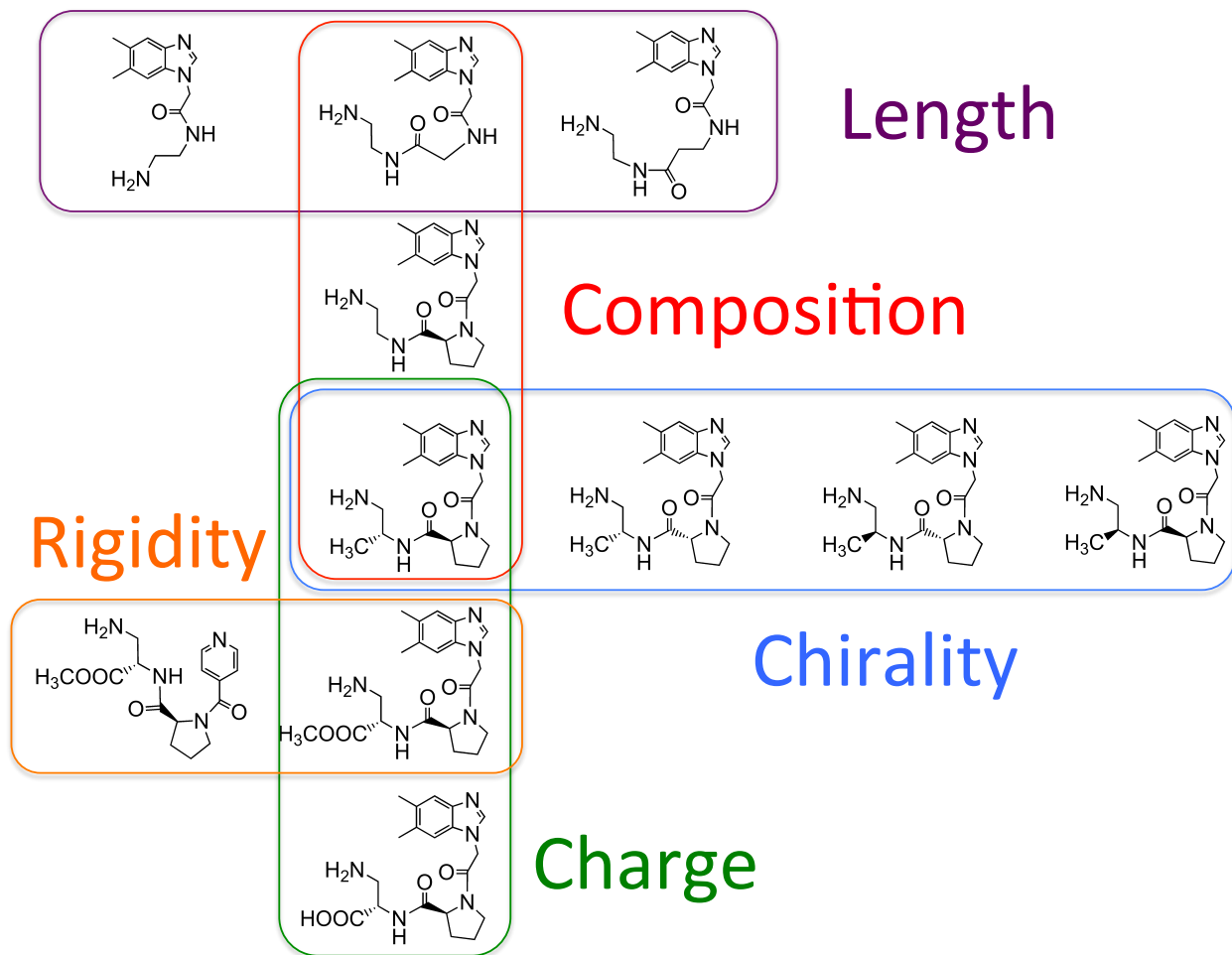


Figure 23: Eleven loop structures of peptide B12 derivatives differing in length, configuration, rigidity, charge and chirality.

Other factors that might influence the “base on” stability have been investigated as well. We focused on the impact of length, chirality, configuration, rigidity and charge on the base on/base off equilibrium (Figure 23).

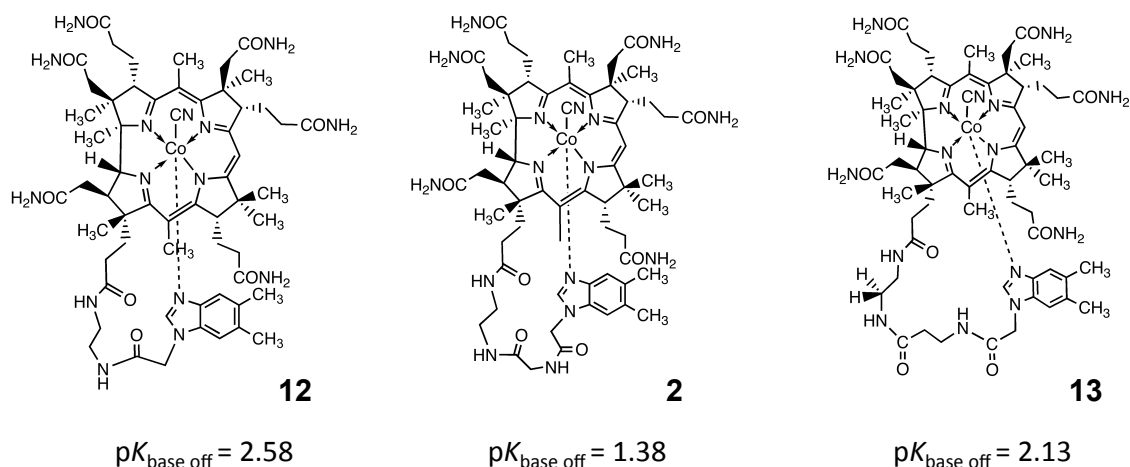


Figure 24: Structures of compounds **2**, **12** and **13**. Charges on the corrin rings have been omitted.

Proper length is critical to the strength of intramolecular coordination based on the following consideration. Construction of part of the intramolecular ring is basically to connect two fixed point A and point B in the ideal structure of B12 (Figure 25: case 1). Modifications of the loop are expected to result in a change of its folding, which will change the head-to-tail distance (Figure 25: case 2 or 3). The modified loops need to be stretched (case 2) or compressed (case 3) to fit the distance between the two points A and B. In either of the above mentioned cases, the stability of the intramolecular coordination could be undermined because of compromising the ideal conformation.

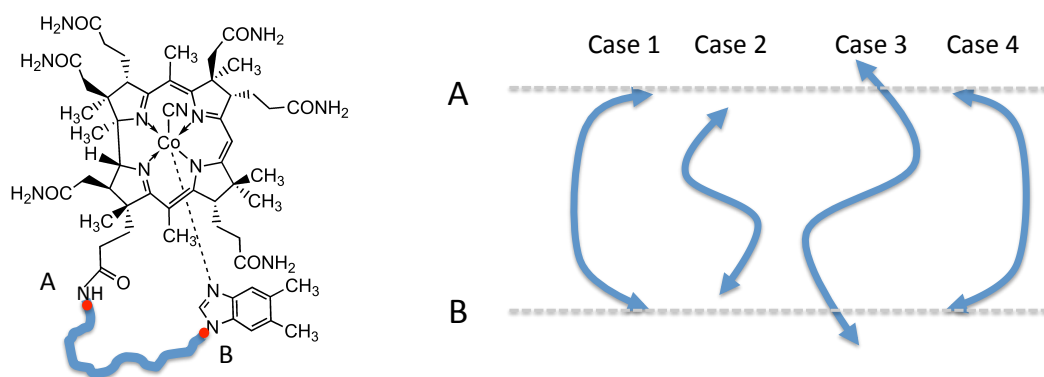


Figure 25: (left) Point A and B are positions in the ideal structure of B12. (right) The head-to-tail distance of the different loops can be longer (case 3) or shorter (case 2) than the distance of AB. Case 4 represents the mirror image of case 1 and has the same head-to-tail distance. Charges on the corrin rings have been omitted.

We assumed that a short loop would cause tension in the intramolecular ring, which in turn would compromise the base on stability. Compound **12** with a shorter loop (Figure 24, **12**) than the prototype (**2**, Figure 24, middle) was synthesized to demonstrate this point. The spectrophotometric pH titration experiments showed that the $pK_{\text{base off}}$ value of **12** is 2.58, which suggested that the base on stability of **12** is 16 times weaker than that of **2** (Figure 24). A long loop can avoid such tension, but lack of structure and preorganisation is a huge disadvantage as shown with **13** having an extra methylene group (Figure 24) compared to **2**. The $pK_{\text{base off}}$ value of **13** is 2.13, and its base on stability is 6 times weaker than that of **2**.

Chiral configuration is another critical factor that determines the strength of intramolecular coordination. Apart from the simulation of the original conformation, mirror-simulation could be another possibility (Figure 25: case 1 and 4) for conformational simulation, since the mirror image does not change the head-to-tail distance. In an ideal situation, when the conformation of the AB loop part is not influenced by the surrounding environment, the mirror-simulated loop will have the same stability as the original one.

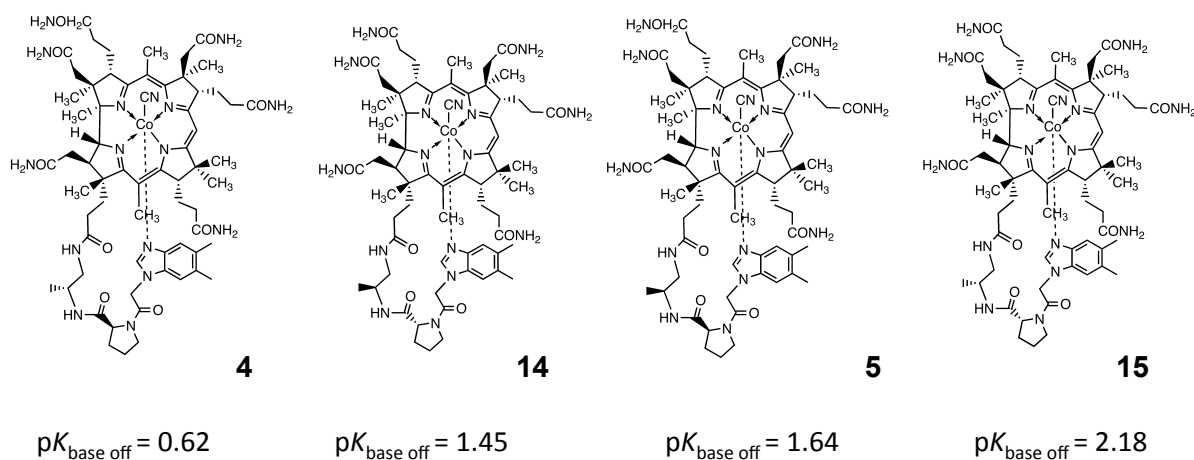


Figure 26: Peptide B12 derivatives with different chiral configurations. Charges on the corrin rings have been omitted.

To prove this assumption, four peptide B12 derivatives with different configurations at C176 as well as the proline subunit were synthesized and their base on stabilities were compared (Figure 26, **4**, **14**, **5**, **15**). We obtained thereby two pairs of mirror-imaged AB

loops (**4** and **14**, **5** and **15**). The connecting points A and B with either a peptide bond or Dmbz moiety have planar conformation, and the mirror image should therefore not undermine the ideal conformations, so **4** and **14** (or **5** and **15**) are expected to have the same $pK_{\text{base off}}$ value. which was not supported by the spectrophotometric pH titration experiments (Figure 26, 0.62 v.s. 1.45, 1.62 v.s. 2.18). This behavior suggests that the the base on stabilities of these compound are influenced by the environment such as the corrin ring part or the solvents.

As mentioned before, the mirror-image proposal is based on the assumption that the loops are in an isolated environment and they can adopt the ideal conformation without interference. However, as part of the whole molecules, the original loop and mirror-imaged loop were in different chemical environments and therefore this might result in different base on stabilities. This proposal was supported by the comparison of ^1H NMR spectra of **4** and **14**, which can be easily differentiated in the region between AB.

We also investigated the effect of the solvent on the conformation of the loops. From the ^1H NMR spectrum of **4**, we observed two sets of signals for the base on species in both D_2O and MeOD (in D_2O : $\approx 9:1$ and in MeOD: $\approx 1:1$, according to the integrals of H10 signals). These NMR experiments suggest that the aqueous environment stabilizes one conformation of **4**, probably because this conformation can form some hydrogen bonds inside the molecule. For these speculations, further experimental and computational studies are necessary.

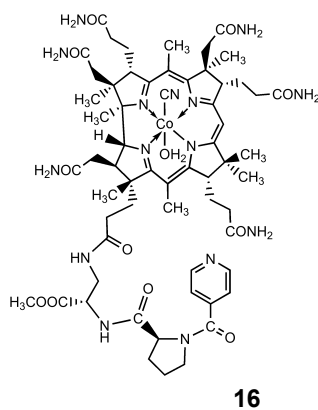


Figure 27: The structure of compound **16**. Charges on the corrin rings have been omitted.

Another example of a more rigid loop structure showed that the conformational mimic demands high precision. With a base exchange from Dmbz to pyridine that is directly connected to proline via an amide bond (Figure 27, **16**), intramolecular coordination was not anymore possible.

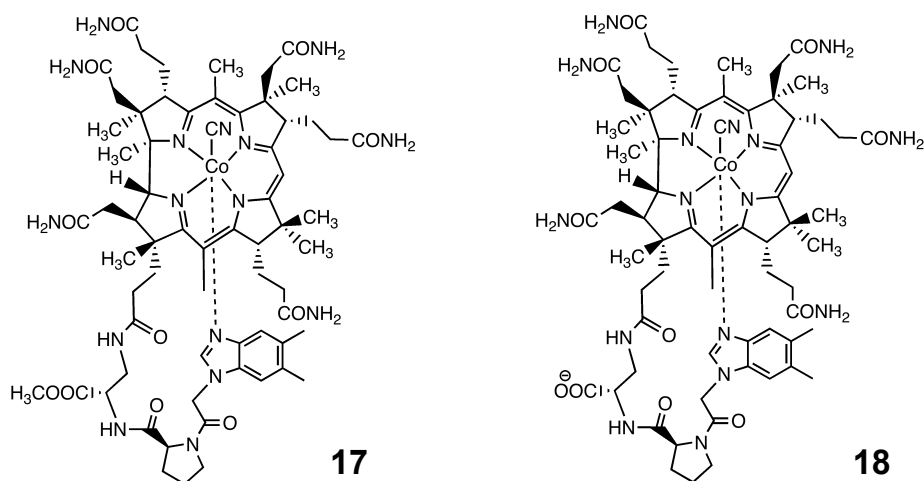
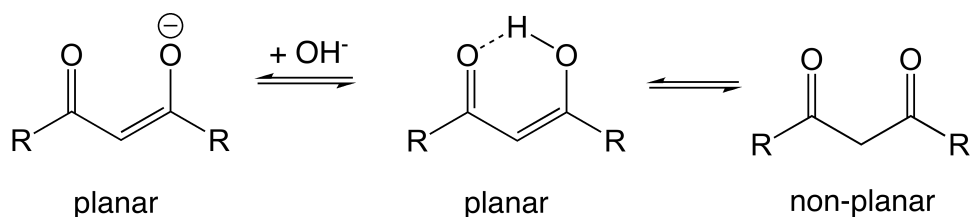


Figure 28: The structure of compounds **17** and **18**. Charges on the corrin rings have been omitted.

The influence of the charge of the loop on intramolecular coordination was also investigated with peptide B12 having methyl ester and carboxylate acid groups at position C176 (Figure 28, **17** and **18**, $pK_{\text{base off}}$ values are 0.77 and 0.78 respectively). As expected, the charge did not effect the base on stability because it is too far away from the coordination site. A charge effect might be expected if protonation (or deprotonation) is directly exerted to the loop skeleton and induces a change of conformation with a reduced or an increased energetic state. For example, a hypothetical $-\text{CO}-\text{CH}_2-\text{CO}-$ moiety within the backbone could response to an increased pH by a conformational change from non-planar to planar due to deprotonation of the enol form (Scheme 8).



Scheme 8: Conformational change between the tautomers.

2.2 Diastereomeric aquacyano cobinamide

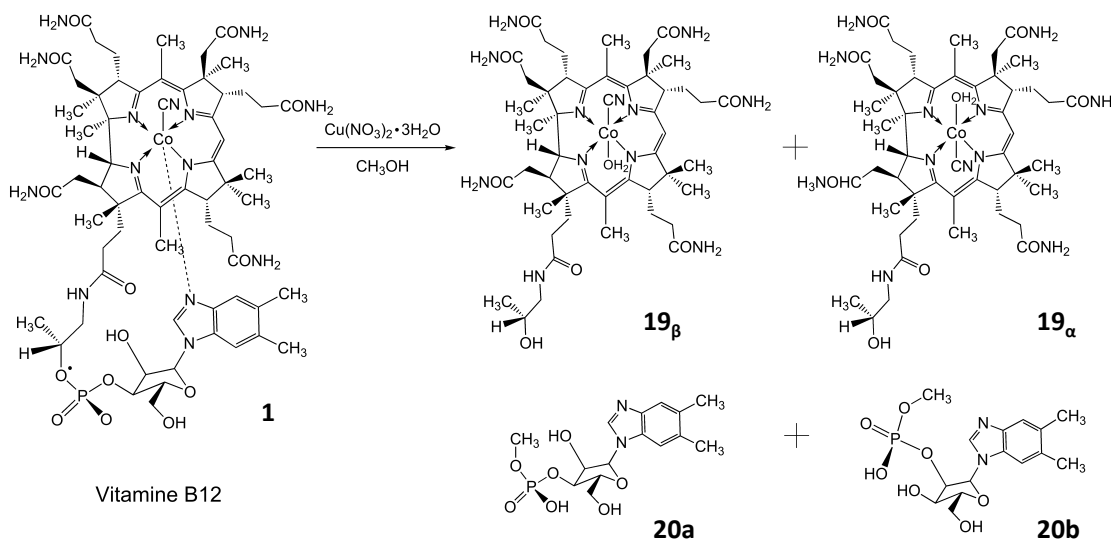
Cobinamides (Cbi) are “incomplete” corrinoids and their axial ligands strongly influence the electronic properties of the corrin ring. Different combinations of axial ligands result in distinctive UV/vis absorbance.^[112] The formation of dicyano-Cbl from diastereomeric mixtures of aquacyano cobinamides has been successfully applied for cyanide sensing.^[90]

There are different protocols for the preparation of Cbi from B12. Most widely used for this purpose are Ce(III) salts.^[110,128] The disadvantage of this methodology is the need to generate dicyano-B12 from B12 with additional cyanide prior to the phosphodiester cleavage with the metal salt and the complicated workup procedures. Brown and co-workers developed a useful method for the phosphodiester hydrolysis of alkylcobalamins under strictly anhydrous conditions.^[129] Improvements of existing synthetic protocols as well as the development of novel modified B12-derivatives are important for further progress and new applications of corrinoids.

Apart from improvements of existing synthetic methods, the characterization of the aquacyano Cbi isomers is also critical for analytical purposes. Friedrich et al. devoted much effort to characterize axial diastereomers of aquacyano Cbi.^[101,111,130] Brown et al. used chemically ¹³C enriched axial ligands and the corresponding Cbl analogs to assign the α - and β -cyanide positions in the mixture of diastereomeric aquacyano Cbi with NMR spectroscopy. Overlap of the ¹³C NMR signals impedes unfortunately the identification of the isolated isomers. For applications such as cyanide detection, only diastereomeric mixtures of “incomplete” aquacyano corrinoids have been employed, and initial kinetic studies suggested differences in cyanide coordination. The identification and evaluation of well-defined isomers are important in regard of future improvements of corrin-based chemosensors.

2.2.1 Synthesis and characterization of aquacyano cobinamide

Based on an earlier report of Müller and Müller^[126], we explored and developed a metal-ion catalyzed transesterification reaction for the synthesis of diastereomeric aquacyano Cbi from B12.



Scheme 9: The synthesis scheme of aquacyano cobinamide. Charges have been omitted.

After screening of different combinations of metal ions (Co^{2+} , Ni^{2+} , Cu^{2+} , Mg^{2+} or Zn^{2+}) and anions (Cl^- , NO_3^- , SO_4^{2-}), we identified $\text{Cu}(\text{NO}_3)_2 \cdot 3\text{H}_2\text{O}$ as the most efficient catalyst for this reaction (Scheme 9). Thorough optimizations led to the following general procedure: B12 (**1**, 20 mg, 15 μmol) and $\text{Cu}(\text{NO}_3)_2 \cdot 3\text{H}_2\text{O}$ (50 mg, 163 μmol) were dissolved in methanol (2 ml) and stirred for 20 min at 100 °C in a Young Tube (1 cm \times 15 cm) sealed with a Teflon cap. After cooling the solution to room temperature, the methanol was removed under reduced pressure. The residue was dissolved in water (5 ml) and desalted with the help of SPE. Subsequently, it was separated by preparative reverse phase HPLC to yield α -cyano- β -aqua-cobinamide (**19 α** ; 6.9 mg, 6.0 μmol , 40%) and α -aqua- β -cyano-cobinamide (**19 β** ; 3.9 mg, 3.4 μmol , 23%) as their corresponding TFA salts.^[131]

The advantage of this method is shown in Figure 29 and includes (i) straightforward procedure, (ii) cyanide free condition and (iii) a convenient workup procedure. More

details are shown in the paper attached in the end (Appendix III).^[131]

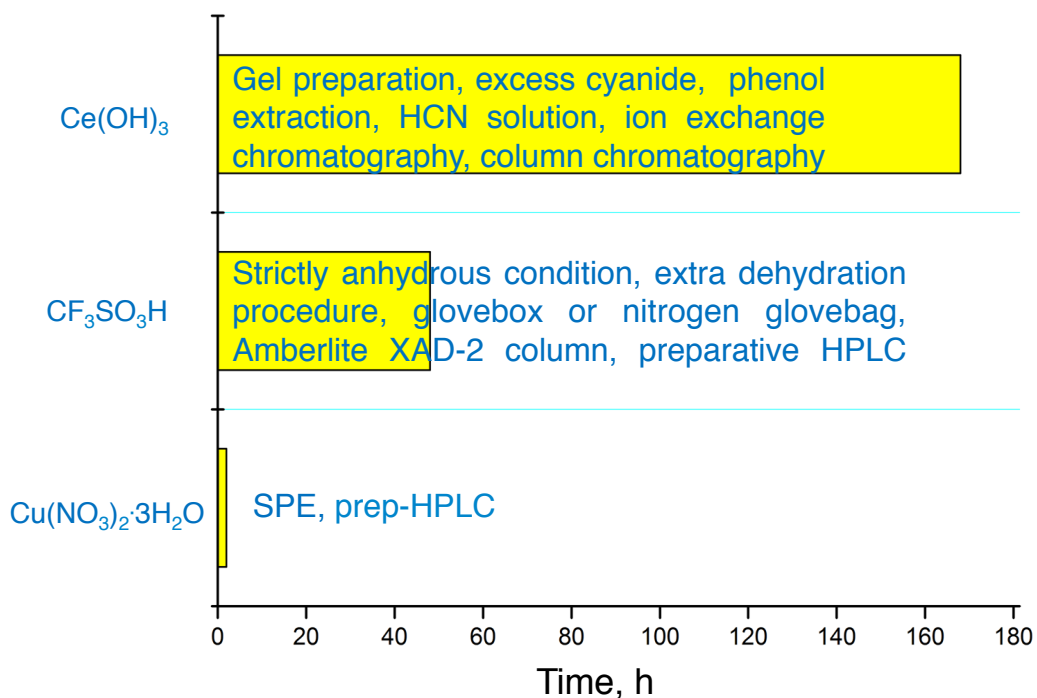
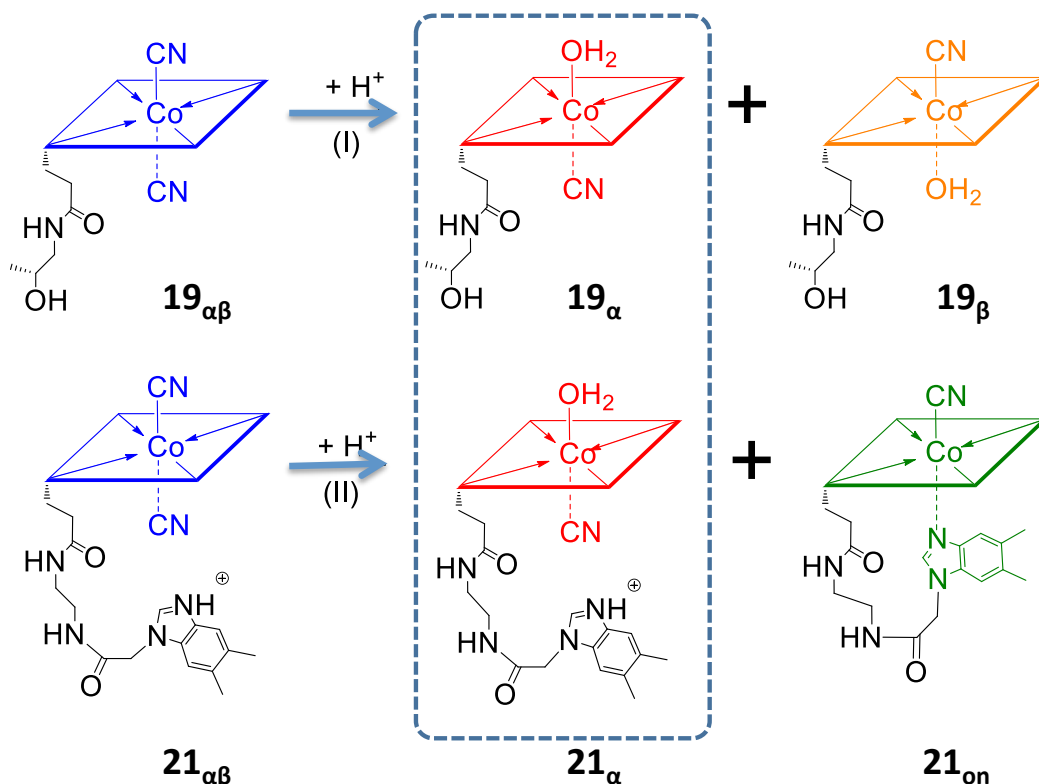


Figure 29: The comparison of three protocols for the synthesis of aquacyano cobinamide.^[131]

After the separation by preparative Reversed-phase HPLC, we shifted our interest to the identification of these two isomers. The two isomers have the same molecular mass and very similar absorption spectra, but distinctive NMR signals. The latter makes it possible to assign the configuration at the cobalt center of **19_α** and **19_β** by comparing their NMR spectra to a reference compound with known structure. The concept is shown in Scheme 10.



Scheme 10: (Top) Synthesis of 19_{α} and 19_{β} from $19_{\alpha\beta}$. (Bottom) Synthesis of 21_{α} and 21_{on} from $21_{\alpha\beta}$.^[132] Charges on the corrin rings have been omitted.

The reference compound α -cyano- β -aqua peptide B12 (21_{α}) was synthesized as a mixture with 21_{on} from dicyano peptide B12 ($21_{\alpha\beta}$) (Scheme 10, bottom). However, due to their difference in stability, the mixture of 21_{on} and 21_{α} will slowly change to pure 21_{on} (Scheme 10, bottom). This transformation can be monitored with both UV/vis and NMR spectra. Subtracting the NMR spectra of 21_{on} from the mixture of 21_{on} and 21_{α} leads to the spectrum of 21_{α} , which is the reference spectrum. We assumed that the NMR spectrum of the corrin was only affected by the axial ligands. Therefore, the NMR spectrum of 21_{α} was expected to be the same as 19_{α} in the corrin ring region, and thus 19_{α} could be identified. More detailed discussions are described in the paper attached in the end of the thesis (Appendix II).^[132]

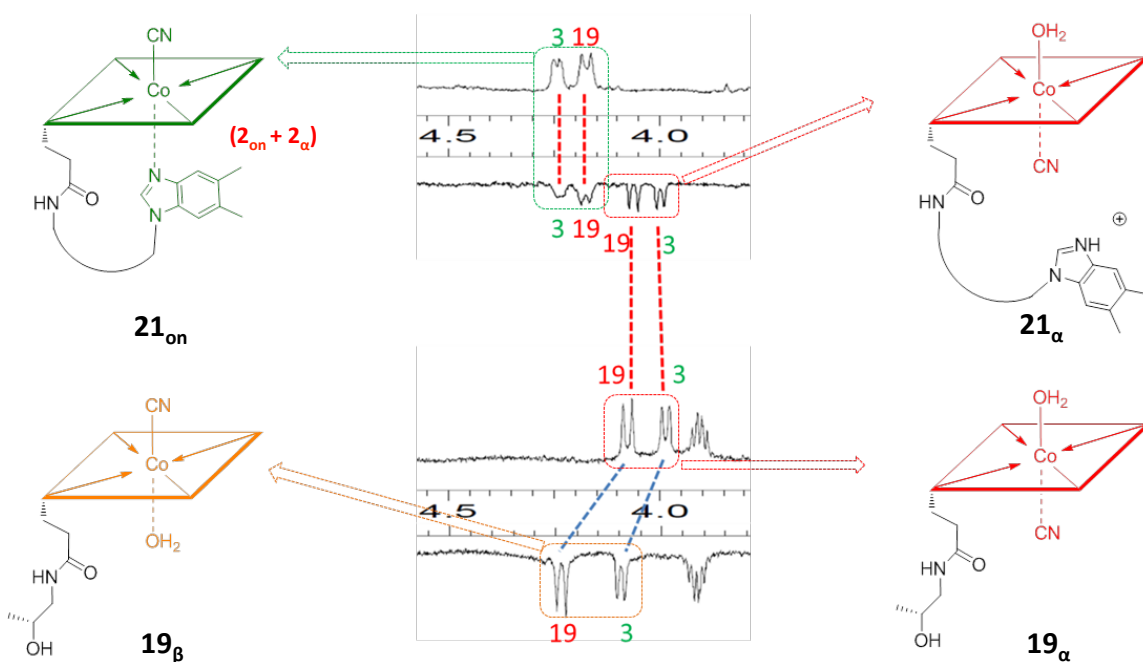


Figure 30: ¹H-NMR comparison of **21_α** and **19_α**. The arrows show the assignment of the peaks to the according compounds.^[132] Charges on the corrin rings have been omitted.

2.2.2 Some unexpected byproducts

Depending on the applied metal salts, different byproducts were detected by MS and/or NMR spectroscopy.

When ZnCl_2 was used as catalyst, byproducts with a 15 units higher m/z ratio than the expected aquacyano Cbi were observed (Figure 31, **23**, less than 5 % according to LCMS; only one out of six possible esters is shown). Further hydrolysis of this byproducts led to a 14 unit lower m/z value. The changes of the molecular masses fit with the chemical groups alternation from amide ($-\text{CONH}_2$, 44) to ester (COOCH_3 , 59) and finally to acid ($-\text{COOH}$, 45). It is well-known that amides react with alcohols to esters at high temperatures.^[133]

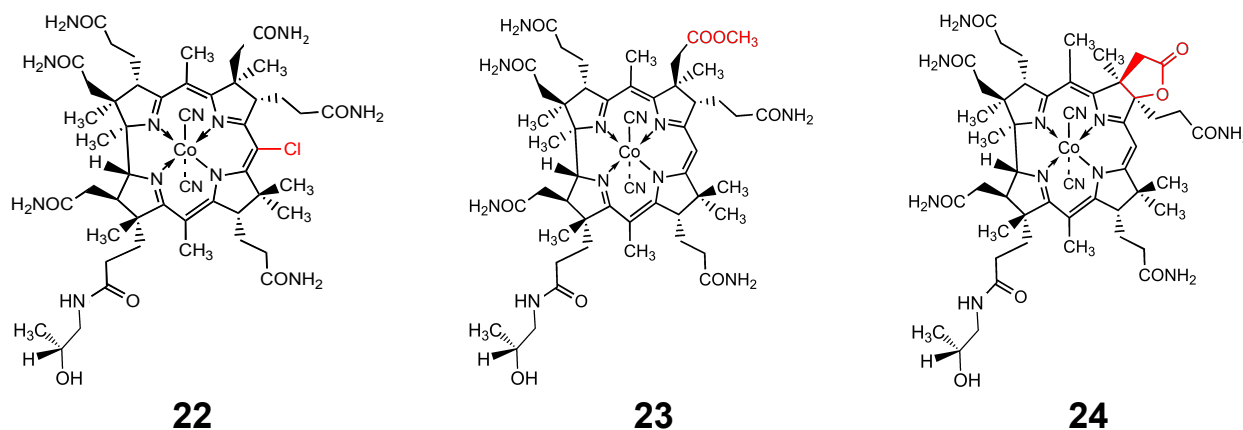
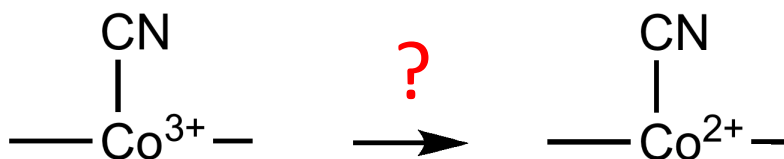


Figure 31: Three possible byproducts during the synthesis of Cbi.

C10-Cl Cbi (Figure 31, **22**) was observed when CuCl_2 was used as catalyst (C10-Cl Cbi : Cbi \approx 1 : 1, according to integrals of the molecule ion peak of the LCMS spectra). The formation of C10-Cl Cbi was deduced from mass and NMR spectra. An m/z ratio of 1049.5 fitted the pattern of substituting a hydrogen with chlorine, and ^1H NMR spectra further confirmed the missing H10 signal. Since C10-Cl Cbi was not observed with $\text{Cu}(\text{NO}_3)_2 \cdot 3\text{H}_2\text{O}$ or ZnCl_2 , we speculated that the chlorination is a combined effort of Cu^{2+} and Cl^- . UV/vis spectrum of the reaction mixture showed an absorption peak at 314 nm, which is characteristic peak for Co(II) species. Exposure of this solution to air led to the disappearance of this peak and showed a typical Co(III) species with an absorption peak at 350 nm. Although a redox mechanism is assumed, the mechanism

of reduction of cobalt is not clear yet (Scheme 11).



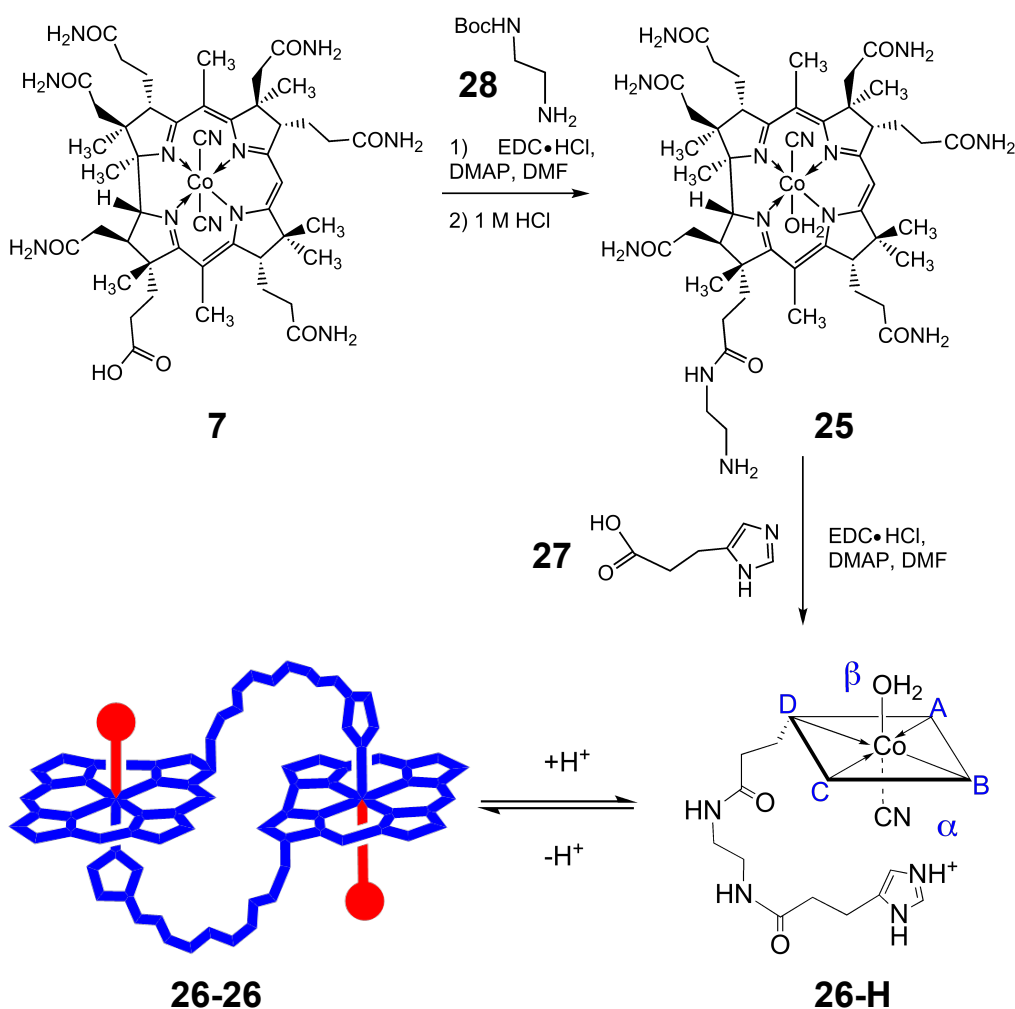
Scheme 11: Reduction of cobalt(III) to Co(II) during the formation of C10-Cl Cbi.

Lactone Cbi (Figure 31, **24**) is a minor byproduct, when $\text{Cu}(\text{NO}_3)_2 \cdot 3\text{H}_2\text{O}$ was applied (less than 5 %, according to the intensity ratio of Lactone Cbi and Cbi). This compound was proposed from a series of MS experiments. An m/z ratio of 1014.5 was first observed during the reaction, and after hydrolization the m/z ratio changed to 1032.6. This mass change is consistent with the cyclization and ring opening process. The common method for lactone formation of Cbi is the use of Chloramine T or bromine as oxidants to activate the cyclization and form the five-membered ring.^[134] In the case of $\text{Cu}(\text{NO}_3)_2$ the possible resource for the oxidant is the nitro group, but the detailed mechanism still needs to be further investigated.

2.3 Self-assembly of a B12 derivative with a flexible loop

Modified heme derivatives are capable to dimerize through side chain-metal interaction.^[117] Although hemes and corrinoids bear similar structures, the intermolecular coordination mode has not been reported for “complete” corrinoids yet. We believe that with careful design dimerization of corrinoids can be achieved, if the convenient intramolecular coordination is inhibited.

2.3.1 Synthesis and design of a loop-modified B12



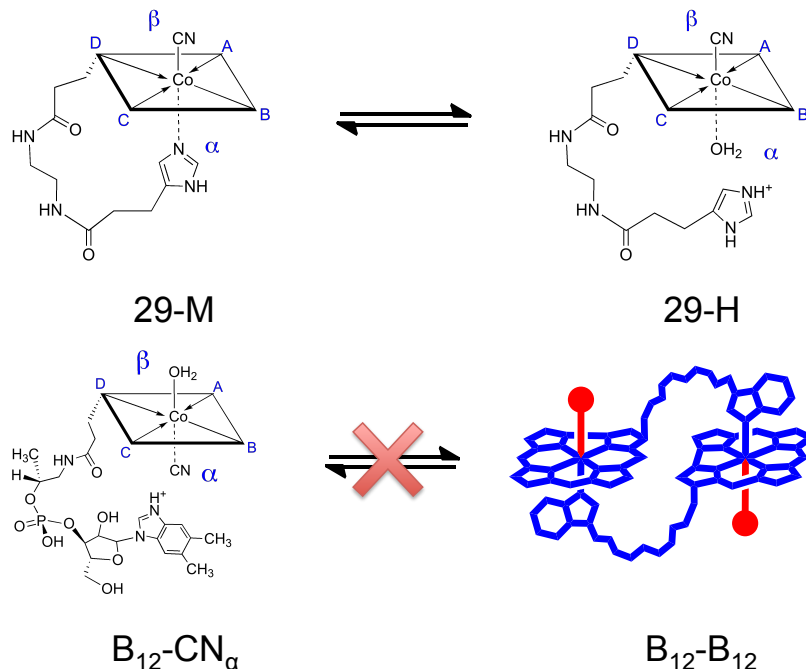
Scheme 12: Synthesis of compound **26-26**.^[135] Charges on the corrin rings have been omitted.

26-H was synthesized from dicyanocobyrinic acid with a yield of 38 % and then dimerized

to **26-26** (Scheme 12). The coordination environment at the cobalt center was proven with UV/vis spectroscopy (base on constitution) and ROESY NMR spectroscopy (β -coordinated imidazole ligand).^[135] The structure of **26-26** was deduced from a dilution experiment. We observed that the “base off” monomer was increasing at lower concentrated solution, which is a unique property of a dimer (multipliers are also possible, but they can be excluded. See part 3.2).

We investigated the configuration at the metal center as well as the artificial loop structure as a structural prerequisite for self-assembly in more detail. The former was tested with the α -aqua- β -cyano compound (**29-H**) which was synthesized with the same method as **26-H**, but they only coordinated intramolecularly (Scheme 13, **29-M**). The importance of the loop structure was proved by comparison with β -aqua- α -cyano B12 ($B_{12}\text{-CN}_\alpha$), which does not dimerise up to 1 mM (Scheme 13, down).

The details of this subject can be found in reference^[136] attached at the end (Appendix IV).



Scheme 13: (Up) “Base on/base off” equilibrium of compound **29-M**. (Down) $B_{12}\text{-CN}_\alpha$ does not dimerize in an “intra base off/ inter base on” fashion. Charges on the corrin rings have been omitted.

2.3.2 Thermodynamic investigations

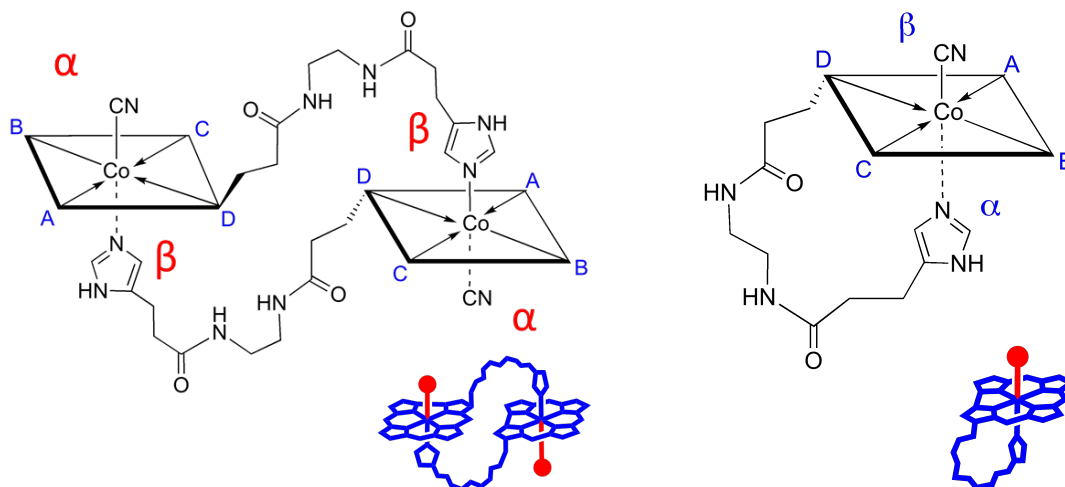
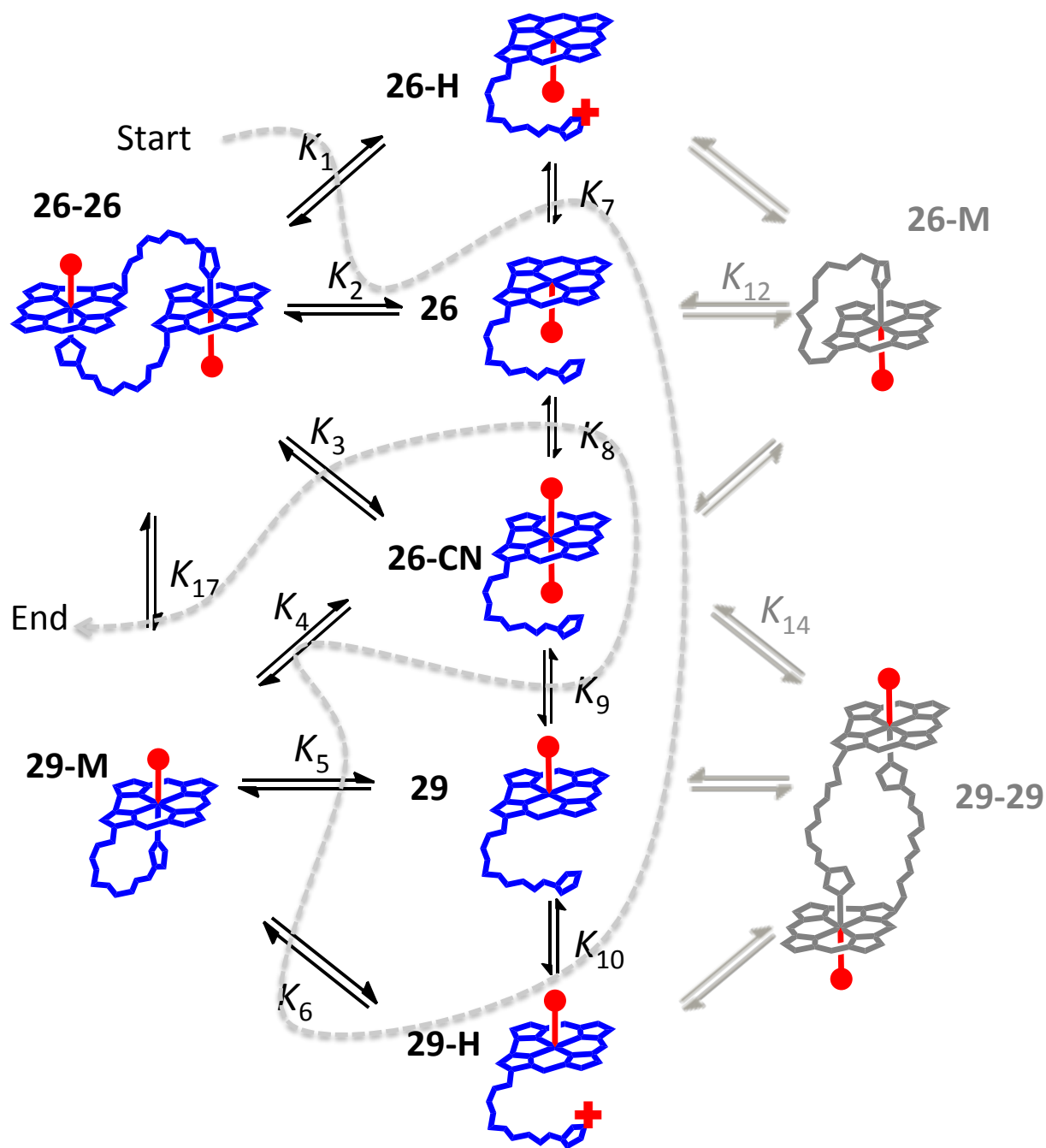


Figure 32: Structures of compound **26-26** (left) and **29-M** (right). Charges on the corrin rings have been omitted. The red dots indicate the cyanide ligands.

We did a thorough thermodynamic study of the “intra-base on” (Figure 32, right) and “inter-base on” (Figure 32, left) compounds with pH titration, cyanide titration, dilution experiments and theoretical calculations. The full equilibrium circle is shown in Scheme 14.

The grey dashed line (Scheme 14) shows the routine of calculation of the equilibria constants. K_1 , K_2 , K_4 and K_6 can be calculated from the experiments directly. K_7 can be derived from K_1 and K_2 . It's reasonable to assume that K_7 equals K_{10} , and with the experimental result of K_6 , we can calculate the value of K_5 . Combining K_5 and K_4 , K_9 can be easily deduced, which equals K_8 . Finally K_3 is calculated through K_2 and K_8 , and with K_4 , K_{17} can be calculated. The results are summarized in Table 2.



Scheme 14: Full equilibrium of compound **26** and **29**. **26-M** and **29-29** are hypothetical structures. The red crosses indicate the changes. The red dots indicate the cyanide ligands. Charges on the corrin rings have been omitted.

Table 2: Equilibrium constants:

Constant	Terms	Equilibrium constant
K_1	$[26-H]^2/[26-26][H]^2$	$7.95 \times 10^7 \text{ M}^{-1}$ [a]
K_2	$[26]^2/[26-26]$	$1.29 \times 10^{-6} \text{ M}$ [a]
K_3	$[26-CN]^2[H]^2/[HCN]^2[26-26]$	$2.67 \times 10^{-6} \text{ M}$ [b]
K_4	$[26-CN][H]/[29-M][HCN]$	5.40×10^{-4} [a]
K_5	$[29]/[29-M]$	3.65×10^{-4} [b]
K_6	$[29-M][H]/[29-H]$	$3.48 \times 10^{-4} \text{ M}$ [a]
K_7	$[26][H]/[26-H]$	$1.27 \times 10^{-7} \text{ M}$ [b]
K_8	$[26-CN][H]/[26][HCN]$	1.44 [b]
K_9	$[26-CN][H]/[29][HCN]$	1.44 [b] (1.83 [c], 0.38 [d])
K_{10}	$[29][H]/[29-H]$	$1.27 \times 10^{-7} \text{ M}$ [b]
K_{12}	$[26]/[26-M]$	/
K_{14}	$[26-CN]^2[H]^2/[HCN]^2[29-29]$	/
K_{17}	$[29-M]^2/[26-26]$	9.15 M [b]

a: experimental determined, b: calculated via the therodynamic cycle, c: reference [60], d: reference [136]

Calculation of the equilibrium constants K_1 and K_6

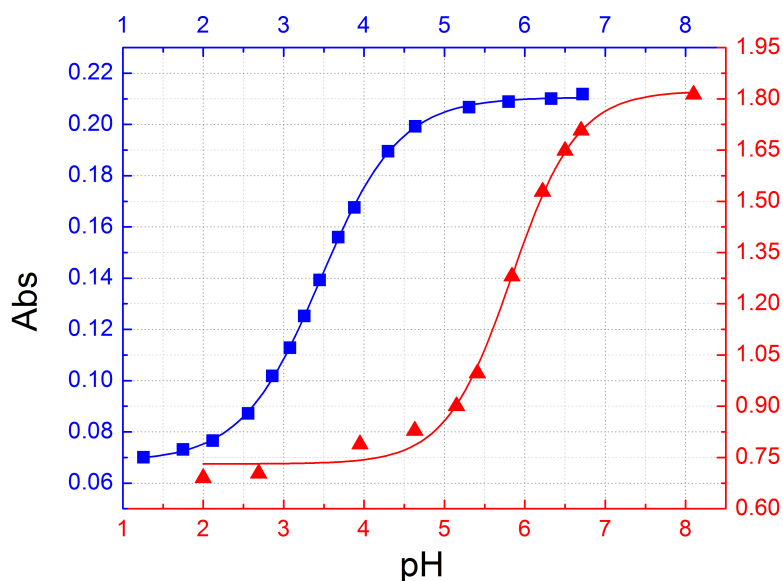


Figure 33: pH titration of monomer (**29-M**, blue) and dimer (**26-26**, red) in KCl solution (0.2 M) at 25° C.

Spectrophotometric pH titration method was applied to determine the $pK_{\text{base off}}$ value of **29-M** and **26-26** (Figure 33). By *Boltzmann* fitting of the titration curve, the $pK_{\text{base off}}$ values of compound **29-M** and **26-26** are 3.46 and 5.83, translating into binding constants K_6 and K_1 of $3.48 \times 10^{-4} \text{ M}^{-1}$ and $7.95 \times 10^7 \text{ M}^{-1}$ respectively.

Calculation of the equilibrium constants K_2

For the determination of the dissociation constant K_2 ($K_2 = [26]^2/[26-26]$), a series of solution with different total cobalt concentrations ($[\text{Co}]_{\text{total}}$) was prepared starting from **26-H** (in a Britton-Robinson buffer at pH 8): 174 μM , 49.3 μM , 35.1 μM , 17.4 μM , 9.79 μM and 4.44 μM . The total “cobalt concentration” ($[\text{Co}]_{\text{total}}$) of a compound was determined from the absorbance of the γ -band at 367-368 nm ($\epsilon_{\gamma}(367-368 \text{ nm}) = 3.04 \times 10^4 \text{ M}^{-1} \text{ cm}^{-1}$)^[112] after conversion of the corresponding corrinoid to the dicyano-compound **26-CN**.

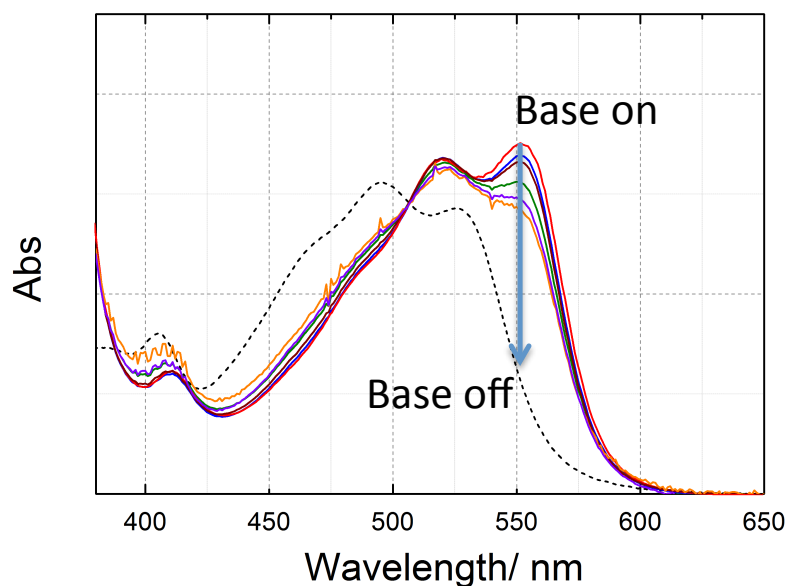


Figure 34: Normalized UV-vis spectra (to the intersection at 508 nm) of **26-26** ($[\text{Co}]_{\text{total}}$: 174 μM , (red)) and mixtures of **26-26** and **26** ($[\text{Co}]_{\text{total}}$: 49.3 μM (blue), 35.1 μM (brown), 17.4 μM (green), 9.79 μM (violet), 4.44 μM (yellow)). Black dashed line indicates the spectrum of **26-H** as a reference for the “base off” constitution.

It was analyzed as follows and the results are summarized in Table 3:

$$2[26 - 26] + [26] = [\text{Co}]$$

$$[26] = \frac{A_{26-26(551)} - A_{x(551)}}{A_{26-26(551)} - A_{26(551)}} \times [\text{Co}]$$

$$[26 - 26] = \frac{A_{x(551)} - A_{26(551)}}{A_{26-26(551)} - A_{26(551)}} \times [\text{Co}]/2$$

$$K_2 = \frac{[26]^2}{[26-26]} = \frac{(A_{26-26(551)} - A_{x(551)})^2}{(A_{x(551)} - A_{1(551)})(A_{26-26(551)} - A_{26(551)})} \times 2[\text{Co}]$$

Table 3: Calculation of the equilibrium constant K_2 at different total cobalt concentrations:

[Co] _{total}	17.4 μM	9.79 μM	4.44 μM	Average
$A_{26-26(551)}$	0.174	0.0979	0.0444	
$A_{26(551)}$	0.0677	0.0388	0.0175	
$A_{x(551)}$	0.155	0.0836	0.0367	
K_2 / M	1.35×10^{-6}	1.51×10^{-6}	1.02×10^{-6}	1.29×10^{-6}

The K_2 values were calculated from solutions with low total cobalt concentrations (17.4 μM, 9.79 μM and 4.44 μM), for which equilibria between **26-26** and **26** was explicitly observed. If the assumption of dimer is right, the K_2 values calculated from different concentrations should be same. As shown in Table 3, the consistency of K_2 values is very well. The average value of K_2 is $1.29 (\pm 0.27) \times 10^{-6} \text{ M}$.

$A_{26-26(551)}$ and $A_{26(551)}$ are the absorbance at 551 nm of pure **26-26** and **26** at the indicated total cobalt concentration and have been calculated with the corresponding extinction coefficients. The extinction coefficient of **26-26** is $\epsilon (551 \text{ nm}) = 2.00 \times 10^4 \text{ M}^{-1} \text{ cm}^{-1}$ and has been derived from the spectrum of **26-26** (87 μM).

It is reasonable to assume that the extinction coefficient of **26** is the same as for **26-H** at a wavelength above 250 nm. The imidazole base in either the protonated or deprotonated form has no UV/Vis absorbance above 250 nm and does not affect the π to π^* transitions of the corrin ring. The extinction coefficient of **26** is $\epsilon (551 \text{ nm}) = 3.96 \times 10^3 \text{ M}^{-1} \text{ cm}^{-1}$.

$A_{x(551)}$ represents the actual absorbance at 551 nm at the indicated concentration.

Calculation of the actual equilibrium constant K_4 and the hypothetical constant K_{14}

Cyanide titration experiments were performed to verify the existence of monomer **29-M** in solution and to exclude the presence of the hypothetical dimer **29-29** with an extraordinary stable “*intra* base-off/ *inter* base-on” coordination mode (Figure 35).

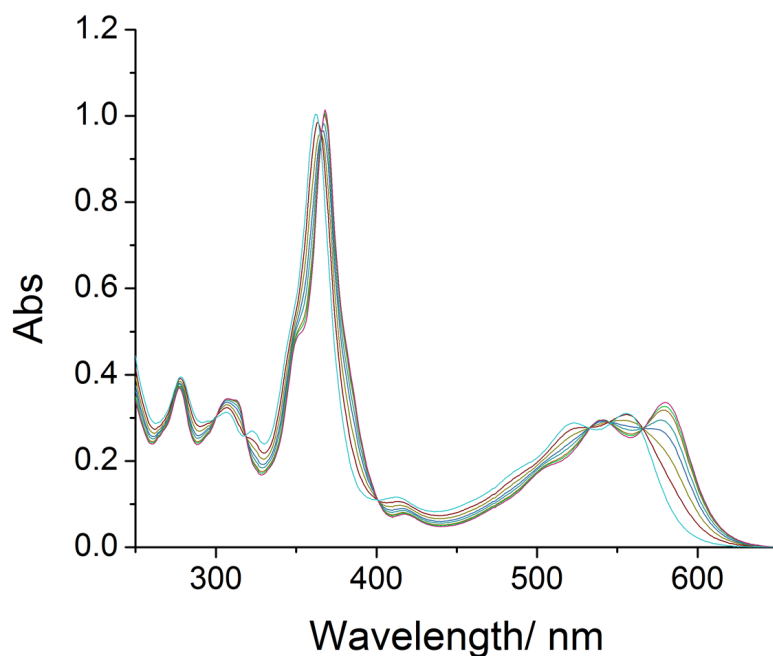


Figure 35: Cyanide titration (c_{CN} : 0 – 160 μM) of **29-M** (33.4 μM) at pH 10 (Britton-Robinson buffer).

Based on the experimental data, the binding constants K_4 and K_{14} were calculated and the consistency was tested (Table 4).

$$K_4 = \frac{[26 - \text{CN}][\text{H}]}{[29 - \text{M}][\text{HCN}]} = \frac{[26 - \text{CN}]K_{\text{HCN}}}{[29 - \text{M}][\text{CN}]}$$

$$K_{14} = \frac{[26 - \text{CN}]^2[\text{H}]^2}{[29 - 29][\text{HCN}]^2} = \frac{[26 - \text{CN}]K_{\text{HCN}}^2}{[29 - \text{M}][\text{CN}]^2}$$

Table 4: Calculation of the equilibrium constants K_4 and K_{14} at different cyanide concentrations:

$[\text{CN}]_0 / \mu\text{M}$	$[1\text{-CN}] / \mu\text{M}$	$[\text{CN}] / \mu\text{M}$	$[2\text{-M}] / \mu\text{M}$	K_4	$[29\text{-}29] / \mu\text{M}$	K_{14} / M
0	0	0	33.4	/	16.7	/
10	9.00	1.00	24.4	6.71×10^{-4}	12.2	21.9×10^{-12}
20	16.2	3.8	17.2	4.50×10^{-4}	8.6	6.96×10^{-12}
30	22.6	7.4	10.8	5.13×10^{-4}	5.4	5.73×10^{-12}
40	26.8	13.2	6.6	5.59×10^{-4}	3.3	4.14×10^{-12}
60	30.65	29.35	3.75	5.08×10^{-4}	1.88	1.92×10^{-12}
160	33.4	126.6	0	/	0	/

A solution of compound **29-H** ($c = 33.4 \mu\text{M}$; Britton-Robinson buffer, pH 10) was prepared in an UV/Vis cuvette (1 mL, 1 cm) and cyanide (0 - 160 μM) was added stepwise (Figure 35).

The total cyanide concentration ($[\text{CN}]_0 = [\text{CN}] + [26\text{-CN}]$, $[\text{CN}]$ indicates the concentration of “free” cyanide) is listed in Table 4. The actual concentration of **26-CN** can be calculated as follows:

$$[26 - \text{CN}] = \frac{A_{x(580)} - A_{29\text{-M}(580)}}{A_{26\text{-CN}(580)} - A_{29\text{-M}(580)}} \times 33.4 \mu\text{M}$$

If we assume monomeric **29-M** ($[29\text{-M}]_0 = 33.4 \mu\text{M}$), the actual concentrations of $[29\text{-M}]$ ($[29\text{-M}] = [29\text{-M}]_0 - [26\text{-CN}]$) and $[\text{CN}]$ in solution can be easily derived (Table 4). The consistency of the five calculated K_4 values from different concentrations (Table 4; blue) is very good and the average value is $5.40 (\pm 1.31) \times 10^{-4}$.

While assuming the hypothetical dimer **29-29** ($[29\text{-}29]_0 = 16.7 \mu\text{M}$), the calculated equilibrium constants (K_{14}) are not anymore in agreement (Table 4; red; The values of K_{14} vary from 1.92×10^{-12} to 21.9×10^{-12} , and the difference is over 11 times), which excludes this structural motif.

Calculation of equilibrium constants K_{10} , K_5 and K_9

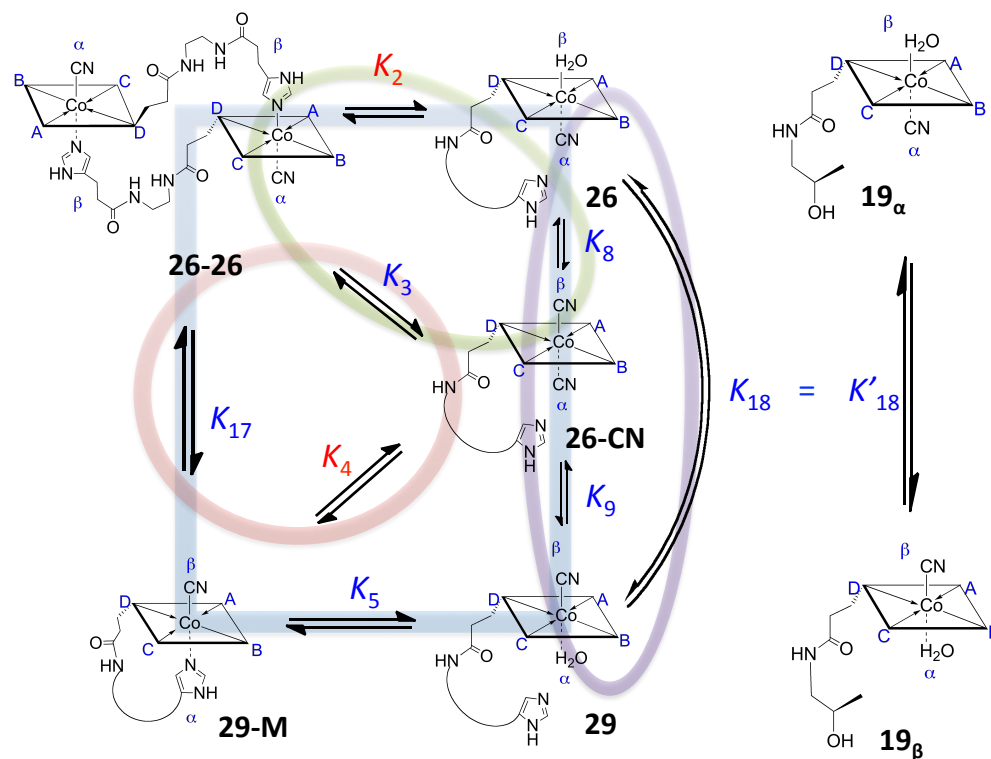
It is reasonable to assume that the acidity constants of the protonated imidazole

moieties of **26-H** and **29-H** are not affected by the appended corrin ring.^[136] Therefore, K_{10} is the same as K_7 (Scheme 14; $K_{7/10} = 1.27 \times 10^{-7}$). Under consideration of the thermodynamic cycle depicted in Scheme 14, the binding constants K_6 and K_{10} , the dissociation constant K_5 for the conversion of **29-M** to **29** with a non-protonated imidazole moiety can be calculated (Scheme 14; Table 2: $K_5 = K_{10}/K_6 = 3.65 \times 10^{-4}$).

With binding constants K_4 and K_5 , the binding constant K_9 for the coordination between cyanide and base-off **29** can be calculated to be 1.44 (Table 1: $K_9 = K_4/K_5$).

Calculation of the equilibrium constants K_{17} , K_3 and K_8

The equilibrium between dimer **26-26** and monomer **29-M** with the opposite constitution of the axially bound ligands ($K_{17} = [29-M]^2/[26-26]$) was calculated from the thermodynamic cycles depicted in Scheme 15 and the following considerations:



Scheme 15: (Left) Equilibria between **26**, **29**, **26-26**, **29-M** and **26-CN** and comparison of the equilibrium between **26** and **29** (K_{18}) with that of (right) **19_α** and **19_β** (K'_{18}). Experimentally determined and calculated constants are shown in red and blue, respectively. Charges on the corrin rings have been omitted.

The value of K_3 (Table 2, Scheme 15), which describes the formation of **26-CN** from **26-26** and cyanide can not be determined directly by cyanide titration, because of fast conversion of **26-26** to **29-M** (K_{17}) in the presence of catalytic amounts of cyanide.

Therefore, we applied a calculation via the thermodynamic cycles depicted in Scheme 15.

We assumed that the equilibrium between **26** and **29** ($K_{18} = [26]/[29]$) is the same as for **19 $_{\alpha}$** and **19 $_{\beta}$** ($K'_{18} = [19_{\alpha}]/[19_{\beta}] = 1^{[111,112]}$), because the dissociated imidazole base is expected not to influence cyanide coordination at the cobalt center. According to the violet colored thermodynamic cycle in Scheme 15 and the binding constant $K_9 = 1.44$ (Table 1), the binding constant K_8 is also 1.44 ($K_8 = K_9/K_{18}$). With K_8 and K_2 (Table 1; $K_2 = 1.29 \times 10^{-6}$ M), we can calculate K_3 ($K_3 = K_2 K_8^2 = 2.67 \times 10^{-7}$ M) following the green coloured thermodynamic cycle (Scheme 15). Finally, we can calculate K_{17} following either the red or blue coloured thermodynamic cycle. Both values of 9.15 and 10.6 M fit very well with each other (red: $K_{17} = K_3/K_4^2 = 9.15$ M; blue $K_{17} = K_2/K_{18}^2 K_5^2 = 10.6$ M) and demonstrated that dimer **26-26** is a kinetically trapped species. By monitoring the NMR spectra, we observed that the dimer could be stable for hours.

2.4 Biological studies of peptide B12 and B12 coenzyme derivatives

In part of project, we cooperated with Prof. Wolfgang Buckel from Marburg University and PD.Helmut Brandl from University of Zurich. Peptide B12 derivatives have potential applications as anti-vitamins in medicine. For this purpose, we wanted to prove that the artificial B12 derivatives are still biologically active but less active than B12.

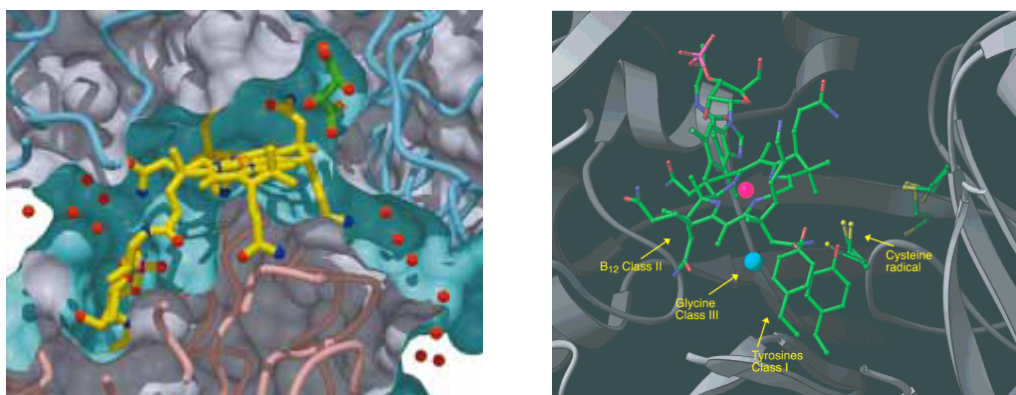


Figure 36: Crystal structures of AdoB12 in glutamate mutase^[21] (left) and ribonucleotide reductase^[137] (right).

We try to understand three key features through bioactivity tests with the peptide B12 derivatives, that are (i) transportation and cellular uptake of B12 derivatives, (ii) the affinity to the apo-enzymes and (iii) the activity of the enzyme. Enzymatic reactions that require the cofactor either in the “base on” or “base off/his on” constitutions were conducted with ribonucleotide reductase^[138] in *Lactobacillus delbrueckii*^[139] (*L. delbrueckii*) and glutamate mutase^[21,140] respectively (Figure 36).

L. delbrueckii (ATCC 7830) has ribonucleotide reductase as the only B12 dependent enzyme. With bacterial growth studies, we evaluated the combinational effect of the cellular uptake, transportation and enzyme activity.

Glutamate mutase is a B12-dependent enzyme which uses adenosylcobalamin to catalyze a reversible carbon skeleton rearrangement reaction between (S)-glutamate and (2S,3S)-3-methylaspartate. This is the first step of the fermentation of glutamate. The enzymatic activities of different cofactors such as backbone or β -ligand modified Cbls have been evaluated by this enzymatic reaction.

2.4.1 *L. delbrueckii* (performed by as well as together with PD. Helmut Brandl)

The experimental procedure is shown in Figure 37. It starts with a *L. delbrueckii* source, which is cultivated in a B12 broth.^[139] After 24 hours' of growth, 1 mL of this pre-culture (broth solution that contains active *L. delbrueckii*) is centrifuged and washed three times with sterilized NaCl solution (0.9 %) to totally remove the broth. Finally, the *L. delbrueckii* is suspended in 1 mL NaCl solution and injected to the each experimental tube as required (Figure 37).

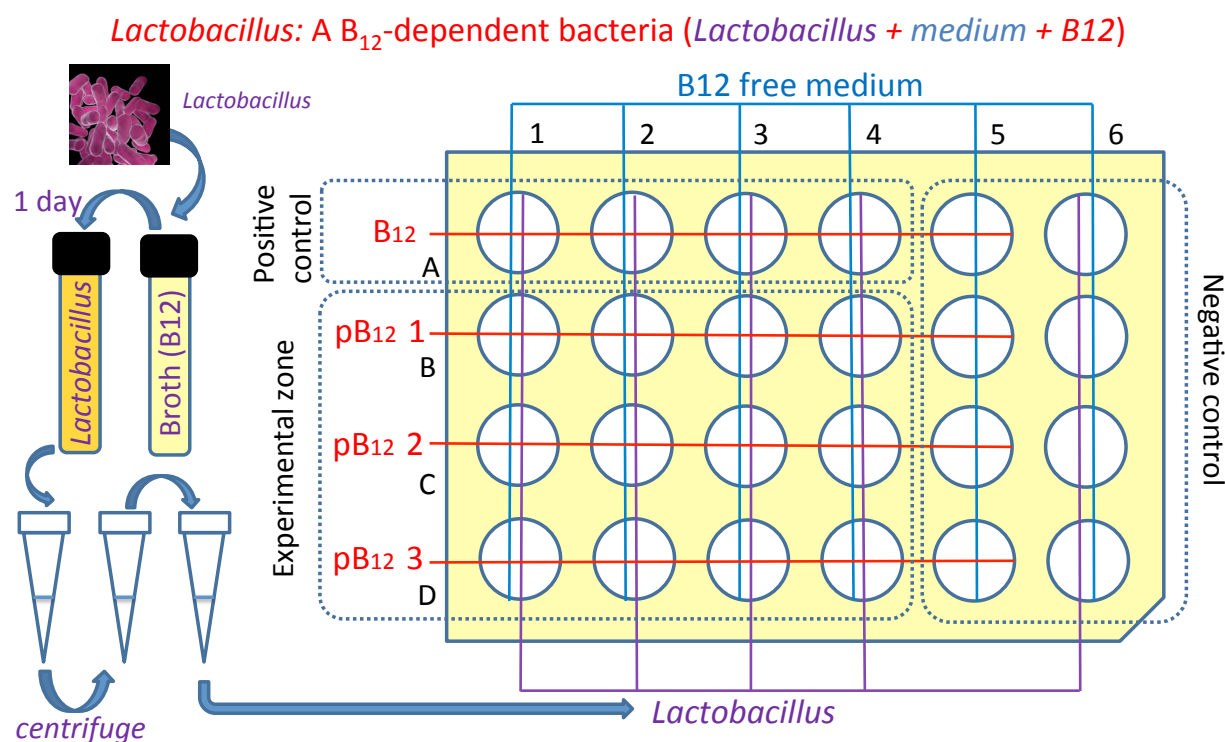


Figure 37: Representative procedures for the *L. delbrueckii* experiments.

The absorbance of each tube will be measured every 6 h and compared to a positive (B12) and a negative (Cbl free) control to evaluate the relative activity.

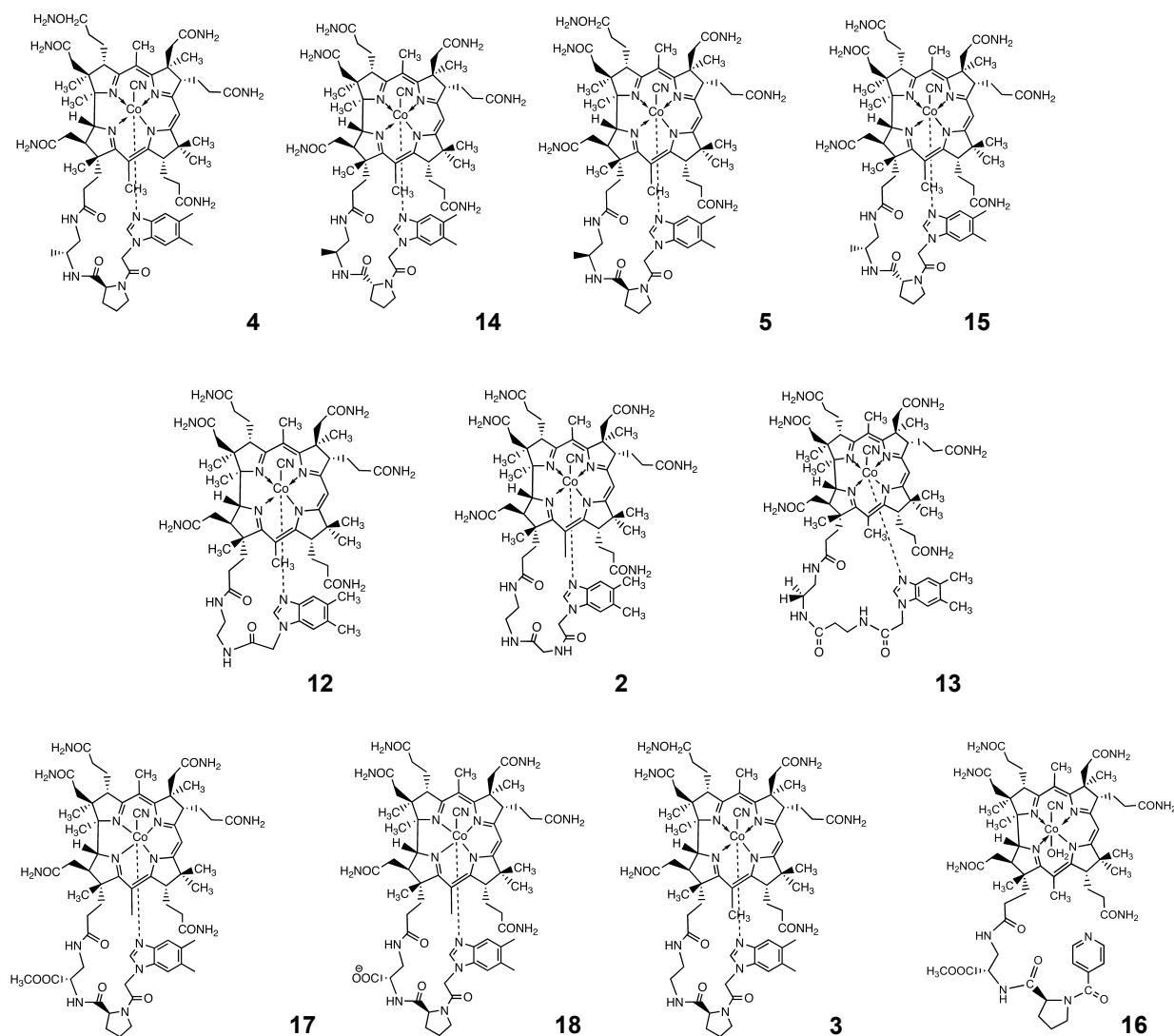


Figure 38: The structures of eleven tested peptide B12 derivatives. Charges on the corrin rings have been omitted.

We tested 11 peptide B12 derivatives (Figure 38), cobyrinic acid (**7**) and B12 (**1**) in these experiments and the results are summarized in Figure 39.

As shown in Figure 39, compound **2** - **5**, **12** - **14** and **17** were the most active ones from the preliminary studies. However, there is no clear connection between the base on stabilities and their bioactivities. Similar results have been observed by Toraya with methylene B12 derivatives tested with diol dehydratase^[58]. This is expected since multiple steps of uptake, transportation and metabolism are assumed to respond to the modification differently and the consequences are difficult to estimate. The important

information from this experiment is the positive results suggesting that the peptide B12 derivatives can still be recognized by multiple proteins and can catalyze the corresponding enzymatic reactions.

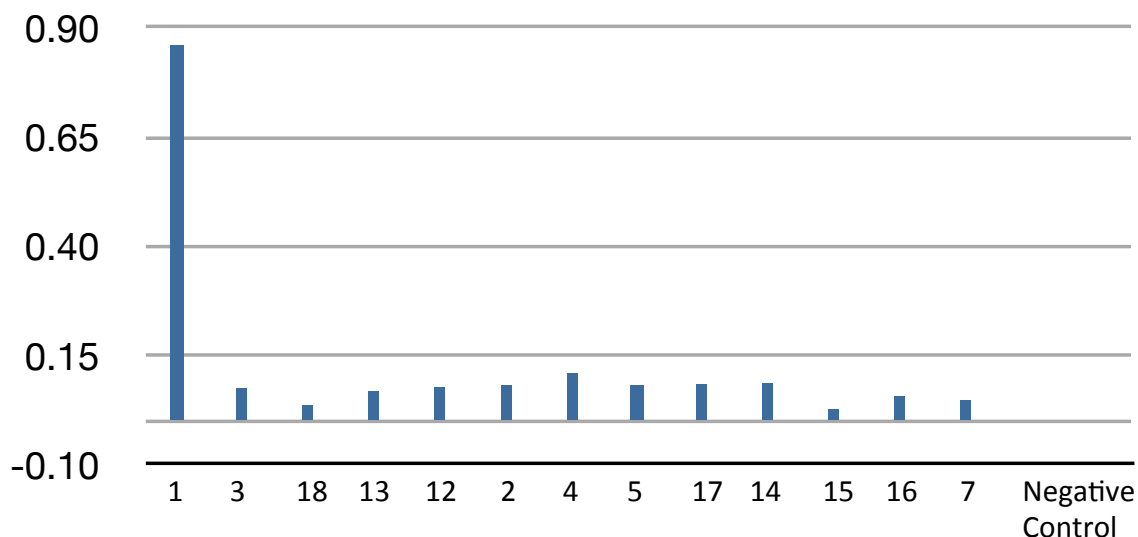


Figure 39: The absorbance value after 48 hours growth of *L. delbrueckii* with compound **1 - 5, 7, 12 - 18**. The last column is the negative control without any B12 derivatives and **1** is the positive control with B12. The absorbance is shown with the negative control as the base line (abs = 0).

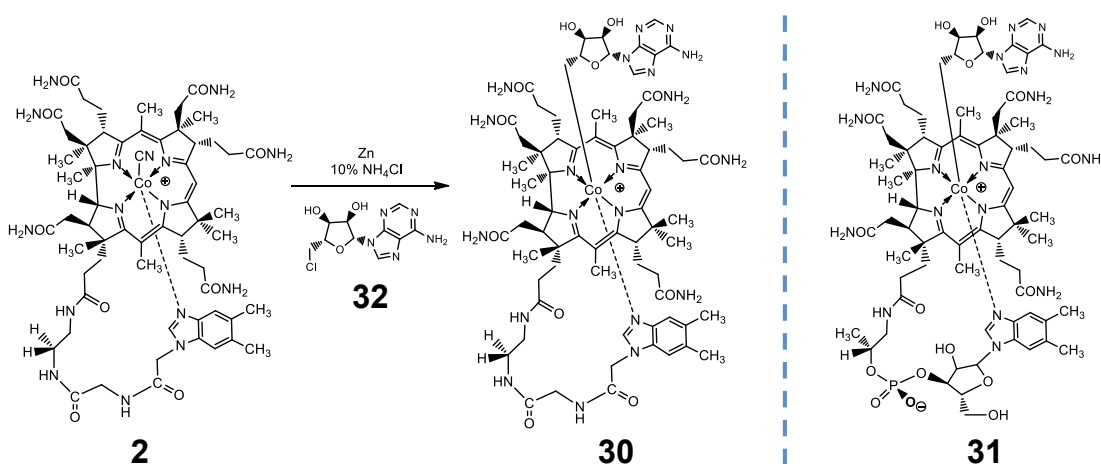
These results need to be further confirmed and additional competition experiments are planned.

2.4.2 Glutamate mutase

α -modified adenosyl peptide B12

We synthesized adenosyl peptide B12 to investigate the impact of the loop structure in the enzymatic reaction of glutamate mutase. The synthetic strategy is shown in Scheme 16. Peptide B12 (**2**) was reduced by Zn in a 10 % aqueous NH_4Cl solution and then reacted with 5'-Cl-5'-deoxy-adenosine (**32**) to give Ado-pB12 (**30**) with a yield of 55 %.

[76]



Scheme 16: Synthesis scheme of Adenosyl peptide B12 (**30**, left); AdoB12 (**31**, right).

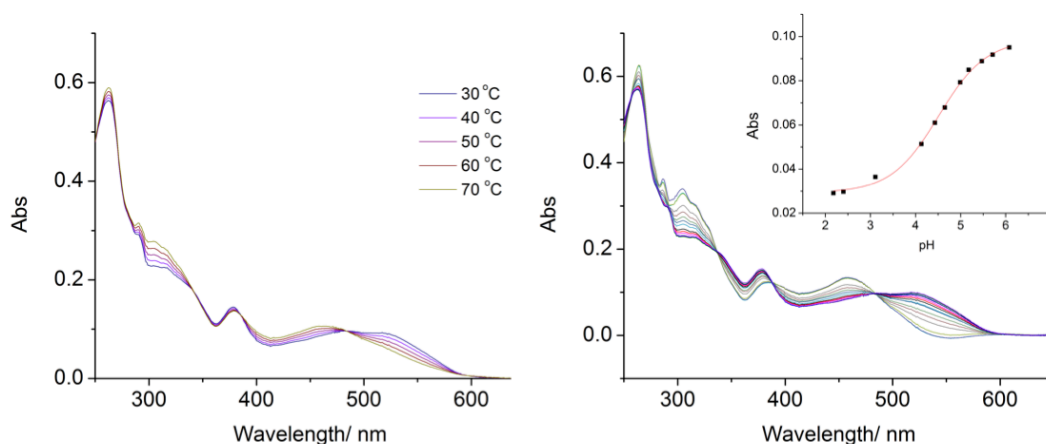


Figure 40: (left) Temperature dependent UV/vis spectra of **30** in KCl solution (0.2 M, pH 6.7); (right) pH titration of **30** in KCl solution (0.2 M) at 20 °C, inset: the absorbance at 517 nm v.s. the corresponding pH values.

The pH titration (Figure 40, right) shows that the $pK_{\text{base off}}$ value of **30** is 4.5, which is 0.8 unit higher than that of natural AdoCbl (**31**). By comparison of the pH titration spectra and the temperature dependent switch experiment of **30** (Figure 40, left), we can deduce the “base on/base off” proportion to be 1 at 70° C. By using the following equations 1 - 4, we got the values of ΔH_0 (- 31 kJ/mol) and ΔS_0 (- 86 J/molK). The ΔG value at 25 °C is -5.4 kJ/mol, which is slightly lower than the corresponding value of AdoCbl (-2.57 kJ/mol).^[54]

$$\text{Eq.1 } K_{\text{base off}} = (1 + K_{\text{on}}) K_{\text{bz}}$$

$$\text{Eq.2 } \Delta G = -RT \ln K_{\text{on}}$$

$$\text{Eq.3 } \Delta H_0 = \Delta G_{20} + T_{20} \Delta S_0$$

$$\text{Eq.4 } \Delta H_0 = \Delta G_{70} + T_{70} \Delta S_0$$

Enzymatic activity tests were conducted by Fredrick Edwin Lyatuu in cooperation with Prof. Wolfgang Buckel from Marburg University. The replacement of the loop caused a decrease of the enzymatic activity in proteins with different ratios of the GlmS and GlmE subunits to less than 10 % of the activity (k_{cat}) of the natural coenzyme (Table 5). The similar K_m values suggest that the coenzyme B12 (**31**) and peptidocoenzyme B12 (**30**) have close affinity to the glutamate mutase, but the lower catalytic efficiency (k_{cat}/K_m) might be caused by the detailed binding position change due to the interaction of the dissociated, artificial loop that affects the environment and this catalysis at the opposite site of the macrocycle.

Table 5: Comparison of the enzymatic activities between coenzyme B12 and peptide coenzyme B12 at different ratios of GlmS:GlmE:

	K_m (μM)		V_{max} (U/mg GlmE)		k_{cat} (s ⁻¹)		k_{cat}/K_m (s ⁻¹ M ⁻¹)	
	14	2	14	2	14	2	14	2
Coenzyme B12	0.52±0.06	1.12±0.04	1.39±0.40	1.39±0.40	1.24±0.36	1.24±0.36	2.38x 10 ⁶	1.10 x 10 ⁶
Peptidocoenzyme B12	0.35±0.05	1.07±0.04	0.10±0.01	0.13±0.01	0.09±0.01	0.12±0.01	2.57 x 10 ⁵	1.12 x 10 ⁵

Both biological studies showed that the peptide B12 derivatives (**2** and **30**) are still bioactive, either bound in “base on” or “base off/his on” constitutions. The results suggest a broad application of peptide B12, and the tests with other proteins are undergoing.

β -modified Cbls

This part of the project was also accomplished in cooperation with Prof. Buckel. The aim is to investigate the interaction of the upper ligand with the protein. We synthesized two compounds (Figure 41, **33** and **34**) as described in the experimental section.

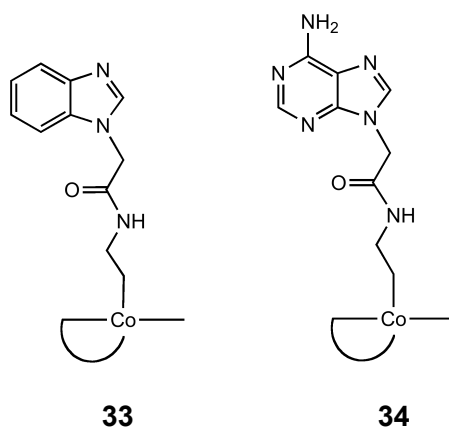


Figure 41: Structure of alkyl Cbl derivatives **33** and **34**.

Compound **33** and **34** kept the same number of atoms between the base and the cobalt center. These two compounds were tested with glutamate mutase, but were inactive. This behavior is reasonable because the radical upper ligand is the catalytically active species in the enzymatic reaction and small modification can result in the deactivation of the enzyme.^[76]

3. Conclusion and outlook

3.1 Peptide B12

We introduced a new class of vitamin B12 mimics with a peptide linker tethering the corrin macrocycle with the Dmbz base. Various modifications of the linker such as length, charge, stereochemistry and nature of the base have been discussed and analyzed in this thesis, providing a guideline for further structural modifications. Electrochemical and spectrophotometric studies with four different peptide B12 derivatives demonstrated that the appropriate design of the peptide backbone allows readjusting the coordination as well as the accompanying redox properties at the Co centre.

Initial results of peptide B12 analogs for biological applications with *L. delbrueckii* and glutamate mutase performed in cooperation with PD Helmut Brandl from University of Zurich and Fredrick Lyatuu and Prof. Wolfgang Buckel from the University of Marburg have demonstrated the deactivation effect of these backbone modified B12 derivatives in both “base on” and “base off/his on” enzymes. The interaction of this class of compound with the human transporting proteins transcobalamin II, intrinsic factor and haptocorrin are momentarily under investigation at the Paul Scherrer Institute.

Structural modification can be easily implemented into peptide B12 and a further increase of the base on stability accompanied by a lowering of the reduction potential are therefore expected in the near future. Peptide B12 with extraordinarily low reduction potentials of the Co(III)/Co(II) couple are very promising to suppress the enzymatic activities of “base on” enzymes. Presumably, additional factors have to be considered. The introduction of additional stabilizing hydrogen bonds in the loop part, which assists intramolecular coordination, is proposed. Another strategy is to intra-cross link the loop part with covalent bonds. If preorganization to the base on form is correct, this approach will greatly impede the reverse opening to the base-off form.

Apart from the improvement of the coordination properties, high binding constants to the related enzymes are critical, especially for biological studies. Further modifications of

the side chains of the loop part such as increasing the number of hydrogen bond donors for stabilizing interactions with the protein are proposed. This strategy might help to block the natural cofactor and suppress the corresponding enzymatic activities.

3.2 Diastereomers of aquacyano cobinamides and intercoordinated Cbls

We identified $\text{Cu}(\text{NO}_3)_2 \cdot 3\text{H}_2\text{O}$ and ZnCl_2 in MeOH as a useful one-step alternative for the preparation of aquacyano cobinamides from B12. Advantages of these reagents compared to the well-established $\text{Ce}(\text{OH})_3$ and $\text{CF}_3\text{SO}_3\text{H}$ methods is the shorter reaction time and the simplified work-up procedure. Further improvement of the synthesis method could be focused to lower the reaction temperature and perform the reaction in water instead of methanol.

We applied a new backbone-modified vitamin B12 derivative with an unusual configuration at the cobalt center for the identification of the two axial diastereomers of aquacyano cobinamides (Cbi) with ^1H NMR spectroscopy. Kinetic studies of the coordination of cyanide to the isolated diastereomers of aquacyano cobinamides are momentarily under investigation by my colleague Christine Männel-Croisé.

On the basis of the above mentioned studies, we developed a self-complementary, artificial B12 derivative that dimerizes in an unprecedented “intra base off/inter base on” mode. It was demonstrated that this novel coordination motif depends on both, the configuration at the metal centre as well as the flexibility of the artificial, connecting linker. We envisage constructing dimers with even more sophisticated loop structures which could be applied as molecule receptors or hosts to selectively bind certain guest molecules into the cavity of the macrocycle.

4 Experimental procedures

All chemicals were of reagent grade and used without further purification.

Deuterated solvents were obtained from Armar Chemicals (Döttingen, Switzerland).

Chromafix C18ec for solid phase extraction (SPE) was obtained from Macherey Nagel.

In general the compound was dissolved in little water, transferred to the adsorbent, washed with water and eluted with MeOH.

HPLC solvents were 0.1 aqueous trifluoroacetic acid (A) and methanol (B). HPLC analyses were performed on a Merck-Hitachi L-7000 system equipped with a diode array UV-Vis spectrometer and Macherey Nagel Nucleosil C-18ec RP columns (5 μm particle size, 100 Å pore size, 250 x 3 mm. Flow rate: 0.5 ml min⁻¹). Preparative HPLC separations were performed on a Varian Prostar system equipped with two Prostar 215 pumps, a Prostar 320 UV/Vis detector and Macherey Nagel Nucleosil C-18ec RP columns (7 μm particle size, 100 Å pore size, 250 x 40 mm. Flow rate: 40 ml min⁻¹).

UV-Vis spectra were recorded on a Cary 50 spectrometer using quartz cells with a path length of 1 cm. The $pK_{\text{base-off}}$ values were obtained from the analysis of a Boltzmann function: $y = A2 + (A1 - A2) / (1 + \exp((x - x0) / dx))$ fitting.

NMR spectra were recorded on a Bruker AV-500 spectrometer (Karlsruhe, Germany) or a Varian OXFORD NMR 200. The chemical shifts are given in ppm relative to the signal from the deuterated solvent. Coupling constants J are given in Hz. The data processing was carried out with ACD/SpecManager (Advanced Chemistry Development).

Mass spectra were recorded either in the positive or negative mode on an Esquire HCT from Bruker (Bremen, Germany).

CV spectra were recorded with a 757 VA computrace electrochemical analyzer (Ω , Metrohm).

UPLC solvents were 0.1% aqueous formic acid (C) and acetonitrile (D). UPLC measurements were performed on an Acquity™ Ultra performance LC and ACQUITY UPLC® BEH C18 column (1.7 μm 2.1x50mm; flow rate: 0.5 ml min⁻¹). The UPLC gradient was: 7 % D for 0.1 min, then in 2.9 min to 17 % D, then in 1 min to 100 % D, and finally 100% D for 1 min.

High-resolution electrospray mass spectra were recorded on a Bruker maXis QTOF-MS instrument (Bruker Daltonics GmbH, Bremen, Germany). The samples were dissolved

in MeOH and analyzed via continuous flow injection at 3 $\mu\text{L}/\text{min}$. The mass spectrometer was operated in positive ion mode with a capillary voltage of 4 kV, an endplate offset of -500 V , nebulizer pressure of 5.8 psig, and a drying gas flow rate of 4 L/min at 180°C . The instrument was calibrated with a sodium formate solution (500 μl H_2O : 500 μl iPrOH : 20 μl HCOOH : 20 μl 0.1M NaOHaq). The resolution was optimized at 30'000 FWHM in the active focus mode. The accuracy was better than 2 ppm in a mass range between m/z 118 and 1600. All solvent used were purchased in best LC-MS qualities.

4.1 Experimental procedures

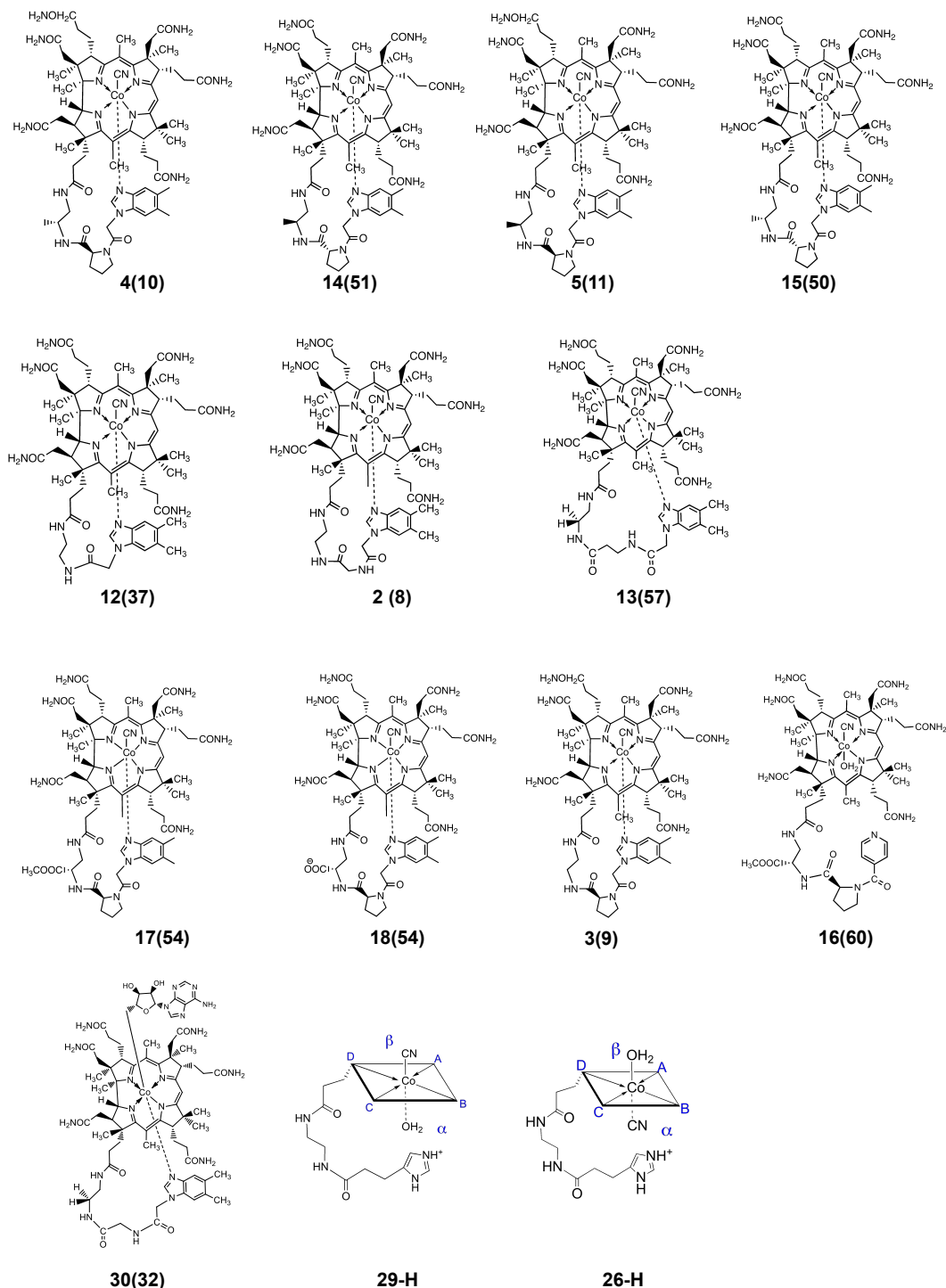


Figure 42: The structures of B12 derivatives (The numbers in the brackets indicate the related loop compounds or the β -ligands). Charges on the corrin rings have been omitted.

Compound 2. **7** (4.9 mg, 5.0 μ mol) was dissolved in dry DMF (1 mL) and cooled to 0°C, after which 4-dimethylaminopyridine (DMAP, 1.0 mg, 8.0 μ mol) and **8** (3.4 mg, 10 μ mol) were added. After 10 min, N-(3-Dimethylaminopropyl)-N'-ethylcarbodiimide hydrochloride (EDC·HCl, 3.0 mg, 15 μ mol) was added and the solution was allowed to warm up to room temperature. After 4 h, the solvent was removed under reduced pressure and the residue was washed with acetone. The mixture was further purified by preparative HPLC to afford **2** (**2**⁺·**CF₃COO**⁻) (4.2 mg, 3.4 μ mol, 62 %).

¹H-NMR (see Table 6).

UV/Vis (c = 0.30 mM, 0.2 M KCl, pH = 5.98): 550 nm (3.95), 520 nm (3.89), 411 nm (3.55), 362 nm (4.45), 322 nm (3.91), 304 nm (3.99), 279 nm (4.24).

HR-MS: [M]⁺ calcd for C₆₁H₈₄CoN₁₆O₉: 1243.59337, found: 1243.59334.

HPLC-UV/Vis: R_t = 14.5 min

Compound 3. **7** (4.9 mg, 5.0 μ mol) was dissolved in dry DMF (1 mL) and cooled to 0°C before NEt₃ (10 μ L, 70 μ mol) and ethylchloroformate (5 μ L, 55 μ mol) were added. After 1 min, N-Boc-ethylenediamine (16 mg, 0.10 mmol) was added and the reaction was quenched with water after 10 min. The crude product (**41**) was precipitated with acetone, filtrated, dissolved in HCl (1 mL, 1 M) and stirred for 1 h. The solution was lyophilized to yield **25**. The intermediate **25** was dissolved without further purification in DMF (1 mL) and cooled to 0°C, after which DMAP (1.0 mg, 8 μ mol) and **9** (4.5 mg, 15 μ mol) were added. After 10 min, EDC·HCl (3.0 mg, 15 μ mol) was added. The solution was allowed to warm up to room temperature and the solvent was removed under reduced pressure after 4 h. The residue was washed with acetone and further purified with preparative HPLC to afford **3** (**3**⁺·**CF₃COO**⁻) (3.2 mg, 2.3 μ mol, 46 %).

¹H-NMR (see Table 6).

UV-Vis (c = 0.28 mM, 0.2 M KCl, pH = 5.98): 549 nm (3.93), 520 nm (3.91), 411 nm (3.57), 361 nm (4.44), 323 nm (3.90), 279 nm (4.27).

HR-MS: [M]⁺ calcd for C₆₄H₈₈CoN₁₆O₉: 1283.62467, found: 1283.62422.

HPLC-UV-Vis: R_t = 16.7 min

Compound 4. 10 (3.5 mg, 6.0 μmol) and DMAP (1.8 mg, 15 μmol) were dissolved in DMF (0.1 mL). The reaction was stirred for 3 days at room temperature before **7** (4.9 mg, 5.0 μmol) dissolved in DMF (1.5 mL) was added. The reaction was cooled down to 0°C before EDC·HCl (8.0 mg, 40 μmol) was added. The solution was allowed to warm up to room temperature. After 4 h, the solvent was removed under reduced pressure. The residue was further purified by preparative HPLC to afford **4** (**4**⁺**CF₃COO**⁻) (3.0 mg, 2.1 μmol , 42 %).

¹H-NMR, ¹³C-NMR: (see Table 6)

UV/Vis (c = 0.32 mM, 0.2 M KCl, pH = 5.98): 551 nm (3.96), 520 nm (3.91), 411 nm (3.58), 362 nm (4.47), 323 nm (3.90), 279 nm (4.23).

HR-MS: [M]⁺ calcd for C₆₅H₉₀CoN₁₆O₉: 1297.64032, found: 1297.63949.

HPLC-UV-Vis: R_t = 17.8 min

Compound 5. The synthesis was performed with **11** (7.0 mg, 12 μmol) and **7** (4.9 mg, 5.0 μmol) as described for **4** to yield **5** (**5**⁺**CF₃COO**⁻) (5.6 mg, 4.0 μmol , 80 %).

¹H-NMR: (see Table 6)

UV/Vis (c = 0.33 mM, 0.2 M KCl, pH = 5.98): 551 nm (3.94), 520 nm (3.89), 409 nm (3.73), 362 nm (4.44), 322 nm (3.96), 279 nm (4.24).

HR-MS: [M]⁺ calcd for C₆₅H₉₀CoN₁₆O₉: 1297.64032, found: 1297.63997.

HPLC-UV-Vis: R_t = 17.2 min

Synthesis of 12. Intermediate **25** was synthesised from dicyanocobyrinic acid (4.9 mg, 5.0 μmol) as described in compound **3**. It was dissolved in DMF (1 mL) and cooled to 0°C, after which DMAP (1.0 mg, 8 μmol) and **7** (4.5 mg, 15 μmol) were added. After 10 min, EDC·HCl (3.0 mg, 15 μmol) was added. The solution was allowed to warm up to room temperature. After 4 h the solvent was removed under reduced pressure. The residue was washed with acetone and further purified with preparative HPLC to afford **12** (3.8 mg, 2.9 μmol , 58 %) as the corresponding TFA salt.

¹H NMR (500 MHz, [D₂]D₂O): (see Table 8) HR-MS: [M]⁺calcd for C₅₉H₈₁CoN₁₅O₈: 1186.57191, found: 1186.57087; UV/Vis (c = 30 μM , 0.2 M KCl, pH = 5.98): 548 nm

(3.96), 521 nm (3.94), 413 nm (3.72), 361 nm (4.43), 279 nm (4.27), HPLC-UV/Vis: R_t = 14.2 min; $pK_{\text{base-off}}$ = 2.58.

Compound 13. **7** (5 mg, 5 μmol) was dissolved in dry DMF (1 mL) and cooled to 0°C, after which 4-dimethylaminopyridine (DMAP, 1.0 mg, 8.0 μmol) and **57** (6 mg, 19 μmol) were added. After 10 min, N-(3-Dimethylaminopropyl)-N'-ethylcarbodiimide hydrochloride (EDC·HCl, 3.0 mg, 15 μmol) was added and the solution was allowed to warm up to room temperature. After 7 h, the solvent was removed under reduced pressure and the residue was washed with acetone. The mixture was further purified by preparative HPLC to afford **13** (**13**⁺·**CF₃COO**⁻) (2.1 mg, 1.6 μmol , 32 %).

¹H-NMR (see Table 7).

MS (ESI-MS): m/z (%): 1257.6 (100) [M]⁺.

HPLC-UV-Vis: R_t = 15.7 min

Compound 14. **51** (5.0 mg, 8.6 μmol) and DMAP (5.0 mg, 41 μmol) were dissolved in DMF (0.2 mL). The reaction was stirred at room temperature for 2 days (to remove the Fmoc protecting group) before **7** (4.0 mg, 4.0 μmol) dissolved in DMF (2 mL) was added. The reaction was cooled down to 0°C before EDC·HCl (6.0 mg, 30 μmol) was added. The solution was allowed to warm up to room temperature. After 4 h, the solvent was removed under reduced pressure. The residue was further purified by preparative HPLC to afford **14** (**14**⁺·**CF₃COO**⁻) (2.4 mg, 1.7 μmol , 43 %).

¹H-NMR: (see Table 7)

MS (ESI-MS): m/z (%): 1297.8 (100) [M]⁺.

HPLC-UV-Vis: R_t = 16.5 min

Compound 15. **50** (5.0 mg, 8.6 μmol) and DMAP (4.0 mg, 33 μmol) were dissolved in DMF (0.2 mL). The reaction was stirred for 2 days at room temperature before **7** (5.0 mg, 5.0 μmol) dissolved in DMF (2 mL) was added. The reaction was cooled down to 0°C before EDC·HCl (8.0 mg, 40 μmol) was added. The solution was allowed to warm up to room temperature. After 6 h, the solvent was removed under reduced pressure. The residue was further purified by preparative HPLC to afford **15** (**15**⁺·**CF₃COO**⁻) (2.3 mg, 1.8 μmol , 36 %).

¹H-NMR: (see Table 7)

MS (ESI-MS): m/z (%): 1297.8 (100) [M]⁺.

HPLC-UV-Vis: R_t = 16.3 min

Compound 16. 7 (4 mg, 4 μmol) was dissolved in dry DMF (1 mL) and cooled to 0°C, after which 4-dimethylaminopyridine (DMAP, 1.0 mg, 8.0 μmol) and **60** (3 mg, 9.4 μmol) were added. After 10 min, N-(3-Dimethylaminopropyl)-N'-ethylcarbodiimide hydrochloride (EDC·HCl, 4.0 mg, 20 μmol) was added and the solution was allowed to warm up to room temperature. After 6 h, the solvent was removed under reduced pressure and the residue was washed with acetone. The mixture was further purified by preparative HPLC to afford **16** (**16**⁺·**CF₃COO**⁻) (3.2 mg, 2.3 μmol, 58 %).

¹H-NMR (not characterised).

MS (ESI-MS): m/z (%): 1260.8 (100) [M]⁺.

HPLC-UV-Vis: R_t = 15.0 min

Compound 17. 7 (10 mg, 10 μmol) was dissolved in dry DMF (2 mL) and cooled to 0°C, after which 4-dimethylaminopyridine (DMAP, 2.0 mg, 16.0 μmol) and **54** (6 mg, 15 μmol) were added. After 10 min, EDC·HCl (8.0 mg, 40 μmol) was added and the solution was allowed to warm up to room temperature. After 3 h, the solvent was removed under reduced pressure and the residue was washed with acetone. The mixture was further purified by preparative HPLC to afford **17** (**17**⁺·**CF₃COO**⁻) (5.5 mg, 3.8 μmol, 38 %).

¹H-NMR (see Table 7).

MS (ESI-MS): m/z (%): 1341.9 (100) [M]⁺.

HPLC-UV-Vis: R_t = 16.0 min

Compound 18. 17 (1 mg, 0.7 μmol) and KCN (5 mg) were dissolved in H₂O (2 mL), and the solution was stirred for 2 h at 50 °C. The solution was purified by C18 filter to afford **18** (1 mg, 0.7 μmol, 100%).

¹H-NMR (see Table 7).

MS (ESI-MS): m/z (%): 1327.7 (100) [M+H]⁺.

HPLC-UV-Vis: R_t = 14.5 min

Synthesis of 19_{α} and 19_{β} . $19_{\alpha\beta}$ (20.8 mg, 20 mmol) was dissolved in 0.1% aqueous TFA (10 mL) and the reaction solution was stirred for 10 min. 19_{α} (10.1 mg, 8.8 mmol, 44 %) and 19_{β} (10.3 mg, 9.0 mmol, 45 %) were separated by preparative HPLC as the corresponding TFA salts.

^1H NMR (500 MHz, $[\text{D}_2]\text{D}_2\text{O}$): (see Table 8); MS (ESI-MS): m/z (%): 1015.6 (100) $[\text{M} - \text{H}_2\text{O}]^+$; HPLC-UV/Vis: $R_t = 8.8$ min (19_{α}), $R_t = 13.5$ min (19_{β}).

Compound 30: compound **2** (2 mg, 0.0015 mmol) was dissolved in an aqueous NH_4Cl solution (10 %; 5 ml). The solution was purged with argon for 20 min. Zn pellets (1 g) were washed with an aqueous HCl solution (3 ml, 1 M) freshly and were added to the reaction mixture in two portions. After 1 h, the chloro-precursor **32** (1.2 mg, 0.0042 mmol) was added and the reaction was stirred for 24 h under protection from light. The zinc pellets were filtered off and it was separated by preparative reverse phase HPLC in a dark room to afford **30** (0.8 mg; 0.00051 mmol, 34%).

^1H -NMR: see table 9

HPLC-UV-vis: 15.6 min

MS (ESI-MS): m/z (%): 1467.8 (100) $[\text{M}]^+$

Compound 26-26 and 29-M: Dicyanocyclopropanecarboxylic acid (**7**, 9.8 mg, 10 μmol) was dissolved in dry DMF (2 mL) and cooled to 0 °C before DMAP (3.0 mg, 2.5 μmol) and EDC·HCl (9.0 mg, 45 μmol) was added. After 5 min, *N*-Boc-ethylenediamine (**28**, 16 mg, 0.10 mmol) was added and the reaction was allowed to warm up to room temperature. After 6 hours, the solvent was removed under reduced pressure and it was precipitated with acetone. The precipitate was dissolved in aqueous HCl (3 mL, 1 M) and it was stirred for 3 h. The solution was lyophilized to yield crude **25**. The latter was dissolved in DMF (1 mL) and it was cooled to 0°C, after which DMAP (1.0 mg, 8 μmol) and deamino histidine (**27**, 4.5 mg, 15 μmol) were added. After 10 min, EDC·HCl (3.0 mg, 15 μmol) was added. The solution was allowed to warm up to room temperature. It was stirred for 10 h and the solvent was removed under reduced pressure. The residue was washed with acetone and further purified with preparative HPLC to afford **26-H** (5.2 mg, 3.8

μmol , yield: 38 %) and **29-H** (5.6 mg, 4.1 μmol , yield: 41 %) as TFA salts. **26-26** and **29-M** are derived from **26-H** and **29-H** in water at pH 8.1 and pH 6.9, respectively.

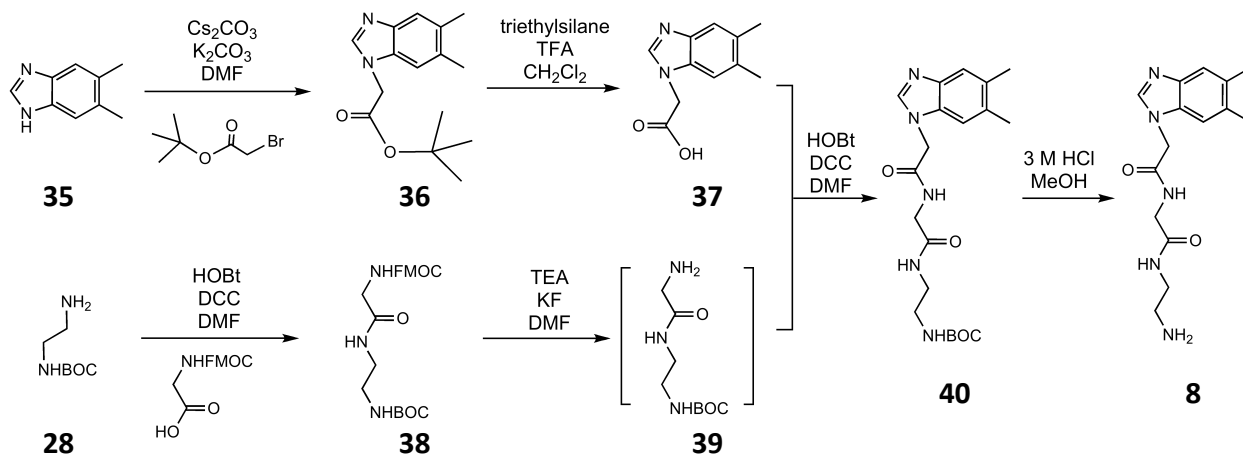
UPLC-UV-vis: $R_t = 0.9$ min (**26-H**) and $R_t = 1.7$ min (**29-H**)

$^1\text{H-NMR}$ of **26-26**, **29-M**, **26-H** and **29-H**: see table 8.

ESI-MS: m/z (%): Compound **26-26**: 1122.6 (100) $[\text{M}/2]^+$, Compound **29-M**: 1122.6 (100) $[\text{M}]^+$

UV-vis spectrum of **26-26** ($c = 87$ μM , 0.2 M KCl, pH = 8.1): 551 nm (4.31), 521 nm (4.28), 411 nm (3.84), 322 nm (4.21), 303 nm (4.27), 277 nm (4.37).

UV-vis spectrum of **29-M** ($c = 24$ μM , 0.2 M KCl, pH = 6.9): 555 nm (3.96), 524 nm (3.95), 411 nm (3.67), 362 nm (4.49), 322 nm (3.94), 306 nm (4.00), 278 nm (4.10).



Scheme 17: Synthesis of the linker **8**.

Compound 36. 5,6-dimethylbenzimidazole (**35**, 1.46 g, 10 mmol) was dissolved in *N,N*-dimethylformamide (DMF) (20 mL), after which Cs_2CO_3 (0.3 g, 1.5 mmol) and K_2CO_3 (1.38 g, 10 mmol) were added. *Tert*-butyl bromoacetate (1.65 mL, 10.5 mmol) was added dropwise after 5 min and it was stirred for 10 h at room temperature. The solvent was removed under reduced pressure and the product was extracted with ethyl acetate (35 mL) from water (10 mL). The organic layer was washed with water and brine (2 x 10 mL each), dried over Na_2SO_4 and then concentrated under reduced pressure. The

crude product was purified by flash chromatography on silica gel (dichloromethane (DCM): ethyl acetate (EA) = 3:2) to afford **36** (1.08 g, 4.2 mmol, 42 %) as a white solid.

TLC (Silicagel 60 F₂₅₄, DCM:EA = 3:2): R_f = 0.32.

¹H-NMR (200 MHz, [D₃]MeOD): δ = 1.45 (s, 9 H), 2.36 (s, 3 H), 2.38 (s, 3 H), 4.97 (s, 2 H), 7.20 (s, 1 H), 7.44 (s, 1 H), 7.99 (s, 1 H).

MS (ESI-MS): m/z (%): 261.1 (100) [M + H]⁺.

Compound 37. A solution of **36** (0.52 g, 2 mmol) in DCM (5 mL) was treated with triethylsilane (3 mL), cooled to 0°C, after which trifluoroacetic acid (TFA, 6 mL) was added dropwise. After 5 min, the solution was allowed to warm up to room temperature and was stirred for 6 h. The solvent was removed under reduced pressure and the residue was azeotroped with DCM (3 x 5 mL) to yield **37** (0.41 g, 2 mmol, 100 %) as a white solid. An analytically pure sample of **37** was obtained by recrystallization from acetone.

¹H-NMR (200 MHz, [D₃]MeOD): δ = 2.47 (s, 6 H), 5.31 (s, 2 H), 7.60 (s, 1 H), 7.62 (s, 1 H), 9.19 (s, 1 H).

MS (ESI-MS): m/z (%): 205.3 (100) [M + H]⁺.

Compound 38. Fmoc-glycine (297 mg, 1.0 mmol) was dissolved in DMF (1 mL) and the solution was cooled down to 0°C. First, 1-hydroxybenzotriazole (HOBt, 150 mg, 1.1 mmol) and dicyclohexylcarbodiimide (DCC, 227 mg, 1.1 mmol) were added and after 10 min of stirring, N-BOC-ethylenediamine (**28**, 160 μ L, 1.0 mmol) was added. The reaction was stirred for 12 h at room temperature and the solvent was removed under reduced pressure. The residue was dissolved in DCM (5 mL) and washed with brine (5 mL). The organic layer was dried over Na₂SO₄, filtrated, and concentrated under reduced pressure. The residue was further purified by flash chromatography on silica gel (DCM : EA : MeOH = 12 : 8 : 5) to afford **38** (320 mg, 0.73 mmol, 73 %) as a white solid.

TLC (Silicagel 60 F₂₅₄, DCM : EA : MeOH = 12 : 8 : 5): R_f = 0.52.

¹H-NMR (500MHz, [D₆]DMSO): δ = 1.37 (s, 9H), 2.98 (m, 2 H), 3.11 (m, 2 H), 3.58 (d, *J* = 5.5, 2 H), 4.22 (m, 1 H), 4.28 (d, *J* = 7, 2 H), 7.31 – 7.88 (m, 8 H).

MS (ESI-MS): m/z (%): 462.3 (100) [M + Na]⁺.

Compound 40. Solution A: **38** (44 mg, 0.10 mmol) was dissolved in DMF (1 mL), after which triethylamine (NEt₃, 35 μ L, 0.28 mmol) and KF (35 mg, 0.6 mmol) were added. The mixture was stirred for 14 h. Solution B: **37** (20 mg, 0.1 mmol) was dissolved in DMF (1 mL), after which HOBt (15 mg, 0.11 mmol) and DCC (23 mg, 0.11 mmol) were added. After 10 min, solution A was added to solution B and the mixture was stirred for 14 h. The solvent was removed under reduced pressure. The residue was purified by flash chromatography on silica gel (DCM : EA : MeOH = 12 : 8 : 5) to afford **40** (25 mg, 0.062 mmol, 62 %) as a white solid.

TLC (Silicagel 60 F₂₅₄, DCM : EA : MeOH = 12 : 8 : 5): R_f = 0.43.

¹H-NMR (500 MHz, [D₃]MeOD): δ = 1.43 (s, 9 H), 2.37 (s, 3 H), 2.39 (s, 3 H), 3.15 (m, 2 H), 3.27 (m, 2 H), 3.88 (s, 2 H), 5.02 (s, 2 H), 7.29 (s, 1 H), 7.44 (s, 1 H), 8.04 (s, 1 H).

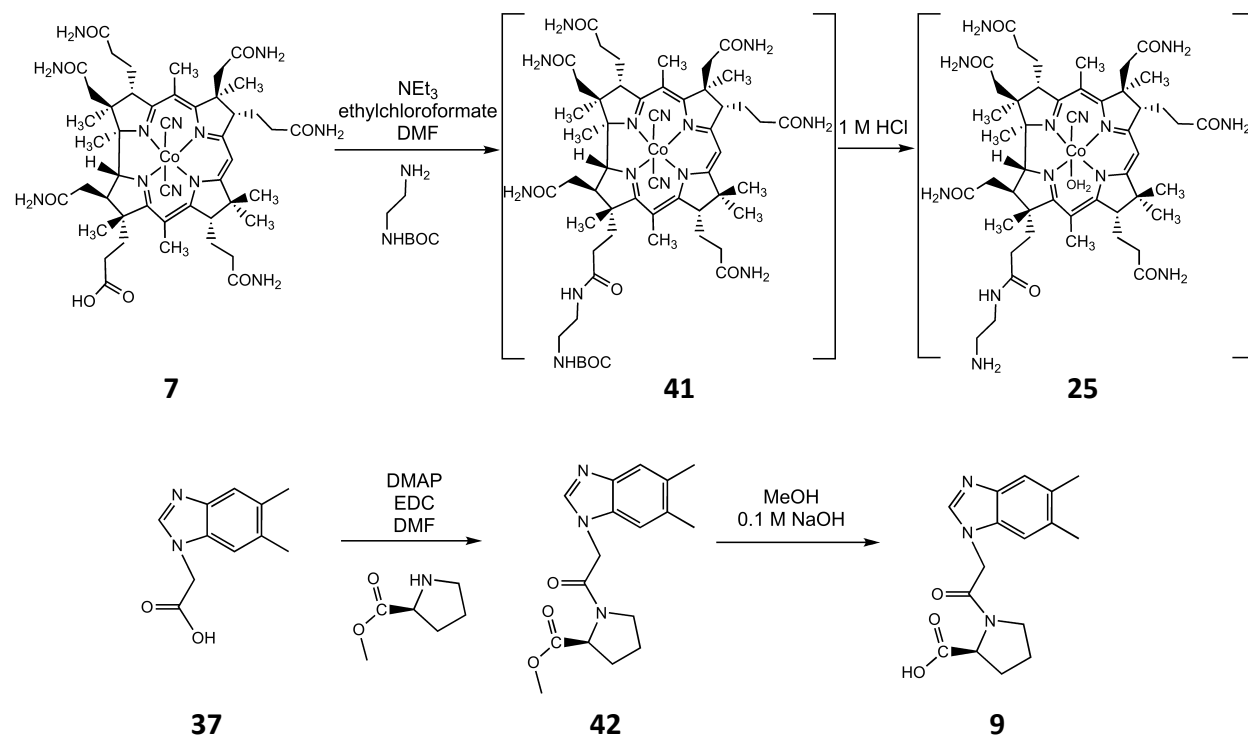
MS (ESI-MS): m/z (%): 404.3 (100) [M + H]⁺.

Compound 8. **40** (20 mg, 0.050 mmol) was dissolved in methanol (10 mL), after which aqueous HCl (3 M, 3 mL) was added. The turbid solution was stirred for 4 h until it turned clear. After removal of the organic solvent under reduced pressure, it was lyophilized to afford **8** (15 mg, 0.050 mmol, 100 %).

¹H-NMR (500 MHz, [D₃]MeOD): δ = 2.47 (s, 3 H), 2.48 (s, 3 H), 3.08 (t, *J* = 6, 2 H), 3.51 (t, *J* = 6, 2 H), 3.98 (s, 2 H), 5.41 (s, 2 H), 7.62 (s, 1 H), 7.72 (s, 1 H), 9.36 (s, 1 H).

¹³C-NMR (125 MHz, [D₃]MeOD): δ = 20.55, 20.72, 38.30, 41.00, 43.84, 114.00, 115.37, 130.57, 131.90, 138.65, 138.83, 142.29, 168.15, 172.49.

MS (ESI-MS): m/z (%): 304.3 (100) [M + H]⁺.



Scheme 18: Synthesis of the linker **9** and the intermediate **25**. Charges on the corrin rings have been omitted.

Compound 25. **7** (4.9 mg, 5.0 μmol) was dissolved in dry DMF (1 mL) and cooled to 0°C before NEt_3 (10 μL , 70 μmol) and ethylchloroformate (5 μL , 55 μmol) were added. After 1 min, *N*-Boc-ethylenediamine (16 mg, 0.10 mmol) was added and the reaction was quenched with water after 10 min. The crude product (**41**) was precipitated with acetone, filtrated, dissolved in HCl (1 mL, 1 M) and stirred for 1 h. The solution was lyophilized to yield crude **25**., which was used directly in the next step without purification.

Compound 42. **37** (20.4 mg, 0.10 mmol) was dissolved in DMF (1 mL) and cooled to 0°C, after which DMAP (2.0 mg, 16 μmol) and (*L*)-Proline methyl ester hydrochloride (20 mg, 0.12 mmol) were added. After 10 min, EDC·HCl (28 mg, 0.14 mmol) was added and the solution was allowed to warm up to room temperature. It was stirred for 2 h and the solvent was removed under reduced pressure. The residue was purified by flash

chromatography on silica gel (DCM : EA : MeOH = 12 : 8 : 5) to afford **42** (22 mg, 0.070 mmol, 70 %).

TLC (Silicagel 60 F₂₅₄, DCM : EA : MeOH = 12 : 8 : 5): R_f = 0.55.

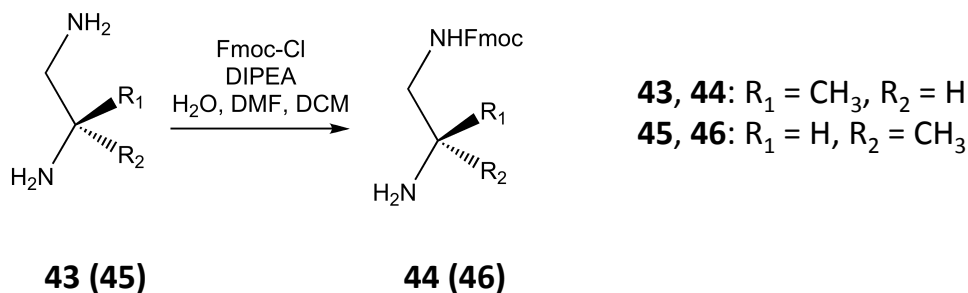
¹H-NMR (500 MHz, [D₃]MeOD) (main rotamer): δ = 2.10 – 2.35 (m, 3 H), 2.36 (s, 3 H), 2.39 (s, 3 H), 3.69 (s, 3 H), 3.70 – 3.85 (m, 3 H), 4.49 (m, 1 H), 5.20 (s, 2 H), 7.25 (s, 1 H), 7.43 (s, 1 H), 7.98 (s, 1 H). (The characteristic presence of *syn/anti* rotamers originating from the restricted rotation around the tertiary amide bond has been observed as indicated by a doubling of relevant resonances^[141]. A ratio of approx. 85 :15 of the two isomers was calculated from the signals 7.98 and 7.96.).

MS (ESI-MS): m/z (%): 316.1 (100) [M + H]⁺.

Compound 9. **42** (16 mg, 50 μmol) was dissolved in methanol (1 mL) and aqueous NaOH (3 mL, 0.1 M) was added. After 2 h, the solution turned clear. After removal of the organic solvent, the solution was acidified to pH 5 with HCl solution (32%) and lyophilized to afford **9** (15 mg, 50 μmol, 100 %).

¹H-NMR (500 MHz, [D₃]MeOD)(main rotamer): δ = 1.90 – 2.36 (m, 4 H), 2.37 (s, 6 H), 3.81 (m, 1 H), 3.72 (m, 1 H), 4.39 (m, 1 H), 5.18 (s, 2 H), 7.33 (s, 1 H), 7.43 (s, 1 H), 8.10 (s, 1 H). (A ratio of approx. 65 : 35 of *syn/anti* rotamers was calculated from the signals at 8.10 and 8.17. The total integral of 18 is consistent with the molecular formula of compound **9** (C₁₆H₁₉N₃O₃)).

MS (ESI-MS): m/z (%): 302.2 (100) [M + H]⁺, 300.2 (100) [M – H]⁻.



Scheme 19: Synthesis of the compound **44**, and **46**.

Compound 44. (R)-(+)-1,2-Diaminopropane dihydrochloride (**43**, 30 mg, 0.2 mmol) was dissolved in water (20 μL) before DMF (6 mL) and N-ethyldiisopropylamine (DIPEA, 50 μL) were added. The solution was cooled down to 0°C before *Fmoc*-Cl (25 mg, 0.10 mmol) dissolved in DCM (1 mL) was added dropwise. After 2h, a saturated aqueous

NaHCO₃ solution (5 mL) and DCM (5 mL) were added and the organic layer was concentrated under reduced pressure. Methanol (0.1 mL) and water (5 mL) were added. The water was removed after centrifugation and the precipitate was lyophilized to yield **44** (12 mg, 0.040 mmol, 20 %).

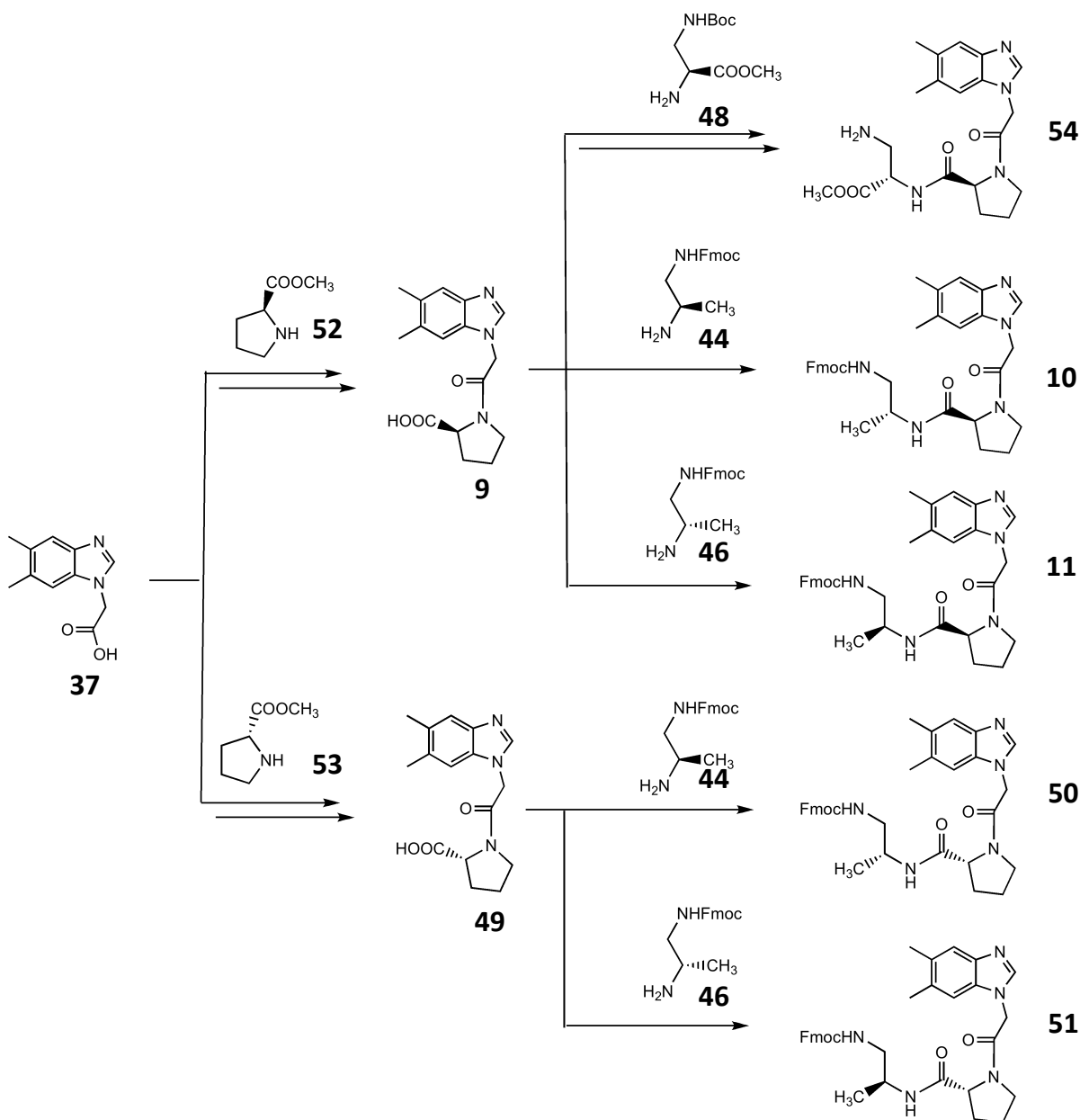
¹H-NMR (500 MHz, [D₆]DMSO): δ = 1.10 (d, *J* = 5.5, 3 H), 3.08 (m, 1 H), 3.15 (m, 2 H), 4.23 (t, *J* = 6, 1 H), 4.37 (d, *J* = 6, 2 H), 7.33 (t, *J* = 7, 2 H), 7.43 (t, *J* = 7, 2 H), 7.69 (d, *J* = 7.5, 2 H), 7.90 (d, *J* = 7.5, 2 H). (The protection at the indicated nitrogen of **44** has been confirmed by ¹H-NMR, ¹³C-NMR, ¹H-COSY, CH-COSY, COLOC (data not shown). An ¹H-NMR spectra of *Fmoc*-NH-CH(CH₃)-CH₂-NH₂ has been reported by McMurray^[142] that differs significantly from that of **44**).
¹³C-NMR (125 MHz, [D₃]MeOD): δ = 159.6, 145.4, 142.8, 129.0, 128.3, 126.2, 121.1, 68.1, 45.2, 16.5.

MS (ESI-MS): *m/z* (%): 297.1 (100) [M + H]⁺.

Compound 46. The synthesis was performed with (S)-(+)-1,2-Diaminopropane dihydrochloride (**45**, 30 mg, 0.20 mmol) as described for **44** to yield **46** (14 mg, 0.047 mmol, 24 %).

¹H-NMR (500 MHz, [D₆]DMSO): 1.12 (d, *J* = 5.5, 3 H), 3.11 (d, *J* = 2, 1 H), 3.17 (m, 2 H), 4.24 (t, *J* = 6.5, 1 H), 4.37 (d, *J* = 6.5, 2 H), 7.34 (t, *J* = 7.5, 2 H), 7.42 (t, *J* = 7.5, 2 H), 7.69 (d, *J* = 7.5, 2 H), 7.90 (d, *J* = 7.5, 2 H).

MS (ESI-MS): *m/z* (%): 297.1 (100) [M + H]⁺.



Scheme 20: Synthesis of the linker **10**, **11**, **50**, **51** and **54**.

Compound 10. **9** (11 mg, 37 μmol) was dissolved in DMF (3 mL). HOBt (8.4 mg, 60 μmol) and DCC (12 mg, 60 μmol) were added to the solution, after which **44** (9.0 mg, 30 μmol) was added after 10 min. The solvent was removed under reduced pressure after 2h of stirring at room temperature. The residue was purified by flash chromatography on silica gel (DCM : EA : MeOH = 12 : 8 : 5) to afford **10** (3.5 mg, 6.2 μmol , 21 %).

TLC (Silicagel 60 F₂₅₄, CH₂Cl₂ : EA : MeOH = 12 : 8 : 5): R_f = 0.44.

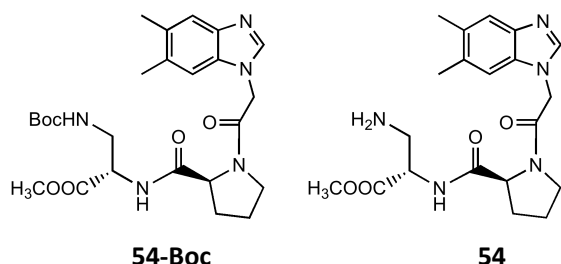
¹H-NMR (500 MHz, [D₃]MeOD): 1.08 (d, *J* = 6.5, 3 H), 1.90 – 2.40 (m, 12 H), 3.05 – 3.26 (m, 2 H), 3.72 – 4.40 (m, 5 H), 5.03 – 5.19 (m, 2 H), 7.17 – 7.93 (m, 11 H). (A ratio of the two *syn/anti* isomers of approx. 80:20 was calculated from the signals at 1.08 and 1.20 ppm (CH₃CH). The total integral of 35 is consistent with the molecular formula of compound **10** (C₃₄H₃₇N₅O₄).) MS (ESI-MS): *m/z* (%): 580.3 (100) [M + H]⁺.

Compound 11. The synthesis was performed with **46** (11 mg, 37 μmol) as described for **10** to afford **11** (7.1 mg, 12 μmol, 32 %).

TLC (Silicagel 60 F₂₅₄, DCM : EA : MeOH = 12 : 8 : 5): R_f = 0.44.

¹H-NMR (500 MHz, [D₃]MeOD)(main rotamer): 1.09 (d, *J* = 6.5, 3 H), 1.94 - 2.03 (m, 4 H), 2.15 – 2.20 (m, 1 H), 2.30 – 2.38 (m, 7 H), 3.07 (m, 1 H), 3.23 (m, 1 H), 3.70 – 4.38 (m, 5 H), 5.18 (s, 2 H), 7.26 – 7.29 (m, 3 H), 7.35 – 7.39 (m, 3 H), 7.60 (dd, *J* = 2, *J* = 7.5, 2 H), 7.78 (d, *J* = 7.5, 2 H), 7.97 (s, 1 H). (A ratio of the *syn/anti* rotamers of approximately 80 : 20 was calculated from the signals at 1.09 and 1.18 ppm (CH₃CH). The total integral of 35 is consistent with the molecular formula of compound **11** (C₃₄H₃₇N₅O₄).)

MS (ESI-MS): *m/z* (%): 580.3 (100) [M + H]⁺.

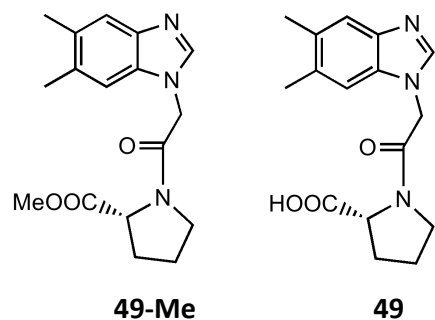


Compound 54. 9 (9.0 mg, 0.03 mmol) was dissolved in DMF (1 mL) and cooled to 0°C, after which DMAP (2.0 mg, 16 μmol) and **48** (10.2 mg, 0.04 mmol) were added. After 10 min, EDC·HCl (10 mg, 0.05 mmol) was added and the solution was allowed to warm up to room temperature. It was stirred for 2 h and the solvent was removed under reduced pressure. The residue was purified by flash chromatography on silica gel (DCM : EA : MeOH = 12 : 8 : 5) to afford **54-Boc**, which was then dissolved in TFA/CH₂Cl₂ solution. After 2 hours, the solvent was removed under reduced pressure to give **54** (7.2 mg, 0.018 mmol, 60%).

TLC (Silicagel 60 F₂₅₄, DCM : EA : MeOH = 12 : 8 : 5): R_t = 0.40.

¹H-NMR (500 MHz, [D₃]MeOD): 2.00 - 2.45 (m, 4 H), 2.49 (s, 6 H), 3.10 - 3.75 (m, 4 H), 2.30 – 2.38 (m, 7 H), 3.07 (m, 1 H), 3.23 (m, 1 H), 3.70 – 4.38 (m, 3 H), 4.51 (m, 2H), 5.58 (s, 2 H), 7.64 (s, 1 H), 7.73 (s, 1 H), 9.25 (s, 1 H).

MS (ESI-MS): m/z (%): 402.2 (100) [M + H]⁺.



Compound 49. **37** (45 mg, 0.22 mmol) was dissolved in DMF (2 mL) and cooled to 0°C, after which DMAP (10 mg, 82 μmol) and (S)-Proline methyl ester hydrochloride (**53**, 31 mg, 0.20 mmol) were added. After 10 min, EDC·HCl (50 mg, 0.26 mmol) was added and the solution was allowed to warm up to room temperature. It was stirred for 2 h and the solvent was removed under reduced pressure. The residue was purified by flash chromatography on silica gel (DCM : EA : MeOH = 12 : 8 : 5) to afford white solid **49-Me**, which was then dissolved in a mixture of methanol (1 mL) and aqueous NaOH (3 mL, 0.1 M). After 2 h of stirring at 20°C, the solution turned clear. After removal of the organic solvent, the solution was acidified to pH 5 with aqueous HCl (32%) and purified by SPE with C18 filter to give **49** (34 mg, 0.011 mmol, 55 %)

¹H-NMR (500 MHz, [D₃]MeOD)(main rotamer): 2.02 – 2.36 (m, 4 H), 2.40 (m, 6 H), 3.77 (m, 1 H), 3.83 (m, 1 H), 4.48 (m, 1 H), 5.28 (s, 2 H), 7.43 (s, 1 H), 7.47 (s, 1 H), 8.37 (s, 1 H). (A ratio of approx. 69 : 31 of *syn/anti* rotamers was calculated from the signals at 8.37 and 8.49.

The total integral of 18 is consistent with the molecular formula of compound **49** (C₁₆H₁₉N₃O₃).

MS (ESI-MS): m/z (%): 302.4 (100) [M + H]⁺.

Compound 50. The synthesis was performed with **44** (12 mg, 40 μmol) as described for **10** to afford **50** (6.0 mg, 10 μmol, 25 %).

TLC (Silicagel 60 F₂₅₄, DCM : EA : MeOH = 12 : 8 : 5): R_t = 0.42.

¹H-NMR (500 MHz, [D₃]MeOD)(main rotamer): 1.09 (d, *J* = 7, 3 H), 1.94 - 2.03 (m, 4 H), 2.15 - 2.20 (m, 1 H), 2.30 - 2.36 (m, 7 H), 3.07 (m, 1 H), 3.23 (m, 1 H), 3.70 - 4.38 (m, 5 H), 5.19 (s, 2 H), 7.26 - 7.29 (m, 3 H), 7.36 - 7.40 (m, 3 H), 7.59 - 7.62 (m, 2 H), 7.78 (d, *J* = 7.5, 2 H), 7.98 (s, 1 H). (A ratio of the *syn/anti* rotamers of 82 : 18 was calculated from the signals at 1.09 and 1.18 ppm (CH₃CH). The total integral of 35 is consistent with the molecular formula of compound **50** (C₃₄H₃₇N₅O₄).)

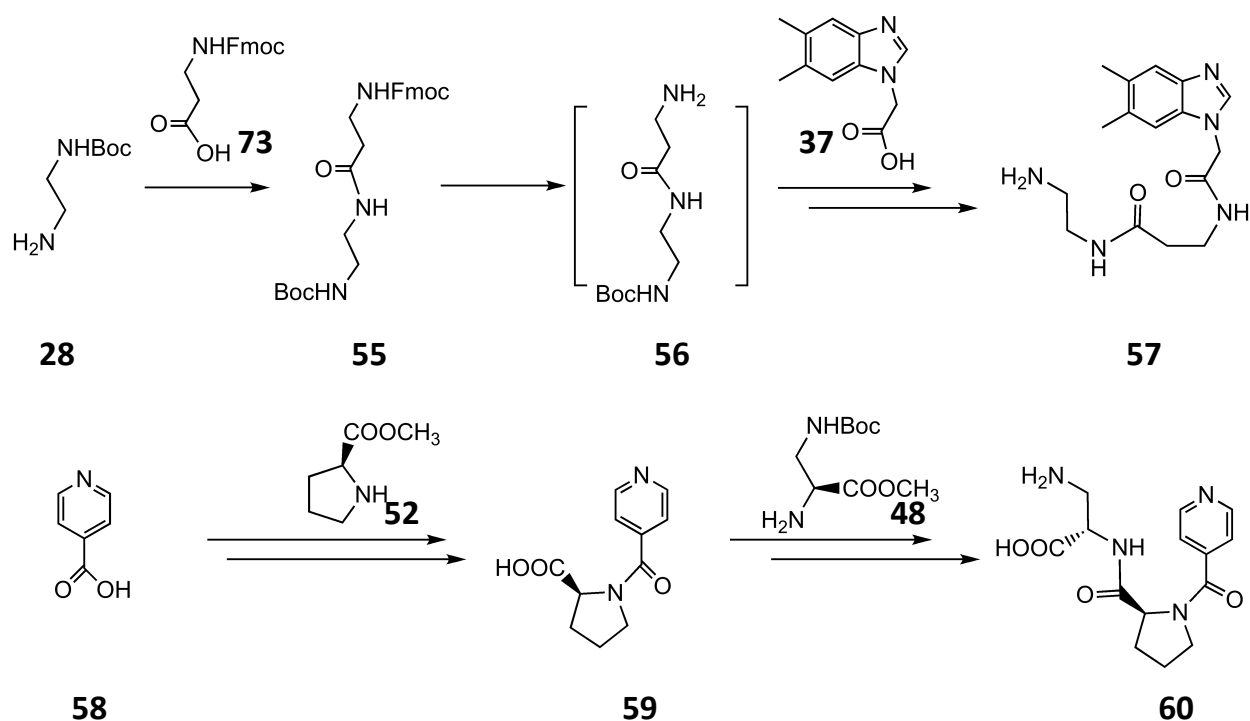
MS (ESI-MS): *m/z* (%): 580.3 (100) [M + H]⁺.

Compound 51. The synthesis was performed with **46** (13 mg, 44 μmol) as described for **10** to afford **51** (8.9 mg, 15 μmol, 35 %).

TLC (Silicagel 60 F₂₅₄, DCM : EA : MeOH = 12 : 8 : 5): R_t = 0.36.

¹H-NMR (500 MHz, [D₃]MeOD)(main rotamer): 1.08 (d, *J* = 7, 3 H), 1.94 - 2.40 (m, 12 H), 3.10 (m, 1 H), 3.25 (m, 1 H), 3.73 - 4.38 (m, 5 H), 5.18 (m, 2 H), 7.26 - 7.39 (m, 6 H), 7.50 (m, 2 H), 7.76 (m, 2 H), 7.92 (s, 1 H). (A ratio of the *syn/anti* rotamers of approximately 80 : 20 was calculated from the signals at 1.08 and 1.20 ppm (CH₃CH). The total integral of 35 is consistent with the molecular formula of compound **51** (C₃₄H₃₇N₅O₄).)

MS (ESI-MS): *m/z* (%): 580.3 (100) [M + H]⁺.



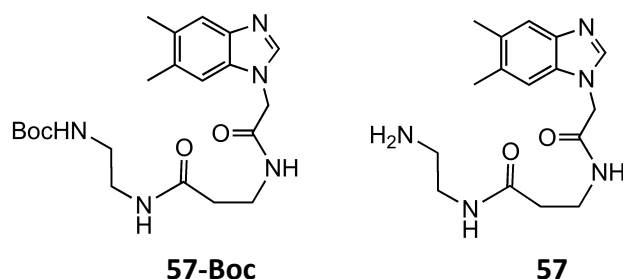
Scheme 21: Synthesis of linker **56**, **57** and **60**.

Compound 55. **73** (31 mg, 0.1 mmol) was dissolved in DMF (1 mL) and the solution was cooled down to 0°C. First, 1-hydroxybenzotriazole (HOBt, 15 mg, 0.11 mmol) and dicyclohexylcarbodiimide (DCC, 22.7 mg, 0.11 mmol) were added and after 10 min of stirring, N-BOC-ethylenediamine (**28**, 16 μ L, 0.1 mmol) was added. The reaction was stirred for 5 h at room temperature and the solvent was removed under reduced pressure. The residue was purified by flash chromatography on silica gel (DCM : EA : MeOH = 24 : 16 : 5) to afford **55**. (36 mg, 0.079 mmol, 79 %) as a white solid.

TLC (Silicagel 60 F₂₅₄, DCM : EA : MeOH = 24 : 16 : 5): R_f = 0.61.

¹H-NMR (500MHz, [D₆]DMSO): 1.42 (s, 9 H), 3.10 - 3.50 (m, 8 H), 4.20 (t, 1 H), 4.34 (d, *J* = 7, 2 H), 7.31 (t, 2 H), 7.39 (t, 2 H), 7.64 (d, *J* = 7, 2 H), 7.79 (d, *J* = 6, 2 H).

MS (ESI-MS): *m/z* (%): 476.3 (100) [M + Na]⁺.



Compound 57. **55** (18 mg, 0.040 mmol) and DMAP (10 mg, 0.082 mmol) were dissolved in DMF (0.3 mL) and after 20 h, **55** turned into **56** indicated as by TLC. To this solution, **37** (10 mg, 0.050 mmol) and DMF (2 mL) were added. The reaction was stirred for 7 h before the solvent was removed under reduced pressure. The residue was purified by flash chromatography on silica gel (DCM : EA : MeOH = 12 : 8 : 5) to afford **57-Boc**, which was dissolved and stirred in aqueous HCl (3 mL, 1 M) at 55 °C for 1 h. The solution was lyophilised to afford **57** (8.5 mg, 0.027 mmol, 67 %).

$^1\text{H-NMR}$ (500 MHz, $[\text{D}_3]\text{MeOD}$): δ = 2.47 (s, 3 H), 2.48 (s, 3 H), 2.51 (t, 2 H), 3.04 (t, 2 H), 3.46 (t, 2 H), 3.56 (t, 2 H), 5.30 (s, 2 H), 7.63 (s, 1 H), 7.66 (s, 1 H), 9.36 (s, 1 H).

MS (ESI-MS): m/z (%): 318.3 (100) $[\text{M} + \text{H}]^+$.

Compound 59. **58** (32 mg, 0.26 mmol) was dissolved in DMF (2 mL) and cooled to 0°C, after which DMAP (10 mg, 82 μmol) and (L)-Proline methyl ester hydrochloride (**52**, 25 mg, 0.19 mmol) were added. After 10 min, EDC·HCl (60 mg, 0.31 mmol) was added and the solution was allowed to warm up to room temperature. It was stirred for 4 h and the solvent was removed under reduced pressure. The residue was purified by flash chromatography on silica gel (DCM : EA : MeOH = 12 : 8 : 5) to afford the methyl ester of **59**, which was hydrolysed to **59** with aqueous KOH (5 mL, pH 13) during 2 h. The solution of **59** was neutralised by aqueous HCl (0.1 M) and purified by SPE with C18 filter to give pure **59** (39 mg, 0.18 mmol, 95 %).

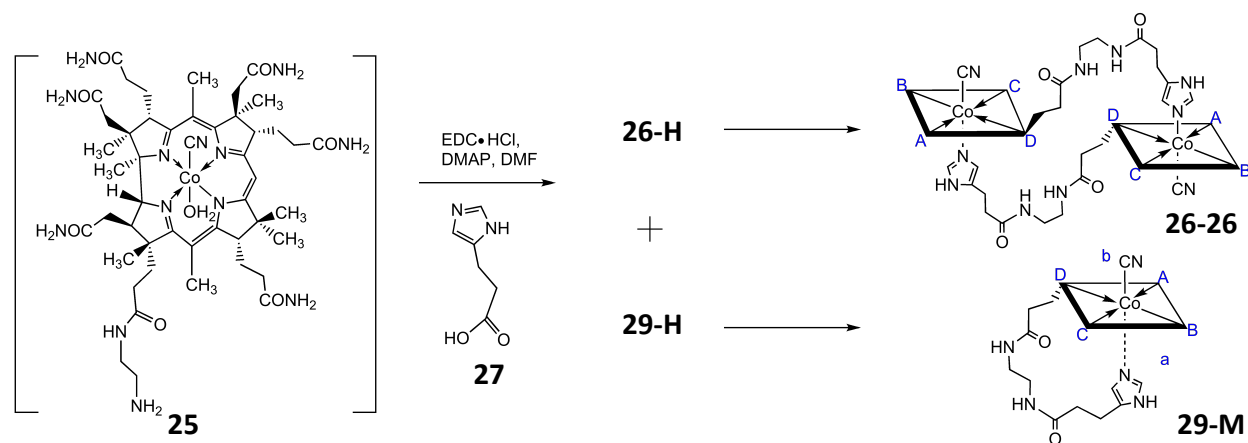
$^1\text{H-NMR}$ (500 MHz, $[\text{D}_3]\text{MeOD}$) (main rotamer): 1.95 - 2.12 (m, 4 H), 3.49 - 3.78 (m, 2 H), 4.63 (t, 1 H), 7.95 (d, J = 5, 2 H), 8.87 (d, J = 5.5, 2 H) (A ratio of the *syn/anti* rotamers of approximately 76 : 24 was calculated from the signals at 8.87 and 8.81 ppm)

MS (ESI-MS): m/z (%): 221.6 (100) $[\text{M} + \text{H}]^+$.

Compound 60. **59** (36 mg, 0.16 mmol) was dissolved in DMF (3 mL) and the solution was cooled down to 0°C, after which DMAP (10 mg, 82 µmol) and **48** (60 mg, 0.24 mmol) were added. After 10 min, EDC·HCl (60 mg, 0.31 mmol) was added and the solution was allowed to warm up to room temperature. It was stirred for 2 h and the solvent was removed under reduced pressure. The residue was purified by flash chromatography on silica gel (DCM : EA : MeOH = 12 : 8 : 5) to afford **60-Boc**, which was dissolved in a mixture of CH₂Cl₂ (3 mL) and TFA (1 mL) for 1 h to afford **60**. The solvent was removed under reduced pressure, and the residue was redissolved in water and purified by C18 filter to give pure **60** (35 mg, 0.11 mmol, 69 %).

¹H-NMR (500 MHz, [D₃]MeOD)(main rotamer): 1.98 (m, 1 H), 2.09 (m, 2 H), 2.39 (m, 1 H), 3.16 – 3.70 (m, 4 H), 3.82 (s, 3 H), 4.57 (t, 1 H), 4.93 (t, 1 H), 7.66 (d, *J* = 4, 2 H), 8.73 (d, *J* = 5, 2 H) (A ratio of the *syn/anti* rotamers of approximately 93 : 7 was calculated from the signals at 8.73 and 8.67 ppm)

MS (ESI-MS): *m/z* (%): 321.4 (100) [*M* + H]⁺.



Scheme 22: Synthesis of compound **26-26** and **29-M**. Charges have been omitted.

Compound 26-26 and 29-M: Dicyanocyno cobyric acid (**7**, 9.8 mg, 10 µmol) was dissolved in dry DMF (2 mL) and cooled to 0 °C before DMAP (3.0 mg, 2.5 µmol) and EDC·HCl (9.0 mg, 45 µmol) was added. After 5 min, N-Boc-ethylenediamine (**28**, 16 mg, 0.10 mmol) was added and the reaction was allowed to warm up to room temperature. After 6 hours, the solvent was removed under reduced pressure and it was precipitated with acetone. The precipitate was dissolved in aqueous HCl (3 mL, 1 M) and it was stirred for 3 h. The solution was lyophilized to yield crude **25**. The latter was dissolved in

DMF (1 mL) and it was cooled to 0°C, after which DMAP (1.0 mg, 8 µmol) and deamino histidine (**27**, 4.5 mg, 15 µmol) were added. After 10 min, EDC·HCl (3.0 mg, 15 µmol) was added. The solution was allowed to warm up to room temperature. It was stirred for 10 h and the solvent was removed under reduced pressure. The residue was washed with acetone and further purified with preparative HPLC to afford **26-H** (5.2 mg, 3.8 µmol, yield: 38 %) and **29-H** (5.6 mg, 4.1 µmol, yield: 41 %) as TFA salts. **26-26** and **29-M** are derived from **26-H** and **29-H** in water at pH 8.1 and pH 6.9, respectively.

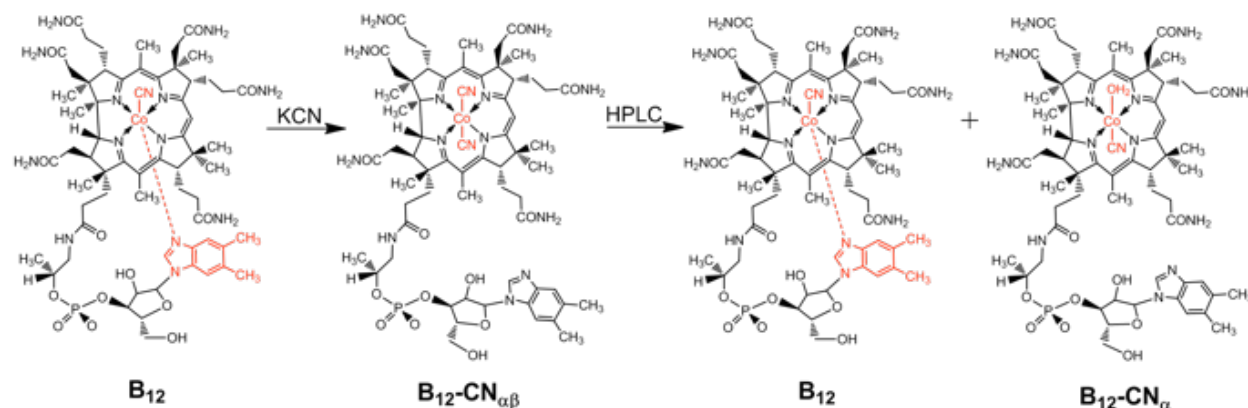
UPLC-UV-vis: R_t = 0.9 min (**26-H**) and R_t = 1.7 min (**29-H**)

¹H-NMR of **26-26**, **29-M**, **26-H** and **29-H**: see table 8.

ESI-MS: m/z (%): Compound **26-26**: 1122.6 (100) $[M/2]^+$, Compound **29-M**: 1122.6 (100) $[M]^+$

UV-vis spectrum of **26-26** (c = 87 µM, 0.2 M KCl, pH = 8.1): 551 nm (4.31), 521 nm (4.28), 411 nm (3.84), 322 nm (4.21), 303 nm (4.27), 277 nm (4.37).

UV-vis spectrum of **29-M** (c = 24 µM, 0.2 M KCl, pH = 6.9): 555 nm (3.96), 524 nm (3.95), 411 nm (3.67), 362 nm (4.49), 322 nm (3.94), 306 nm (4.00), 278 nm (4.10).



Scheme 23: Synthesis of compound **B12-CN_α**. Charges on the corrin rings have been omitted.

B12-CN_α: **B12** (27 mg, 20 µmol) was dissolved in water (5 ml), before KCN (13 mg, 200 µmol) was added. After observation of a colour change from red to violet, the solution was injected directly into the preparative HPLC to yield **B12-CN_α** (17 mg, 12.5 µmol, 62.7 %) (The solvent waste was collected into a bottle containing solid NaOH to

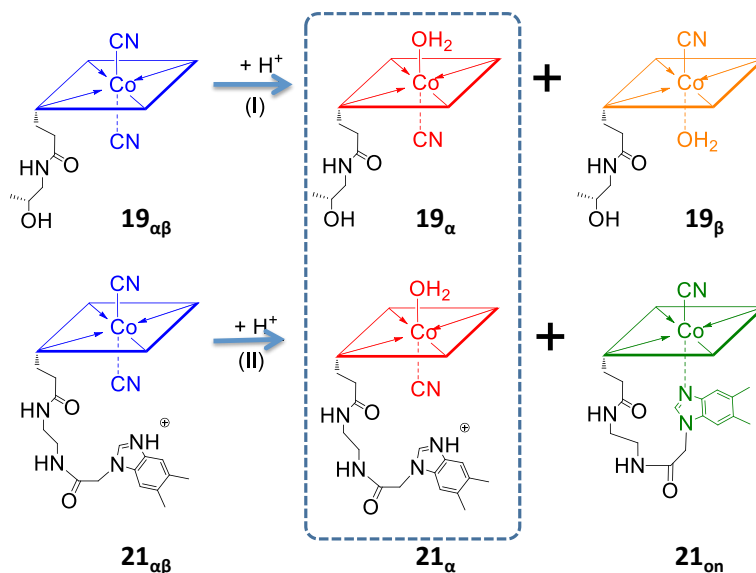
neutralize the acidic solution and to absorb potential HCN as cyanide; an HCN-detector from Dräger was used.)

HPLC-UV-vis: $R_t = 11$ min

$^1\text{H-NMR}$ of **B12-CN $_{\alpha}$** : see table 8 (The chemical shifts of the protons of the corrin ring are consistent with those of Cbi-CN $_{\alpha}$, but differ significantly from those of Cbi-CN $_{\beta}$)

ESI-MS: m/z (%): Compound **B12-CN $_{\alpha}$** : 1355.6 (100) $[\text{M-H}_2\text{O}+\text{H}]^+$

UV-vis spectrum of **B12-CN $_{\alpha}$** ($c = 35 \mu\text{M}$, $\text{pH} = 4.5$): 528 nm (3.88), 496 nm (3.92), 407 nm (3.67), 354 nm (4.49), 321 nm (4.43), 276 nm (4.22).



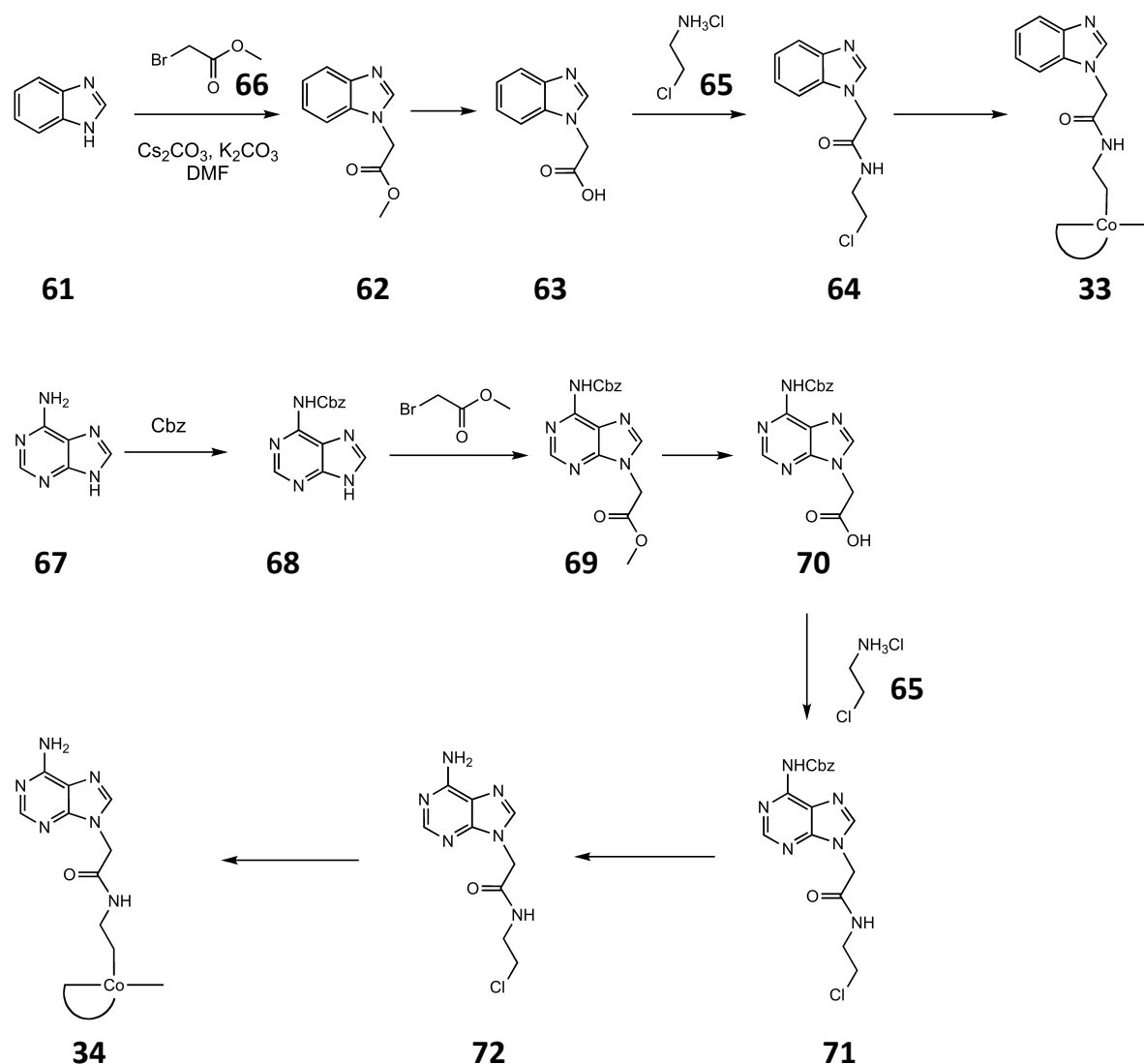
Scheme 25: (Up) Synthesis of **19 $_{\alpha}$** and **19 $_{\beta}$** from **19 $_{\alpha\beta}$** . (Down) Synthesis of **21 $_{\alpha}$** and **21 $_{on}$** from **21 $_{\alpha\beta}$** . Charges on the corrin rings have been omitted.

Synthesis of 21 $_{on}$. Intermediate **25** was synthesised from dicyanocobyrinic acid (4.9 mg, 5.0 μmol) as described in compound **3**. It was dissolved in DMF (1 mL) and cooled to 0°C , after which DMAP (1.0 mg, 8 μmol) and **7** (4.5 mg, 15 μmol) were added. After 10 min, EDC $\cdot\text{HCl}$ (3.0 mg, 15 μmol) was added. The solution was allowed to warm up to room temperature. After 4 h the solvent was removed under reduced pressure. The residue was washed with acetone and further purified with preparative HPLC to afford **21 $_{on}$** (3.8 mg, 2.9 μmol , 58 %) as the corresponding TFA salt.

^1H NMR (500 MHz, $[\text{D}_2]\text{D}_2\text{O}$): (see Table 8) HR-MS: $[\text{M}]^+$ calcd for $\text{C}_{59}\text{H}_{81}\text{CoN}_{15}\text{O}_8$: 1186.57191, found: 1186.57087; UV/Vis ($c = 30 \mu\text{M}$, 0.2 M KCl, pH = 5.98): 548 nm (3.96), 521 nm (3.94), 413 nm (3.72), 361 nm (4.43), 279 nm (4.27), HPLC-UV/Vis: $R_t = 14.2$ min; $\text{pK}_{\text{base-off}} = 2.58$.

Synthesis of ($\mathbf{21_{on}}$ + $\mathbf{21_{\alpha}}$). $\mathbf{21_{on}}$ (1.3 mg, 1.0 μmol) and KCN (1.3 mg, 20 μmol) were dissolved in water (5 mL) to obtain a violet coloured solution of $\mathbf{21_{\alpha\beta}}$. The pH value of the solution was adjusted to 2 with trifluoroacetic acid. After purging the solution with N_2 for 20 min to remove HCN, the reaction solution was adsorbed on a reverse-phase Chromafix[®] C18ec cartridge. It was washed with water (30 mL) and then eluted with MeOH (3 mL). The solvent was removed under vacuum to yield $\mathbf{21_{on}}$ and $\mathbf{21_{\alpha}}$ as a mixture of the corresponding TFA salts (1.3 mg, 100%).

ESI-MS: m/z (%): 1186.6 (100) $[\text{M}]^+$ for $\mathbf{21_{on}}$ or $[\text{M}-\text{H}_2\text{O}]^+$ for $\mathbf{21_{\alpha}}$.



Scheme 24: Synthesis of compound **33** and **34**.

Compound **62**: Benzimidazole (**61**, 0.292 g, 2.5 mmol) was dissolved in *N,N*-dimethylformamide (DMF; 4 ml), before Cs_2CO_3 (0.060 g, 0.9 mmol) and K_2CO_3 (0.276 g, 2.0 mmol) were added. Methyl bromoacetate (0.2 ml, 2.1 mmol) was added dropwise 5 min later. After stirring for 18 h, the organic solvent was removed under reduced pressure. The product was extracted with ethyl acetate (15 ml) from water (4 ml). The organic layer was washed twice with a saturated NaHCO_3 -solution (10 ml) and dried over Na_2SO_4 . It was filtrated, the organic layer was concentrated under reduced pressure (4 ml) and it was precipitated with hexane (3 ml) to yield **62** (66 mg, 0.35 mmol, 14 %).

¹H-NMR (500 MHz, [D₃]MeOD): δ = 8.17 (s, 1 H), 7.70-7.68 (dd, J = 1.5, J = 7.0, 1 H), 7.49-7.48 (dd, J = 1.5, J = 6.5, 1 H), 7.33-7.30 (m, 2 H), 5.20 (s, 2 H), 3.78 (s, 3 H).

MS (ESI-MS): m/z (%): 191.8 (100) [M + H]⁺.

Compound **63**: **62** (66 mg, 0.35 mmol) was dissolved in MeOH (2 ml) and it was added an aqueous KOH- solution (2 M; 0.35 ml) as well as water (0.5 ml). The reaction mixture was stirred at 50°C for 50 minutes. The organic solvent was removed under reduced pressure and the pH was adjusted to 2.5 with an aqueous HCl-solution (6 M; 0.12 ml). Lyophilization yielded pure product **63** (77 mg, 0.36 mmol, 100%).

¹H-NMR (500 MHz, [D₃]MeOD): δ = 9.39 (s, 1 H), 7.89-7.86 (m, 2 H), 7.68-7.66 (m, 2 H), 5.42 (s, 2 H).

MS (ESI-MS): m/z (%): 177.8 (100) [M + H]⁺.

Compound **64**: **63** (21 mg, 0.12 mmol) was dissolved in DMF (3 ml) and 2-chloroethane amine hydrochloride (0.29 mg, 0.25 mmol) was added. The reaction mixture was cooled to 0°C. DMAP (0.49 mg, 0.4 mmol) was added. EDC·HCl (60 mg, 0.3 mmol) was added after 5 min. The reaction was stirred for 3 h at room temperature. The organic solvent was removed under reduced pressure. The crude product was purified by flash chromatography (silica; ethyl acetate (EA)/ dichloromethane (DCM)/MeOH = 8:12:5) to yield pure product **64** (17.3 mg, 0.073 mmol, 61 %).

R_f: 0.5 (Silicagel 60 F₂₅₄, EA/DCM/MeOH = 8/12/5)

¹H-NMR (500 MHz, [D₃]MeOD): δ = 8.17 (s, 1 H), 7.70-7.68 (dd, J = 1.0, J = 8.5, 1 H), 7.49-7.47 (dd, J = 1.5, J = 7.5, 1 H), 7.34-7.31 (m, 2 H), 5.02 (s, 2 H), 3.64-3.61 (m, 2 H), 3.57-3.55 (m, 2 H).

MS (ESI-MS): m/z (%): 238.5 (100) [M + H]⁺.

Compound **68**: Anhydrous DMF (7.5 ml) was added to sodium hydride (304 mg, 7.6 mmol) at -4 °C. Afterward adenine (**67**; 250 mg, 1.9 mmol) was added in small portions. The suspension was stirred vigorously for 3 min and benzyl chloroformate (0.58 ml, 4.8 mmol) was added dropwise. After stirring for 4 h, the reaction mixture was poured into

ice water (15 ml) and the pH was adjusted to 7 with aqueous HCl (1 N). The white precipitate was collected by filtration and was washed with water (1 ml) and ethyl ether (5 ml). Recrystallization from MeOH/DCM (1:1; 10 ml) afforded 171 mg of pure product **62** (0.64 mmol, 33%).

¹H-NMR (500MHz, [D₆]DMSO): δ = 8.59 (s, 1 H), 8.43 (s, 1 H), 7.48-7.34 (*m*, 5 H), 5.28 (s, 2 H).

MS (ESI-MS): *m/z* (%): 270.5 (96) [M + H]⁺, 561.2 (100) [2M + Na]⁺

Compound **69**: **68** (50 mg, 0.19 mmol) was dissolved in DMF (2 ml), before Cs₂CO₃ (5.2 mg, 0.02 mmol) and K₂CO₃ (23.8 mg, 0.17 mmol) were added. Methyl bromacetate (0.03 ml, 0.35 mmol) was added dropwise. After 2.5 h the reaction was stopped and the organic solvent was removed under reduced pressure. The product was extracted with ethyl acetate (15 ml) from water (4 ml). The organic layer was washed twice with an aqueous, saturated NaHCO₃-solution (5 ml) and dried over Na₂SO₄. The organic layer was concentrated under reduced pressure (2 ml) and it was precipitated with hexane (4 ml). The precipitate was filtrated off to yield **69** (30 mg, 0.09 mmol, 47 %).

¹H-NMR (500 MHz, [D₃]MeOD): δ = 8.61 (s, 1 H), 8.31 (s, 1 H), 7.49-7.28 (*m*, 5 H), 5.30 (*d*, 2 H), 5.18 (s, 2 H), 3.78 (s, 3 H).

MS (ESI-MS): *m/z* (%): 342.2 (100) [M + H]⁺.

Compound **70**: **69** (15 mg, 0.05 mmol) was dissolved in MeOH (2 ml) and it was added an aqueous KOH-solution (2 M; 0.1 ml) as well as water (0.5 ml). After 45 min of stirring at room temperature, the solvents were removed under reduced pressure to yield **70** (15 mg, 0.05 mmol, 100%).

¹H-NMR (500 MHz, [D₃]MeOD): δ = 8.58 (s, 1 H), 8.29 (s, 1 H), 7.48-7.33 (*m*, 5 H), 5.30 (*d*, 2 H), 4.86 (s, 2 H).

MS (ESI-MS): *m/z* (%): 328.2 (100) [M + H]⁺.

Compound **71**: **70** (15 mg, 0.05 mmol) was dissolved in DMF (3 ml). After the addition of 2-chloroethane amine hydrochloride (8 mg, 0.07 mmol), the reaction mixture was cooled to 0°C and DMAP (10 mg, 0.09 mmol) and EDC·HCl (18 mg, 0.09 mmol) were added.

The solvents were removed under reduced pressure after 6 h. The crude product was purified by flash chromatography (EA/DCM/MeOH = 16/24/5) to yield **71** (8 mg, 0.02 mmol, 46 %).

R_f: 0.5 (Silicagel 60 F₂₅₄, EA/DCM/MeOH = 8/12/5)

¹H-NMR (500 MHz, [D₃]MeOD): δ = 8.58 (s, 1 H), 8.31 (s, 1 H), 7.48 (d, 2 H), 7.32-7.40 (m, 3 H), 5.50 (s, 2 H), 5.30 (s, 1 H), 5.07 (s, 1 H), 4.43 (m, 1 H), 4.10 (m, 1 H), 3.54 – 3.64 (m, 2 H).

MS (ESI-MS): m/z (%): 387.1 (100) [M + H]⁺.

Compound **72**: **71** (30 mg, 0.077 mmol) was dissolved in MeOH (6 ml) and Pd on charcoal (10 %; 20 mg) was added. The mixture was stirred for 1.5 h at 65°C under an atmosphere of H₂. The precipitate and the catalyst were filtered off, and the solid was washed with water (3x 10 ml). The aqueous phase was collected and the solvent was removed under reduced pressure to yield pure product **72** (6 mg, 0.024 mmol, 31 %).

¹H-NMR (500 MHz, [D₃]MeOD): δ = 8.20 (s, 1 H), 8.10 (s, 1 H), 5.04 (s, 2 H), 3.65 (t, 2 H), 3.58 (t, 2 H).

MS (ESI-MS): m/z (%): 277.4 (100) [M + Na]⁺.

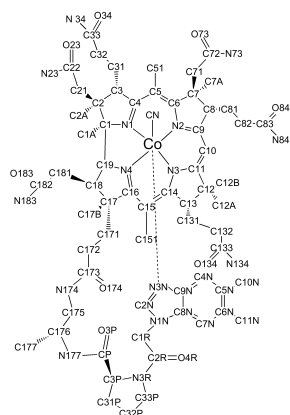
Cobalamins **33** and **34**: B12 (16 mg, 0.012 mmol) was dissolved in an aqueous NH₄Cl solution (10 %; 5 ml). The solution was purged with argon for 20 min. Zn pellets (2 g) were washed with an aqueous HCl-solution (3 ml, 1 M) and were added to the reaction mixture in two portions. After 1 h, the chloro-precursor **64** (or **72**; 4 mg) was added and the reaction was stirred for 24 h under protection from light. The zinc pellets were filtered off and it was separated by preparative reverse phase HPLC in a dark room. The following yields were obtained: **33** (6.1 mg; 33%,) and **34** (12.1 mg; 65 %).

NMR: see table 9.

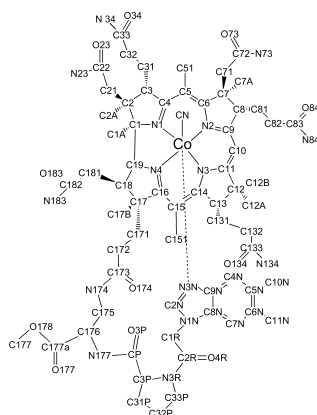
Compound **33**: HPLC-MS: R_t = 19.0 min; m/z (%) 1531.7 (100) [M + H]⁺. Calcd. for C₇₃H₁₀₀CoN₁₆O₁₅P: 1530.7.

Compound **34**: HPLC-MS: R_t = 18.7 min; m/z (%) 1548.8 (100) [M + H]⁺. Calcd. for C₇₁H₉₉CoN₁₉O₁₅P: 1547.7.

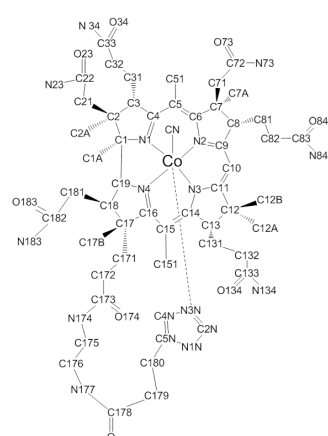
4.2 NMR tables



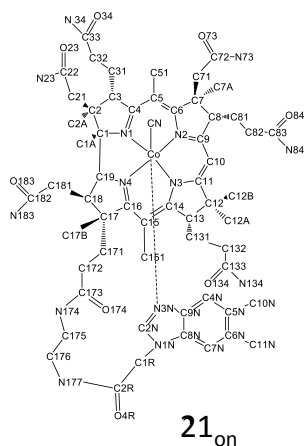
2 – 7, 14 15 and 31



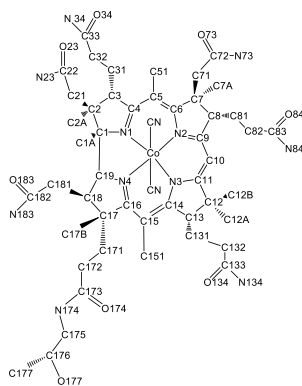
17 and 18



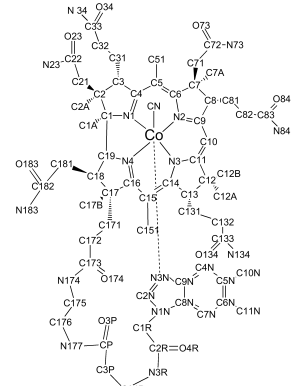
26 and 29 derivatives



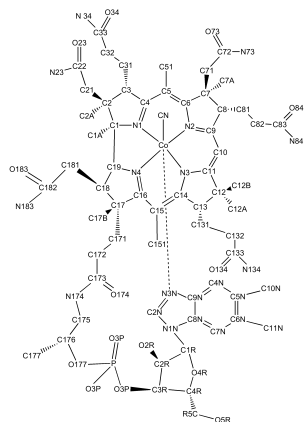
21_{on}



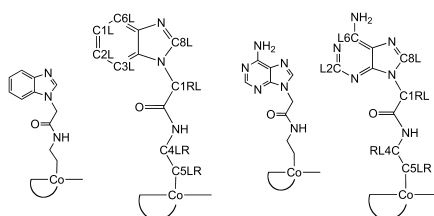
19_α, 19_α and 19_β



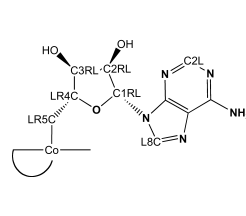
13



1, 31, 33 and 34



33 and 34



30 and 31

Figure 43: Atom labelling for B12 derivatives. Charges have been omitted.

Table 6: NMR chemical shift values of **1** - **5** and **7**

	δ ^1H [ppm]						δ ^{13}C [ppm]		$\Delta\delta$ (1-2)
	1	2	3 ^c	5	4 ^c	7	4	7	
C1							87.9	85.9	
C1A	0.49	0.57	0.64	0.51	0.64	1.54	22.6	24.4	- 0.08
C2							50.0	49.0	
C2A	1.44	1.46	1.46	1.50	1.44	1.58	19.6	19.2	- 0.02
C3	4.22	4.23	3.25	4.23	4.24	3.88	59.2	59.0	- 0.01
C4							182.8	179.4	
C5							110.1	107.7	
C6							168.2	165.6	
C7							54.1	51.9	
C7A	1.90	1.88	1.88	1.89	1.88	1.73	21.8	21.5	+ 0.02
C8	3.46	3.46	3.46	3.51	3.45	3.44	58.5	57.9	+ 0.00
C9							176.6	174.5	
C10	6.11	6.12	6.14	6.15	6.13	5.92	97.8	93.6	- 0.01
C11							179.8	180.3	
C12							51.4	49.6	
C12A	1.48	1.47	1.49	1.48	1.49	1.48	21.6	21.3	+ 0.01
C12B	1.23	1.19	1.20	1.20	1.20	1.23	33.4	33.0	+ 0.04
C13	3.37	3.39	3.40	3.42	3.38	3.34	56.4	55.9	- 0.02
C14							168.7	165.7	
C15							107.0	106.3	
C16							181.4	180.8	
C17							62.3	61.8	
C17B	1.42	1.46	1.48	1.46	1.48	1.35	19.3	20.3	- 0.04
C18	2.78	2.78	2.84	2.77	2.85	2.94	41.7	41.8	+ 0.00
C19	4.12	4.14	4.15	4.15	4.13	3.79	77.9	78.0	- 0.02
C21	2.43	2.43	2.44	2.41	2.45	2.28/2.31	45.5	44.9	+ 0.00

Experimental Procedures

C31	2.01	2.08	2.13	2.09	1.95	2.04/2.34	28.7	27.6	- 0.07
C32	2.55	2.58	2.58	2.57	2.70	2.51/2.60	37.7	37.7	- 0.03
C51	2.57	2.57	2.58	2.56	2.58	2.29	18.2	17.9	+ 0.00
C71	2.22/2.59	2.23/2.62	2.22/2.63	2.23/2.65	2.22/2.61	2.42/2.63	45.6	46.5	- 0.01/- 0.03
C81	1.03/2.02	0.97/2.07	0.92/1.96	1.01/2.00	2.10	1.82/2.17	28.8	29.3	+ 0.06/- 0.05
C82	1.04/1.85	0.97/1.96	0.95/1.81	1.06/1.92	0.95/1.79	2.32	34.4	34.5	+ 0.07/- 0.11
C131	2.00	2.05	1.92/2.10	2.01	1.90/2.11	1.87/2.17	30.7	28.5	- 0.05
C132	2.66	2.73	2.72	2.74	2.70	2.18/2.40	36.9	34.5	- 0.07
C151	2.60	2.58	2.58	2.53	2.59	2.35	17.5	17.6	+ 0.02
C171	2.18/2.53	1.78/2.45	1.78/2.67	1.73/2.47	1.75/2.68	2.06/2.55	35.6	36.0	
C172	1.88/2.64	2.85	2.80	2.60/2.81	1.99/2.26	1.90/2.45	33.8	36.2	
C175	2.98/3.63	3.29/3.57 ^b	3.16/3.80 ^b	3.22/3.55	2.66/3.59		48.1		
C176	4.31	3.09/3.57 ^b	3.60/3.80 ^b	3.97	4.30		46.5		
C177	1.28/1.30			1.17	1.14		19.4		
C181	2.74	2.74	2.70	2.74	2.74	2.77	34.8	35.5	+ 0.00
C3P		3.77/3.96	4.39	4.32	4.34		63.4		
C31P			2.02/2.28	2.07/2.29	1.99/2.30		32.7		
C32P			2.08/2.16	2.07/2.18	2.10		27.1		
C33P			3.78	3.83/3.87	3.75/3.82		50.0		
C1R	6.38	4.94/5.04	4.97/5.17	4.96/5.18	4.95/5.17		49.4		
C2N	7.12	7.01	6.95	7.03	6.94		146.0		+ 0.11
C4N	6.54	6.49	6.50	6.48	6.51		119.3		+ 0.05
C5N							136.0		
C6N							138.1		
C7N	7.31	7.18	7.15	7.04	7.18		113.9		+ 0.13
C8N							134.3		
C9N							139.2		
C10N	2.29	2.29	2.30	2.28	2.30		22.6		+ 0.00
C11N	2.29	2.27	2.28	2.26	2.29		22.2		+ 0.02

Experimental Procedures

Assignment by ^1H -NMR, ^{13}C -NMR, ^1H , ^{13}C -HSQC correlation and comparison with B12 (**1**) and dicyano-cobyrinic acid (**7**). ^aCarboxamide resonances C22, C33, C72, C83, C133, C173, C182 were not assigned. ^bThe protons at C175 and C176 were not assigned specifically. ^cmain rotamer.

Table 7: ^1H -NMR chemical shift values of **12** - **15**, **17** and **18**

	$\delta\ ^1\text{H}[\text{ppm}]$					
	12 ^a	13 ^b	14	15 ^c	17 ^c	18 ^c
C1						
C1A	0.55	0.45	0.67	0.52	0.63	0.63
C2						
C2A	1.53	1.43	1.42	1.37	1.45	1.44
C3	4.22	4.21	4.24	4.25	4.24	4.25
C4						
C5						
C6						
C7						
C7A	1.88	1.88	1.82	1.86	1.87	1.87
C8	3.46	3.45	3.41	3.41	3.44	3.44
C9						
C10	6.15	6.12	6.05	6.07	6.13	6.12
C11						
C12						
C12A	1.47	1.46	1.43	1.46	1.48	1.48
C12B	1.19	1.19	1.16	1.18	1.19	1.19
C13	3.37	3.37	3.39	3.40	3.38	3.38
C14						
C15						
C16						
C17						
C17B	1.47	1.36	1.47	1.39	1.48	1.47
C18	2.74	2.78	2.87	2.62	2.86	2.86
C19	4.16	4.12	4.16	4.11	4.13	4.13
C21	2.40	2.43	2.45	2.44	2.44	2.44
C31	2.12	2.03	2.10	2.05	2.14	2.11
C32	2.58	2.56	2.65	2.57		

Experimental Procedures

C51	2.64	2.58	2.60	2.52	2.58	2.58
C71	2.23/2.63	2.23/2.62	2.21/2.61	2.20/2.60	2.22/2.63	2.22/2.62
C81	0.95/1.98	1.04/2.12	2.16	2.04	0.91/1.98	0.94/1.91
C82	0.97/1.88	1.05/1.48	1.78	0.92/1.79	0.97/1.82	0.95/1.81
C131	1.92/2.03	1.91/2.01	1.87	1.89	1.93/2.10	1.91/2.09
C132	2.71	2.68	2.66	2.65	2.72	2.71
C151	2.57	2.56	2.55	2.57	2.58	2.58
C171	2.33/2.71	1.94/2.72	2.71	2.68	1.75/2.69	1.75/2.68
C172	1.84	2.12/2.42	2.40	2.36	2.14	2.05/2.20
C175	3.64	3.79/3.57/3.33/3.2	3.66	3.67	3.05/3.97	2.90/3.96
C176	3.12	3.79/3.57/3.33/3.2	3.98	4.03	5.06	4.77
C177			1.13	1.06	3.82	
C181	2.74	2.78	2.75	2.78	2.77	2.75
C3P		3.79/3.57/3.33/3.2	4.27	4.29	4.45	4.45
C31P		3.79/3.57/3.33/3.2	1.93/2.36	2.01/2.36	2.06/2.30	2.09/2.29
C32P			2.10	2.13	2.14	2.12
C33P			3.66	3.81	3.80	3.78
C1R	4.66/5.05	4.86/5.28	4.63/5.22	4.72/5.31	4.94/5.18	4.95/5.16
C2N	6.99	6.97	7.41	7.83	6.93	6.93
C4N	6.46	6.49	6.45	6.51	6.50	6.50
C5N						
C6N						
C7N	7.24	7.16	7.31	7.40	7.17	7.18
C8N						
C9N						
C10N	2.29	2.28	2.28	2.30	2.29	2.29
C11N	2.27	2.28	2.28	2.32	2.28	2.28

Assignment by ¹H-NMR, ¹H,¹³C-HSQC correlation and comparison with B12 (1). ^aThe protons at C175 and C176 were not assigned specifically. ^bThe protons at C175, C176, C3P and C31P were not assigned specifically. ^cmain rotamer.

Table 8: Comparison of NMR chemical shift values for **26-26**, **29-M**, **26-H**, **29-H**, α -aqua- β -cyano-cobinamide (**Cbi-CN β**) and β -aqua- α -cyano-cobinamide (**Cbi-CN α**):

	δ ^1H [ppm]						
	29-M	29-H [a]	Cbi-CNβ	26-26	26-H [a]	Cbi-CNα	B12-CNα
	α -imidazole β -cyano	α -aqua β -cyano	α -aqua β -cyano	α -cyano β -imidazole	α -cyano β -aqua	α -cyano β -aqua	α -cyano β -aqua
C1							
C1A	0.69	1.37	1.38	1.54	1.71	1.73	1.67
C2							
C2A	1.50	1.61	1.62	1.54	1.64	1.64	1.56
C3	4.11	4.11	4.11	4.11	3.99	4.00	3.98
C4							
C5							
C6							
C7							
C7A	1.81	1.82	1.82	1.67	1.74	1.74	1.76
C8	3.47	3.68	3.68	3.67	3.68	3.69	3.69
C9							
C10	6.10	6.53	6.52	6.03	6.46	6.45	6.48
C11							
C12							
C12A	1.50	1.41	1.42	1.54	1.35	1.37	1.32
C12B	1.21	1.17	1.18	1.21	1.35	1.35	1.35
C13	3.33	3.48	3.48	3.51	3.57	3.57	3.54
C14							
C15							
C16							
C17							
C17B	1.45	1.61	1.61	1.38	1.58	1.58	1.59
C18	2.71	3.09	3.10	3.40	3.11	3.13	3.07

Experimental Procedures

C19	4.09	4.26	4.25	3.21	4.08	4.08	4.08
C21	2.34/2.47	2.39/2.49	2.37/2.47	1.51/2.05	2.23/2.34	2.24/2.35	2.22/2.33
C31	2.05/2.24			2.18			
C32	2.59			2.59			
C51	2.40	2.37	2.38	2.42	2.42	2.44	2.41
C71	2.26/2.61	2.23/2.57	2.23/2.56	2.71/2.88	2.74	2.74	2.75
C81	1.37/2.17			2.00/2.45			
C82	1.37/2.56			2.20/2.38			
C131	1.96			1.96/2.19			
C132	2.64			2.37			
C151	2.50	2.45	2.47	2.52	2.41	2.41	2.40
C171	2.44/2.50			2.35/2.50			
C172	1.82/2.02			2.11/2.82			
C175	3.18/3.37 ^[b]			3.21/3.40 ^[b]			
C176	3.29 ^[b]			3.34 ^[b]			
C177							
C181	2.74/2.85			2.66			
C3P							
C179	2.15/2.30			2.06/2.42			
C180	2.70			2.68/2.83			
C2N	6.65	8.62		7.05	8.53		
C4N	5.84	7.26		5.35	7.17		

Assignment by ¹H-NMR, ¹³C-NMR, ¹H, ¹³C-HSQC correlation, ROESY and comparison with B12.

^aCompound **1-H** and **2-H** are partially signed for comparison with **Cbi-CN_β** and **Cbi-CN_α**.

^bThe protons at C175 and C176 positions were not assigned specifically.

Table 9: NMR chemical shift values for **30**, **31**, **33** and **34**:

	δ ^1H [ppm]			
	31	30	33	34
C1				
C1A	0.50	0.61	0.48	0.48
C2				
C2A	1.40	1.36	1.40	1.37
C3	4.13	4.18	4.07	4.03
C7A	1.75	1.78	1.76	1.79
C8	3.33	3.44	3.26	3.25
C9				
C10	5.97	6.20	6.02	6.02
C11				
C12				
C12A	1.36	1.42	1.45	1.43
C12B	0.88	0.72	1.14	1.1
C13	2.91	2.96	3.23	3.21
C17B	1.39	1.43	1.36	1.39
C18	2.66	2.52	2.67	2.67
C19	4.36	4.35	4.09	4.13
C21	2.45	2.43	2.21/2.30	2.33
C31	2.00/2.10	2.09	1.98/2.06	2.02/2.08
C32	2.53	2.55	2.48/2.54	2.49/2.55
C51	2.50	2.42	2.45	2.48
C71	1.77/2.26	1.85/2.34	1.66/2.04	1.86/2.26
C81	0.84/1.79	1.00/1.87	0.85/1.80	0.83/1.78
C82	0.95/1.75	1.24/1.84	1.00/1.76	0.83/1.82
C131	2.04/2.24	1.99/2.20	2.09	2.08
C132	2.58	2.51	2.64	2.63
C151	2.47	2.50	2.50	2.5
C171	2.10/2.48	1.97	1.82/2.54	1.81/2.55

Experimental Procedures

C172	1.86/2.58	1.83/2.53	2.10/2.46	2.44
C175	3.18/3.57	3.53/3.35	3.14/3.57	3.14/3.56
C176	4.26	3.43/3.16	4.34	4.33
C177	1.24		1.24	1.21
C181	2.67	2.67	2.63/2.72	2.64/2.73
C3P		3.77/3.94		
C1R	6.27	4.96/4.89	6.27	6.27
C2R	4.26		4.24	4.23
C3R	4.78		4.74	4.72
C4R	4.12		4.10	4.1
C5R	3.77/3.92		3.77/3.92	3.75/3.91
C2N	6.97	7.03	6.95	6.95
C4N	6.27	6.49	6.24	6.25
C5N				
C6N				
C7N	7.19	7.10	7.18	7.17
C8N				
C9N				
C10N	2.24	2.25	2.23	2.22
C11N	2.24	2.24	2.22	2.22
C1RL	5.60		4.83	4.76
C2RL	4.57	4.51		
C3RL	3.78	3.83		
C4RL	2.68	2.75	1.71/2.21	1.68/2.22
C5RL	0.60/1.56	0.47/1.30	0.32/1.11	0.49/1.21
C2L(C1L)	8.26	8.27	7.26(7.41)	8.15
C3L			7.26	
C6L			7.77	
C8L	8.04	8.04	8.12	8.03

Assignment by ^1H -NMR, ^1H , ^{13}C -HSQC correlation and comparison with adenosyl B12.

- [1] J. Stubbe, *Science*, **1994**, 266, 1663-1664.
- [2] R. Banerjee, *Chemistry and Biochemistry of B12*, Wiley, New York, **1999**.
- [3] D. Arigoni, B. Golding, *Vitamin B12 and B12-Proteins*, Wiley-VCH, Weinheim, **1998**.
- [4] www.nobelprize.org
- [5] E. Rickes, N. Brink, F. Koniuszy, T. R. Wood, K. Folkers, *Science*, **1948**, 107, 396-397.
- [6] N. Brink, *J. Am. Chem. Soc.*, **1952**, 74, 2856-2858
- [7] N. Brink, D. Wolf, E. Kaczka, *J. Am. Chem. Soc.*, **1949**, 71, 1854-1856.
- [8] N. Brink, *J. Am. Chem. Soc.*, **1949**, 71, 2951.
- [9] N. Brink, *J. Am. Chem. Soc.*, **1950**, 72, 4442-4443.
- [10] E. Kaczka, *J. Am. Chem. Soc.*, **1953**, 75, 6317-6318.
- [11] B. Ellis, V. Petrow, G. F. Snook, *J. Pharm. Pharmacol.* **1949**, 1, 735-735.
- [12] D. E. Sands, *Introduction to Crystallography*, Dover Publications, **1994**.
- [13] D. C. Hodgkin, J. Kamper, M. Mackay, J. Pickworth, K. N. Trueblood, J. G. White, *Nature*, **1956**, 178, 64-66.
- [14] D. Hodgkin, J. Kamper, J. Lindsey, *Proc. R. Soc. London, Ser. A*, **1957**, 242, 228
- [15] J. P. Glusker, *Protein Sci.*, **1994**, 3, 2465-2469.
- [16] A. Eschenmoser, *Science*, **1977**, 196, 1410-1420.
- [17] R. Woodward, *Pure Appl. Chem.*, **1973**, 33, 145-177.
- [18] R. Woodward, *Symposium on the Chemistry of Natural Products*, **1971**.
- [19] K. Nicolaou, D. Vourloumis, *Angew. Chem. Int. Edit.*, **2000**, 39, 44-122.
- [20] R. Banerjee, R. G. Matthews, *The FASEB journal*, **1990**, 1450-1459.
- [21] R. Reitzer, K. Gruber, G. Jögl, U. Wagner, H. Bothe, W. Buckel, C. Kratky, *Structure*, **1999**, 7, 891-902.
- [22] D. Lexa, J. M. Sayeant, J. Zickler, *J. Am. Chem. Soc.*, **1980**, 102, 2654-2663.
- [23] D. Lexa, J. M. Saveant, *J. Am. Chem. Soc.*, **1976**, 98, 2652-2658.
- [24] D. Lexa, J. M. Saveant, J. Zickler, *J. Am. Chem. Soc.*, **1977**, 99, 2786-2790.
- [25] D. Lexa, J. M. Saveant, *Acc. Chem. Res* **1983**, 16, 235-243.

- [26] C. Drennan, S. Huang, J. Drummond, R. G. Matthews, M. L. Ludwig, *Science*, **1994**, 266, 1669-1674.
- [27] F. Mancia, N. Keep, A. Nakagawa, P. Leadlay, *Structure*, **1996**, 4, 339-350.
- [28] J. Masuda, N. Shibata, Y. Morimoto, T. Toraya, N. Yasuoka, *Structure*, **2000**, 8, 775-788.
- [29] M. D. Sintchak, G. Arjara, B. A. Kellogg, J. Stubbe, C. L. Drennan, *Nat. Struct. Mol. Biol.*, **2002**, 9, 293-300.
- [30] J. Wuerges, G. Garau, S. Geremia, S. Fedosov, T. Petersen, L. Randaccio, *PNAS*, **2006**, 103, 4386-4391.
- [31] F. Mathews, M. Gordon, Z. Chen, K. Rajashankar, S. Ealick, D. Alpers, N. Sukumar, *PNAS*, **2007**, 104, 17311-17316.
- [32] M. J. Albert, V. I. Mathan, S. J. Baker, *Nature*, **1980**, 283, 781-782.
- [33] L. P. Dryden, A. M. Hartman, M. P. Bryant, I. M. Robinson, L. A. Moore, *Nature*, **1962**, 195, 201-202.
- [34] *en.wikipedia.org*
- [35] F. Watanabe, *Exp. Biol. Med.* **2007**, 232, 1266-1274.
- [36] D. Allis, T. Fairchild, R. Doyle, *Mol. BioSys.*, **2010**, 6, 1611-1618.
- [37] R. Banerjee, C. Gherasim, D. Padovani, *Curr. Opin. Chem. Biol.*, **2009**, 13, 484-491.
- [38] A. Marchaj, D. W. Jacobsen, S. R. Savon, K. L. Brown, *J. Am. Chem. Soc.*, **1995**, 117, 11640-11646.
- [39] R. Abeles, D. Dolphin, *Acc. Chem. Res.*, **1976**, 9, 114-120.
- [40] R. G. Matthews, *Acc. Chem. Res.*, **2001**, 34, 681-689.
- [41] C. L. Drennan, R. G. Matthews, M. L. Ludwig, *Curr. Opin. Struct. Biol.*, **1994**, 4, 919-929.
- [42] J. T. Jarrett, M. Amaratunga, C. L. Drennan, J. D. Scholten, R. H. Sands, M. L. Ludwig, R. G. Matthews, *Biochemistry*, **1996**, 35, 2464-2475.
- [43] L. Stryer, *Biochemistry*, New York, W H Freeman, **1988**.
- [44] S. Cortellino, J. Xu, M. Sannai, R. Moore, E. Caretti, A. Cigliano, M. Le Coz, K. Devarajan, A. Wessels, D. Soprano, *Cell*, **2011**, 146, 67-79.

- [45] T. R. Halfdanarson, J. A. Walker, M. R. Litzow, C. A. Hanson, *Eur. J. Haematol.*, **2008**, *80*, 448-451.
- [46] F. Bethell, M. Meyers, *J. Lab. Clin. Med.*, **1948**, *33*, 1477.
- [47] S. Datta, M. Koutmos, K. Patridge, M. Ludwig, R. Matthews, *PNAS*, **2008**, *105*, 4115-4120.
- [48] F. Mancia, G. A. Smith, P. R. Evans, *Biochemistry*, **1999**, *38*, 7999-8005.
- [49] W. Manzanares, G. Hardy, *Curr. Opin. Clin. Nutr. & Meta. Care*, **2010**, *13*, 662-668.
- [50] M. Yoon, PhD thesis, University of Michigan, **2009**.
- [51] D. E. Holloway, E. N. Marsh, *J. Biol. Chem.*, **1994**, *269*, 20425-20430.
- [52] T. Kamachi, T. Toraya, K. Yoshizawa, *J. Am. Chem. Soc.*, **2004**, *126*, 16207-16216.
- [53] L. R. McDowell, *Vitamins in Animal and Human Nutrition*, Wiley-Blackwell, **2000**.
- [54] K. Brown, J. Hakimi, *J. Am. Chem. Soc.*, **1986**, *108*, 496-503.
- [55] K. L. Brown, *Chem. Rev.*, **2005**, *105*, 2075-2150.
- [56] Z. Schneider, A. Stroiński, *Comprehensive B12*, Walter De Gruyter, **1987**.
- [57] T. Toraya, S. Miyoshi, M. Mori, K. Wada, *Biochim. Biophys. Acta*, **1994**, *1204*, 169-174.
- [58] T. Toraya, A. Ishida, *J. Biol. Chem.*, **1991**, *266*, 5430-5437.
- [59] S. Chowdhury, M. Thomas, J. Escalante-Semerena, R. Banerjee, *J. Biol. Chem.*, **2001**, *276*, 1015-1019.
- [60] M. Hamza, X. Zou, R. Banka, K. Brown, R. Eldik, *Dalton Trans.*, **2005**, *2005*, 782-787.
- [61] R. Wang, B. MacGillivray, D. Macartney, *Dalton Trans.*, **2009**, *2009*, 3584-3589.
- [62] F. Wagner, *Proc. R. Soc. London, Ser. A*, **1965**, *288*, 344-347.
- [63] F. H. Zelder, *Inorg. Chem.* **2008**, *47*, 1264-1266.
- [64] J. Jarrett, C. Choi, R. G. Matthews, *Biochemistry*, **1997**, *36*, 15738-15748.
- [65] A. McDermott, *Annu. Rev. Biophys.*, **2009**, *38*, 385-403.
- [66] I. Usón, G. M. Sheldrick, *Curr. Opin. Struct. Biol.*, **1999**, *9*, 643-648.
- [67] P. Ruiz-Sánchez, S. Mundwiler, B. Spingler, N. R. Buan, J. C. Escalante-Semerena, R. Alberto, *J. Biol. Inorg. Chem.*, **2008**, *13*, 335-347.

- [68] P. Ruiz-Sanchez, S. Mundwiler, *Chimia*, **2007**, *61*, 190-193.
- [69] S. Kunze, F. Zobi, P. Kurz, B. Spingler, R. Alberto, *Angew.*, **2004**, *116*, 5135-5139.
- [70] C. Rosenblum, *Talanta*, **1964**, *11*, 255-269.
- [71] D. B. Endres, K. Painter, G. D. Niswender, *Clin. Chem.*, **1978**, *24*, 460-465.
- [72] T. M. Houts, *Clin. Chim. Acta*, **1982**, *126*, 315-322.
- [73] R. Alberto, *Topics in Organometallic Chemistry*, Springer Berlin Heidelberg, Berlin, Heidelberg, **2010**, *32*, 219-246.
- [74] R. Banerjee, *Wiley*, **1999**, New York.
- [75] T. Toraya, T. Shirakashi, S. Fukui, H. Hogenkamp, *Biochemistry*, **1975**, *14*, 3949-3952.
- [76] K. L. Brown, S. Cheng, X. Zou, J. Li, G. Chen, E. J. Valente, J. D. Zubkowski, H. M. Marques, *Biochemistry*, **1998**, *37*, 9704-9715.
- [77] H. Pfeiffer, TH Stuttgart, PhD Thesis, **1967**.
- [78] L. Knapton, H. Marques, *Dalton Trans.*, **2005**, *2005*, 889-895.
- [79] P. Butler, M. Ebert, A. Lyskowski, K. Gruber, C. Kratky, B. Kräutler, *Angew. Chem. Int. Edit.*, **2006**, *45*, 989-993.
- [80] P. A. Butler, S. Murtaza, B. Kräutler, *Monatsh. Chem.*, **2006**, *137*, 1579-1589.
- [81] A. Eschenmoser, *Angew. Chem. Int. Edit.*, **1988**, *27*, 5-39.
- [82] B. Kräutler, *Angew. Chem. Int. Edit.*, **2011**, *50*, 2439-2441.
- [83] M. Yamanishi, T. Labunska, R. Banerjee, *J. Am. Chem. Soc.*, **2005**, *127*, 526-527.
- [84] M. Uyemura, T. Aida, *J. Am. Chem. Soc.*, **2002**, *124*, 11392-11403.
- [85] E. Suarez-Moreira, J. Yun, C. S. Birch, J. H. H. Williams, A. Mccaddon, N. E. Brasch, *J. Am. Chem. Soc.*, **2009**, *131*, 15078-15079.
- [86] V. Sharma, R. Pilz, G. Boss, D. Magde, *Biochemistry*, **2003**, *42*, 8900-8908.
- [87] T. A. Shell, D. S. Lawrence, *J. Am. Chem. Soc.*, **2011**, *133*, 2148-2150.
- [88] C. Männel-Croisé, B. Probst, F. Zelder, *Anal. Chem.*, **2009**, *81*, 9493-9498.
- [89] C. Männel-Croisé, F. Zelder, *Chem. Commun.* **2011**, *47*, 11249-11251.
- [90] C. Männel-Croisé, F. Zelder, *Inorg. Chem.*, **2009**, *48*, 1272-1274.
- [91] F. H. Zelder, C. Männel-Croisé, *Chimia*, **2009**, *63*, 58-62.

- [92] S. Gallo, S. Mundwiler, R. Alberto, R. K. O. Sigel, *Chem. Commun.*, **2011**, 47, 403-405.
- [93] S. Gschösser, K. Gruber, C. Kratky, *Angew. Chem. Int. Edit.*, **2005**, 44, 2284-2288.
- [94] S. Gallo, M. Oberhuber, R. K. O. Sigel, B. Kräutler, *ChemBioChem.*, **2008**, 9, 1408-1414.
- [95] M. Lee, C. B. Grissom, *Org. Lett.*, **2009**, 11, 2499-2502.
- [96] M. Ebbing, K. H. Bonna, O. Nygard, E. Arnesen, P. M. Ueland, J. E. Nordrehaug, K. Rasmussen, I. Njolstad, H. Refsum, D. W. Nilsen, *JAMA*, **2009**, 302, 2119-2126.
- [97] F. Huennekens, P. Digirolamo, K. Fujii, D. Jacobson, K. Vitols, *Adv. Enzy. Regul.*, **1976**, 14, 187-205.
- [98] H. Vlajinac, *Eur. J. Cancer*, **1997**, 33, 101-107.
- [99] V. Koppenhagen, B. Elsenhans, F. Wagner, J. Pfiffner, *J. Biol. Chem.*, **1974**, 249, 6532-6540.
- [100] V. Koppenhagen, *J. Biol. Chem.*, **1970**, 245, 5865-5873.
- [101] B. Zagalak, W. Friedrich, Vitamin B12, *Walter de Gruyter*, **1979**, 647-648.
- [102] J. I. Toohey, *PNAS*, **1965**, 54, 934-942.
- [103] S. Takada, *PNAS*, **1999**, 96, 11698-11700.
- [104] P. E. Nielsen, M. Egholm, R. H. Berg, O. Buchardt, *Science*, **1991**, 254, 1497-1500.
- [105] U. Diederichsen, *Angew. Chem. Int. Edit.*, **1998**, 37, 302-305.
- [106] G. K. Mittapalli, Y. M. Osornio, M. A. Guerrero, K. R. Reddy, R. Krishnamurthy, A. Eschenmoser, *Angew. Chem. Int. Edit.*, **2007**, 46, 2478-2484.
- [107] K. L. Brown, X. Zou, *J. Am. Chem. Soc.*, **1992**, 114, 9643-9651.
- [108] K. Brown, X. Zou, *Inorg. Chem.*, **1991**, 30, 4185-4191.
- [109] K. Brown, D. Zhao, S. Cheng, X. Zou, *Inorg., Chem.*, **1997**, 36, 1764-1771.
- [110] K. L. Brown, J. M. Hakimi, D. M. Nuss, Y. D. Montejano, D. W. Jacobsen, *Inorg. Chem.*, **1984**, 23, 1463-1471.
- [111] M. Moskopididis, W. Friedrich, *Z. Naturforsch. B*, **1968**, 23, 804-812.

- [112] J. M. Pratt, *Inorganic Chemistry of Vitamin B12.*, London, UK, Academic Press Inc. (London) Ltd., **1972**.
- [113] K. Brown, J. M. Hakimi, *Inorg. Chem.* **1984**, *23*, 1756-1764.
- [114] U. Ermler, W. Grabarse, S. Shima, M. Goubeaud, R. K. Thauer, *Science*, **1997**, *278*, 1457-1462.
- [115] J. C. Kendrew, R. E. Dickerson, B. E. Strandberg, R. G. Hart, D. R. Davies, D. C. Phillips, V. C. Shore, *Nature*, **1960**, *185*, 422-427.
- [116] D. T. Denhardt, *Nature*, **1968**, *220*, 131-134.
- [117] C. Hunter, L. D. Sarson, *Angew. Chem. Int. Edit.*, **1994**, *33*, 2313-2316.
- [118] X. Chi, A. Guerin, R. Haycock, C. Hunter, *J. Chem. Soc.*, **1995**, 2567-2569.
- [119] R. A. Haycock, C. A. Hunter, D. A. James, U. Michelsen, L. R. Sutton, *Org. Lett.*, **2000**, *2*, 2435-2438.
- [120] J. K. Sprafke, B. Odell, T. D. W. Claridge, H. L. Anderson, *Angew. Chem. Int. Edit.*, **2011**, DOI 10.1002/anie.201008087.
- [121] S. Murtaza, P. Butler, C. Kratky, K. Gruber, B. Kräutler, *Chemistry*, **2008**, *14*, 7521-7524.
- [122] B. Kräutler, T. Dérer, P. Liu, W. Mühlecker, M. Puchberger, K. Gruber, C. Kratky, *Angew. Chem. Int. Ed.*, **1995**, *34*, 84-86.
- [123] R. B. Hannak, G. Färber, R. Konrat, B. Kräutler, *J. Am. Chem. Soc.*, **1997**, *119*, 2313-2314.
- [124] F. Kreppelt, ETH Zurich, PhD thesis, **1991**.
- [125] P. Chakrabarti, *Helv. Chim. Acta.*, **1982**, *65*, 1555-1562.
- [126] G. Müller, O. Müller, *Z. Naturforsch. B*, **1966**, 1159-1164.
- [127] K. Zhou, F. Zelder, *Angew. Chem. Int. Edit.*, **2010**, *49*, 5178-5180.
- [128] P. Renz, J. R. A. Vogt, *Eur. J. Biochem.*, **1971**, *171*, 655-659.
- [129] X. Zou, D. Evans, K. Brown, *Inorg. Chem.*, **1995**, *34*, 1634-1635.
- [130] W. Friedrich, G. Gross, K. Bernhauer, *Helv. Chim. Acta*, **1960**, *56*, 704-712.
- [131] K. Zhou, F. Zelder, *J. Porphyrins Phthalocyanines*, **2011**, *15*, 555-559.
- [132] K. Zhou, F. Zelder, *Eur. J. Inorg. Chem.*, **2011**, 53-57.
- [133] D. F. Taber, M. Rahimizadeh, *J. Org. Chem.* **1992**, *57*, 4037-4038.

- [134] R. Bonnett, J. R. Cannon, V. M. Clark, A. W. Johnson, L. F. J. Parker, E. L. Smith, A. Todd, *J. Chem. Soc.*, **1957**, 1158-1168.
- [135] K. Zhou, F. Zelder, *Chem. Commun.*, **2011**, 47, 11999-12001.
- [136] W. Reenstra, W. Jencks, *J. Am. Chem. Soc.*, **1979**, 101, 5780-5791.
- [137] J. Stubbe, D. G. Nocera, C. S. Yee, M. C. Y. Chang, *Chem. Rev.*, **2003**, 103, 2167–2201
- [138] K. Larsson, D. T. Logan, P. Nordlund, *Acs. Chem. Biol.* **2010**, 5, 933-942.
- [139] J. Valu, *Appl. Environ. Microbiol.* **1965**, 13, 486-490.
- [140] H. Chen, E. N. G. Marsh, *Biochemistry*, **1997**, 36, 7884-7889.
- [141] S. Jordan, C. Schwemler, W. Kosch, *Bioorg. Med. Chem. Lett.*, **1997**, 7, 681-686.
- [142] P. K. Mandal, J. S. McMurray, *J. Org. Chem.*, **2007**, 72, 6599-6601.

Traveling 12000 kilometers, crossing 7 time zones and knowing nobody here in Zurich, I started my PhD journal at 2008. I had never expected that I would enjoy this experience so much for the past three and a half years. Not only because I had a great project that I was truly devoted into, but also the great people around me helped and pushed me to be a better version of myself.

Dr. Felix Zelder led me into the world of B12, which is absolutely beautiful, but what impressed me the most is his enthusiasm for the project, for the chemistry and for the people. It is his inspiring spirit that catalyzes me and our project, and the sparks of ideals often come out during those inspirational conversations. Therefore I want to thank Felix for being my supervisor and also for being my friend.

Prof. Dr. Roger Alberto is always supportive to me and to my project. He often gave good suggestions to my papers, which is very important and valuable. The every year retreat he supported is always great fun and brings the group members together.

I want to thank Prof. Roland Sigel for being my co-advisor and organizing the graduate retreat every year.

I want to thank Prof. Dr. Albert Eschenmoser for visit and discussion. He is a big inspiration for me to work with B12 chemistry.

I want to thank our collaborator Dr. Helmut Brandl's help in bacteria tests and it's pleasure to work with him. Prof. Wolfgang Buckel is very helpful with enzymatic tests. I really appreciate their help.

Christine Männel-Croisé and René Oetterli are the kind of lab-mates that I couldn't ask for more. They are always there, no matter as colleagues or as friends.

Of course, the people in ACI are excellent to work with. Dr. Karel Zelenka, Dr. Pillar Sanchez, Dr. Thomas Fox, Dr. Paul Schmutz, Dr. Benjamin Probst and Mai Tran are very helpful to share their experiences. Besides, Dr. Laurent Bigler, Prof. Dr. Oliver Zerbe and Dr. Olivier Blacque are very helpful in MS, NMR and computation.

I also want to thank the graduate school for opening my PhD journal and supporting me for the conference, and of course the graduate school retreat is a great opportunity for inter-disciplinary communication and connecting people.

Last but not least, I want to thank all my Chinese friends here in Zurich. You give my life a taste of home. I want to thank my parents most for their support in every step of my life. Without them, none of these would be possible.

Surname: ZHOU
First name Kai
Nationality: Chinese
Date of Birth: 11/10/1982

Education:

07/2008 - 12/2011 PhD study at the Institute of Inorganic Chemistry, University of Zurich, Switzerland
09/2005 - 06/2008 Master Study at the State Key Laboratory of Coordination Chemistry, Nanjing University, China
Diploma subject: Inorganic Chemistry
Title of the thesis: Phosphonate complexes as catalysts for organic reactions
09/2003 - 06/2005 Bachelor Study at Nanjing University, China
01/2003 - 06/2003 International Student Exchange Program with the Hong Kong University of Science and Technology, Hong Kong
09/2001 - 01/2003 Bachelor Study at Nanjing University, China
09/1998 - 06/2001 No.1 High School, Changzhou, Jiangsu, China

Publications:

2010 1. K. Zhou, F. Zelder, *Angew. Chem. Int. Ed.* **2010**, 49, 5178.
2011 2. K. Zhou, F. Zelder, *Chem. Commun.* **2011**, 47, 11999.
3. K. Zhou, F. Zelder, *Eur. J. Inorg. Chem.* **2011**, 53.
4. K. Zhou, F. Zelder, *J. Porphyrins Phthalocyanines*. **2011**, 15, 555.

Awards:

2011 CMSZH Travel Award from the Graduate School of Chemical and Molecular Sciences Zurich.
2011 SCNAT/SCS Chemistry Travel Award from the Swiss Academy of Sciences.

09/2011

Oral Presentation at the Swiss Chemical Society Fall Meeting, EPFL Lausanne,
Switzerland

04/2011

Oral Presentation at the First EuCheMS Inorganic Chemistry Conference, University of
Manchester, UK

09/2010

Poster Presentation at the Swiss Chemical Society Fall Meeting, University of Zurich,
Switzerland

09/2009

Poster Presentation at the Swiss Chemical Society Fall Meeting, EPFL Lausanne,
Switzerland

Publications during PhD Studies:

Appendix I

K. Zhou, F. Zelder, *Angew. Chem. Int. Ed.* **2010**, 49, 5178.

Appendix II

K. Zhou, F. Zelder, *Eur. J. Inorg. Chem.* **2011**, 53.

Appendix III

K. Zhou, F. Zelder, *J. Porphyrins Phthalocyanines*. **2011**, 15, 555.

Appendix IV

K. Zhou, F. Zelder, *Chem. Commun.* **2011**, 47, 11999.

Communications

Biomimetics

DOI: 10.1002/anie.201001928

Vitamin B₁₂ Mimics Having a Peptide Backbone and Tuneable Coordination and Redox Properties**

Kai Zhou and Felix Zelder*

Cobalamines (Cbls) are corrinoids that can adopt different constitutional states, in which the dimethylbenzimidazole base (Dmbz) is either bound (base on) or has been displaced (base off) from the Co center of the macrocycle.^[1,2] This equilibrium plays an important role for the delivery, transformation, and reactivity of vitamin B₁₂ (**1**, CNCbl) and its organometallic analogues.^[3] Small amounts of base-on vitamin B₁₂ (10 µg per day) are channeled through a sophisticated and highly selective pathway into the cells before it is converted to the cofactors adenosylcobalamin (AdoCbl) and methylcobalamin (MeCbl).^[4]

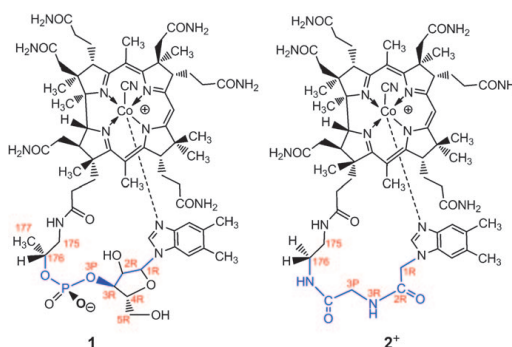
Only recently, the reductive decyanation of base-on CNCbl to a base-off Co^{II} species catalyzed by the trafficking chaperone *MMACHC* was reported.^[5] Difficulties in this reduction are related to mutations of the corresponding *MMACHC* genes,^[4] and medical studies suggest some therapeutic effect for Cbl derivatives that are easier to reduce than **1** to the intermediate Co^I state.^[6,7]

Detailed studies have been reported for the inorganic chemistry of Cbls with different ligands at the β side (upper side),^[8–10] but rather little is known how structural changes at the α side (lower side) of the molecule influence the coordination behavior of the Dmbz base^[11–13] and the corresponding redox properties of the metal ion. Herein, we report on the coordination chemistry and accompanying electrochemical properties of a new class of vitamin B₁₂ mimics in which a peptide linker tethers the corrin macrocycle to the Dmbz base.

Kräutler et al. demonstrated in an elegant study that a single methyl group quite distant from the coordination site stabilizes the base-on form of natural Cbls, as had been predicted earlier by Eschenmoser et al.^[11,14] In another pioneering study, Toraya and Ishida replaced the α-ribofuranotide moiety in vitamin B₁₂ with “methylene bridges” of different length.^[12]

With a view toward future biological applications, we are interested in the development of artificial derivatives of

vitamin B₁₂ with tuneable coordination and electrochemical properties. We decided to investigate the replacement of the ribose phosphodiester moiety of vitamin B₁₂ with peptide structures containing the same number of atoms between the corrin macrocycle and the nitrogen donor of the Dmbz base (Scheme 1), because amides have already been excellent



Scheme 1. Structural formula of vitamin B₁₂ (**1**) and the peptide B₁₂ prototype **2**⁺. The natural linker in **1** and the peptide mimic in **2**⁺ contain the same number of atoms (shown in blue; the complete atom numbering is given in the Supporting Information).

mimics of phosphodiester in other natural products leading to derivatives with interesting novel physico-chemical properties and biological functions.^[17–20]

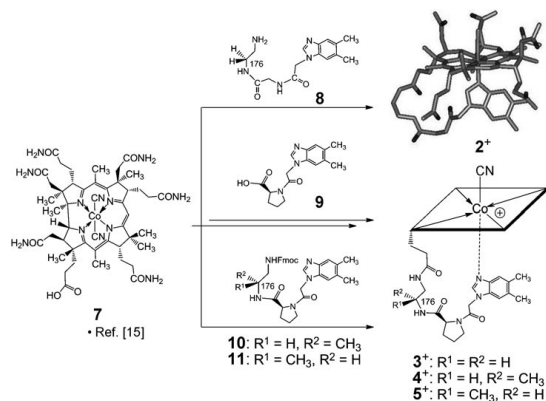
An energy-minimized structure of **2**⁺ (Scheme 2, top right) was obtained from semiempirical quantum chemical calculations (PM3, Spartan '06 software) in which the Dmbz base is in a similar position as in its natural counterpart **1**. The artificial linker **8** was synthesized in six steps and coupled with dimethylaminopyridine and *N*'-(3-dimethylaminopropyl)-*N*-ethylcarbodiimide hydrochloride to dicyanocobyrinic acid **7**^[15] to yield **2** in 62 % yield (Scheme 2).^[16]

The high-resolution mass spectrum of **2** displays the signal of a [*M*]⁺ ion at *m/z* 1243.59334 (*m/z*_{calc} 1243.59337) consistent with the molecular formula C₆₁H₈₄CoN₁₆O₉. Compound **2** was further characterized by UV/Vis spectroscopy, RP-HPLC, ¹H NMR analysis, and ¹H,¹³C-HSQC correlations.^[16] The UV/Vis spectra of base-on vitamin B₁₂ (**1**) and **2** are identical, but differ significantly (Δλ_{max} = 29 nm) from the absorption spectra of aquocyno-cobinamide indicating that **2** occurs in its base-on form.^[16] The corresponding ¹H NMR spectra show only minor shifts for the signals of the corrin macrocycle as well as the Dmbz base, but differ substantially for the connecting linker (Figure 1).^[16]

[*] K. Zhou, Dr. F. Zelder
Institute of Inorganic Chemistry, University of Zurich
Winterthurerstrasse 190, 8057 Zurich (Switzerland)
Fax: (+ 41) 446-356-802
E-mail: zelder@aci.uzh.ch

[**] We thank R. Alberto, A. Eschenmoser, T. Fox, and O. Zerbe for helpful discussions and L. Bigler for recording the HR-ESI-MS spectra. A generous gift of vitamin B₁₂ from DSM Nutritional Products AG (Basel/Switzerland) is acknowledged. This work was supported by the Swiss National Science Foundation (grant no. 200021-117822).

Supporting information for this article is available on the WWW under <http://dx.doi.org/10.1002/anie.201001928>.



Scheme 2. Synthesis of peptide B₁₂ derivatives 2⁺–5⁺ from dicyanocobyrinic acid (7)^[15] and peptide linkers 8–11.^[16] Compounds 2⁺–5⁺ were isolated as 2⁺·CF₃COO[−]–5⁺·CF₃COO[−] (2[−]–5[−]). Derivative 2⁺ (top right) is shown as the energy-minimized structure (Spartan '06, PM3 semiempirical calculation; H atoms not shown). Fmoc = 9-fluorenylmethoxycarbonyl.

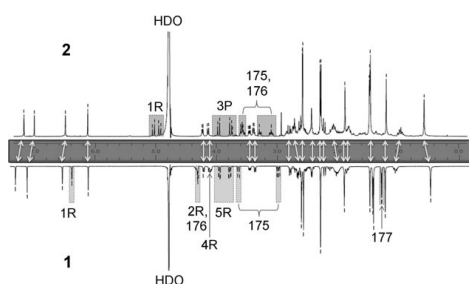


Figure 1. ¹H NMR spectrum of **2** (top) and **1** (bottom) in D₂O. The arrows indicate corresponding positions of signals arising from the corrin ring and the Dmbz base. The assignments refer to the protons of the linker (Scheme 1).

The intramolecular dissociation of the Dmbz base (Table 1, top left) of **2** was studied by spectrophotometric pH titration. The stability of the coordinated base-on form of **2** ($pK_{\text{base-off}} = 1.38$) is 19 times lower (K^* ; Table 1 entry 2 vs. 1) than that of the natural counterpart, which displays strong intramolecular coordination and a low $pK_{\text{base-off}}$ value of 0.1.^[2] On the other hand, the value indicates that the preference of **2** for the base-on constitution is 25 times greater than that of another artificial vitamin B₁₂ analogue, **6**,^[12,21] in which the linker contains a phosphodiester (Table 1 entry 6). The altered coordination properties of **2** affect the reduction of the octahedral cobalt(III) to the square-pyramidal cobalt(II) complex with loss of the β -cyano group (Table 1, top right) and was investigated with cyclic voltammetry (CV) in water ([Tris] = 0.2 M, pH 8.0; Tris = tris(hydroxymethyl)aminomethane). The CV trace of **2** displays a cathodic E_{pc}^* value at -1.056 V, a value 70 mV more positive than in **1**. The facilitated reduction of cobalt(III) in **2** can be explained by

a lower electron density at the metal center resulting from the weaker coordination of the Dmbz base.

We envisaged that an enhanced rigidity of the linker structure might lead to a tighter intramolecular coordination which would make the reduction from cobalt(III) to cobalt(II) more difficult. First, we decided to replace the glycine unit in the linker of **2** with (L)-proline to yield **3** (Scheme 2). We thought that this cyclic building block might act as a turn mimic; it would mimic the α -ribose moiety of natural cobalamines and thus stabilize the base-on form. Compound **3** (Scheme 2) was synthesized as described in the Supporting Information. The stability of the base-on form of **3** ($pK_{\text{base-off}} = 0.97$) increased by a factor of 2.6 compared to the prototype **2**, and electrochemical studies showed that **3** is—as expected—more difficult to reduce to Co^{II} than **2** ($\Delta V = -21$ mV; Table 1, entry 3).

In natural cobalamines the methyl group at C176 of *R* configuration plays an important role in the stabilization of the base-on form,^[11] and we envisaged a comparable effect for the peptide B₁₂ mimics. To test this hypothesis, derivative **4**, which has an *R*-configured

Table 1: Base-on/base-off (left) and Co^{III}/Co^{II} equilibria (right).

Entry	Compound	$K_{\text{base-off}}^*$		E_{pc}^*	
		base off, Co ^{III}	base on, Co ^{III}	base on, Co ^{III}	base on, Co ^{II}
1	1	0.1 ^[d]	19	−1.126	
2	2	1.38	1	−1.056	
3	3	0.97	2.6	−1.077	
4	4	0.62	5.8	−1.096	
5	5	1.64	0.55	−1.039	
6	6 ^[d]	2.8 ^[d]	0.04	n.r. ^[e]	

[a] $K^* = K_{\text{base-off(1)}}/K_{\text{base-off(2)}}$. [b] $E_{\text{pc}}^* = E_{\text{pc}} - E_0^*$ (see the Supporting Information). [c] Ref. [2]. [d] Refs. [12, 21]. [e] n.r. = not reported.

methyl group at C176, was synthesized from **10** and **7** (Scheme 2).^[16] The base-on form of **4** ($pK_{\text{base-off}} = 0.62$) was favored by a factor of two, and the reduction from Co^{III} to Co^{II} was more difficult than in **3** ($\Delta V = -19$ mV; Table 1 entry 4 vs. 3), which lacks this modification. The influence of the remote methyl group on the base-on/base-off equilibrium in **4** is almost identical to that observed for natural cobalamines;^[11] this underscores the utility of peptide structures as artificial linkers in vitamin B₁₂ analogues.

In earlier studies Eschenmoser et al. claimed that a change in configuration at C176 from *R* to *S* may destabilize the base-on constitution of vitamin B₁₂.^[14] This behavior can be explained by an additional *gauche* effect in the base-on form.^[16] Encouraged by our findings with **4**, we synthesized and characterized its epimer **5** (Scheme 2). This derivative, in

Communications

which the methyl group at C176 has an *S* configuration, displays a $pK_{\text{base-off}}$ of 1.64, an tremendous tenfold destabilization of the base-on form compared to that of **4**. It is remarkable that the energetically unfavorable conformation of the cyclic base-on structure of **5** outweighs the entropic gain obtained from the preorganization of the linker structure; this is reflected in a higher $pK_{\text{base-off}}$ value of **5** compared to that of the prototype **2** (Table 1 entry 5 vs. 2). The switch of configuration at C176 also has electrochemical consequences: derivative **5** is roughly 60 mV easier to reduce than its epimer **4**.

The peptide B_{12} mimics **2–5** show a linear correlation between the cathodic E_{pc}^* values of the $\text{Co}^{\text{III}}/\text{Co}^{\text{II}}$ reduction and their $pK_{\text{base-off}}$ values ($\Delta V = 57 \text{ mV}$, $\Delta pK_{\text{base-off}} = 1.02$; Figure 2). Since the same β -cyano group is released from the cobalt center during reduction from cobalt(III) to

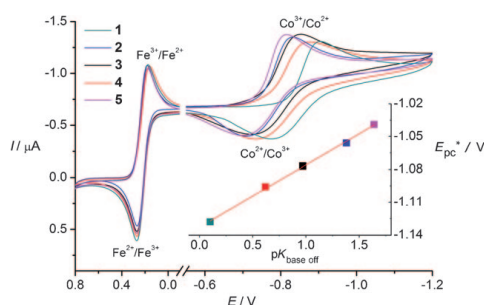


Figure 2. CV spectra of **1–5** in water ([Tris] = 0.2 M, pH 8.0) (reference electrode: Ag/AgCl, internal reference: $\text{K}_3\text{Fe}(\text{CN})_6$). Inset: Plot of $pK_{\text{base-off}}$ vs. E_{pc}^* . The value $pK_{\text{base-off}}(1) = 0.1$ is from reference [2].

cobalt(II) (Table 1, top right), the entropy of the reaction must be comparable and thus the reduction potentials are directly related to the enthalpy of the Co–CN bond. A lower $pK_{\text{base-off}}$ value corresponds to a stronger coordination of the Dmbz base and increasing back-donation from the Co ion to the β -cyano group. This may subsequently hamper reduction and shift the redox potential to a more negative value.

In summary, we have introduced a new class of vitamin B_{12} mimics in which a peptide linker tethers the corrin macrocycle to the Dmbz base. Studies with four different peptide B_{12} derivatives demonstrated that through the appropriate design of the peptide backbone both the coordination and the accompanying redox properties at the Co center can be adjusted. This implies that it might be possible to fine-tunereactivity in cofactor-catalyzed reactions in which an intermediate base-on cobalt(II) species is the catalytically

active species. The development of organometallic peptide B_{12} analogues for biological applications as well as further modifications of the linker for physico-chemical studies are subjects of current research.

Received: March 31, 2010

Published online: June 22, 2010

Keywords: bioinorganic chemistry · coordination chemistry · electrochemistry · peptides · vitamins

- [1] B. Kräutler, D. Arigoni, B. Golding, *Vitamin B₁₂ and B₁₂[−] Proteins*, Wiley-VCH, Weinheim, **1998**.
- [2] K. L. Brown, *Chem. Rev.* **2005**, *105*, 2075.
- [3] R. Banerjee, *Chemistry and Biochemistry of B₁₂*, 1st ed., Wiley-Interscience, New York, **1999**.
- [4] R. Banerjee, C. Gherasim, D. Padovani, *Curr. Opin. Chem. Biol.* **2009**, *13*, 484.
- [5] J. Kim, C. Gherasim, R. Banerjee, *Proc. Natl. Acad. Sci. USA* **2008**, *105*, 14551.
- [6] I. Mellman, H. F. Willard, P. Youngdahlturner, L. E. Rosenberg, *J. Biol. Chem.* **1979**, *254*, 1847.
- [7] J. P. Lerner-Ellis, J. C. Tirone, P. D. Pawelek, C. Dore, J. L. Atkinson, D. Watkins, C. F. Morel, T. M. Fujiwara, E. Moras, A. R. Hosack, G. V. Dunbar, H. Antonicka, V. Forgetta, C. M. Dobson, D. Leclerc, R. A. Gravel, E. A. Shoubridge, J. W. Coulton, P. Lepage, J. M. Rommens, K. Morgan, D. S. Rosenblatt, *Nat. Genet.* **2006**, *38*, 93.
- [8] J. M. Pratt in *Inorganic Chemistry of Vitamin B₁₂* (Ed.: J. M. Pratt), Academic Press, New York, **1972**, p. 44.
- [9] L. Hannibal, C. A. Smith, D. W. Jacobsen, N. E. Brasch, *Angew. Chem.* **2007**, *119*, 5232; *Angew. Chem. Int. Ed.* **2007**, *46*, 5140.
- [10] H. A. Hassanin, L. Hannibal, D. W. Jacobsen, M. F. El-Shahat, M. S. A. Hamza, N. E. Brasch, *Angew. Chem.* **2009**, *121*, 9071; *Angew. Chem. Int. Ed.* **2009**, *48*, 8909.
- [11] P. Butler, M. O. Ebert, A. Lyskowski, K. Gruber, C. Kratky, B. Kräutler, *Angew. Chem.* **2006**, *118*, 1004; *Angew. Chem. Int. Ed.* **2006**, *45*, 989.
- [12] T. Toraya, A. Ishida, *J. Biol. Chem.* **1991**, *266*, 5430.
- [13] R. B. Wang, B. C. MacGillivray, D. H. Macartney, *Dalton Trans.* **2009**, 3584.
- [14] A. Eschenmoser, *Angew. Chem.* **1988**, *100*, 5; *Angew. Chem. Int. Ed. Engl.* **1988**, *27*, 5; F. Kreppelt, PhD Thesis, Dissertation no. 9458, ETH-Zürich, **1991**.
- [15] G. Müller, O. Müller, *Z. Naturforsch. B* **1966**, *21*, 1159.
- [16] See the Supporting Information.
- [17] P. E. Nielsen, M. Egholm, R. H. Berg, O. Buchardt, *Science* **1991**, *254*, 1497.
- [18] U. Diederichsen, H. W. Schmitt, *Angew. Chem.* **1998**, *110*, 312; *Angew. Chem. Int. Ed.* **1998**, *37*, 302.
- [19] P. E. Nielsen, *Acc. Chem. Res.* **1999**, *32*, 624.
- [20] G. K. Mittapalli, K. R. Reddy, H. Xiong, O. Munoz, B. Han, F. De Riccardis, R. Krishnamurthy, A. Eschenmoser, *Angew. Chem.* **2007**, *119*, 2522; *Angew. Chem. Int. Ed.* **2007**, *46*, 2470.
- [21] The structural formula of **6** is shown in the Supporting Information.

SHORT COMMUNICATION

DOI: 10.1002/ejic.201001146

Identification of Diastereomeric Cyano–Aqua Cobinamides with a Backbone-Modified Vitamin B12 Derivative and with ^1H NMR Spectroscopy

Kai Zhou^[a] and Felix Zelder^{*[a]}**Keywords:** Vitamin B12 / NMR spectroscopy / Cobalt / Diastereomers / Bioinorganic chemistry/ Corrinoids

A new backbone-modified vitamin B12 derivative with an unusual configuration at the cobalt center has been used for

the identification of the two axial diastereomers of cyano–aqua cobinamides (Cbi) by using ^1H NMR spectroscopy.

Introduction

Cobinamides (Cbi) are “incomplete” corrinoids lacking the dimethylbenzimidazole (Dmbz) -containing α -ribose-3'-phosphate linker of natural cobalamins (Cbl).^[1,2] These biologically important vitamin B12 (B12) precursors represent useful starting materials for the preparation of chemically modified analogues.^[3,4] Recently, “incomplete” corrinoids have regained considerable attention as biologically inspired catalysts^[5–7] as well as chemosensors for the straightforward detection of cyanide (Figure 1).^[8–10]

Enormous effort has been devoted by Friedrich et al. to characterize axial diastereomers of cyano–aqua Cbi.^[11–13] In other important studies, Brown et al. assigned, by heteronuclear NMR spectroscopy, the α - (lower side) and β - (upper side) positions of various Cbi with the help of chemically enriched axial ligands and the corresponding Cbl analogues.^[14,15] For mixtures of diastereomeric cyano–aqua Cbi, the ^{13}C NMR signals of the axially coordinated cyano ligands partially overlap.^[16] This behavior seems disadvantageous for the unequivocal assignment of the isolated isomers. For applications such as cyanide detection, only diastereomeric mixtures of “incomplete” cyano–aqua corrinoids have been employed,^[17–20] whereas initial kinetic studies suggest differences in cyanide coordination.^[20] The identification and evaluation of well-defined isomers are important with regard to future improvements of corrin-based chemosensors. In this communication, we report the identification of diastereomeric cyano–aqua Cbi with a backbone-modified vitamin B12 derivative and with ^1H NMR spectroscopy.

Results and Discussion

Diastereomeric mixtures of “incomplete” cyano–aqua corrinoids are generally synthesized by non-selective dis-

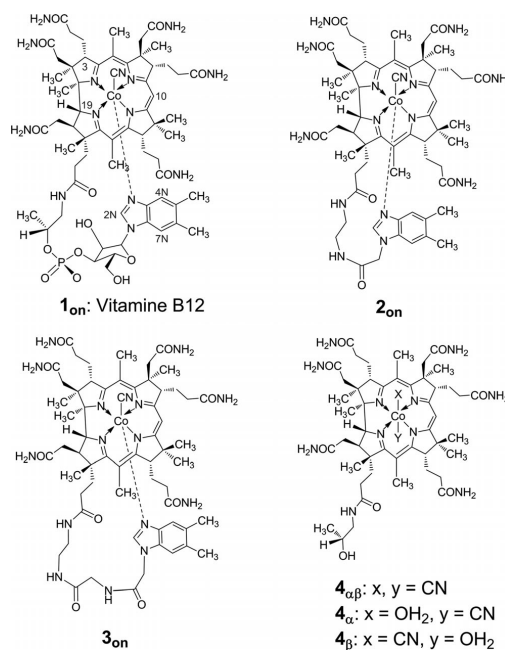


Figure 1. “Complete” cobalamins 1_{on}–3_{on} and “incomplete” Cobinamides 4 _{α β} , 4 _{α} , and 4 _{β} . The subscript “on” refers to the “base on” constitution. The subscripts “ α ” and “ β ” indicate the position of the cyano ligand at the lower and upper side of the macrocycle, respectively (charges have been omitted).

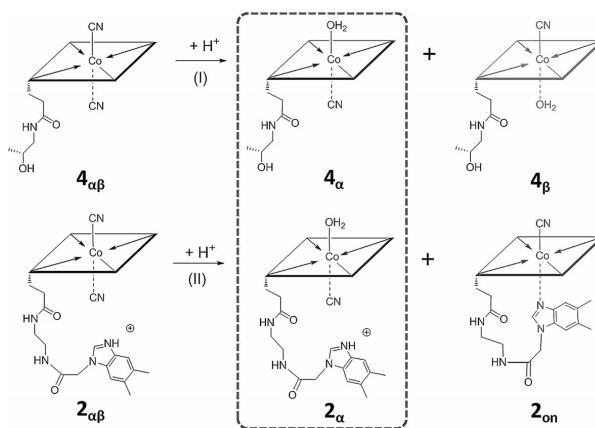
placement of one cyanide from the corresponding dicyano species under acidic conditions.^[20] For instance, α -aqua, β -cyano- (4 _{β}) and α -cyano, β -aqua- (4 _{α}) cobinamide are derived from 4 _{α β} (Scheme 1, I) and separated by preparative reverse-phase C18 chromatography. Differences in their ^1H NMR spectra (Figure 3, bottom) can easily be identified in a clearly arranged region between 3.9 and 6.6 ppm for the

[a] Institute of Inorganic Chemistry, University of Zürich, Winterthurerstrasse 190, 8057 Zürich, Switzerland
 Fax: +41-44-635-6803
 E-mail: zelder@aci.uzh.ch

Supporting information for this article is available on the WWW under <http://dx.doi.org/10.1002/ejic.201001146>.

SHORT COMMUNICATION

K. Zhou, F. Zelder



Scheme 1. Synthesis of **4_α** and **4_β** from **4_{αβ}** (I) and of **2_α** and **2_{on}** from **2_{αβ}** (II). **4_α** and its structural analogue **2_α** are depicted in a frame.

characteristic signals of H3, H10, and H19 of the corrin ring (Table 1, Entries 1 and 2; Figure 3, bottom). These differences are not conclusive with regard to the configuration at the cobalt center. In order to structurally identify these isomers, we planned to design a backbone-modified B12 derivative that mimics the structural and spectroscopic features of cyano-aqua Cbi in solution. We envisaged that the removal of one cyano ligand from a “complete” “base off” dicyano-Cbl derivative (**Cbl_{αβ}**) may lead to a mixture of **Cbl_α** and **Cbl_{on}** (see Supporting Information). “Base off” **Cbl_α** with a well-defined configuration at the metal center would represent a perfect surrogate of its “incomplete” counterpart and has comparable ¹H NMR signals for the protons at the corrin macrocycle.

Table 1. ¹H NMR data for **4_α**, **4_β**, **1_{on}**, **2_{on}** and (**2_{on}** + **2_α**).^[a,b]

Entry	Corrinoid	Configuration	H3 ^[c]	H10	H19 ^[d]	H2N	H4N	H7N
1	4_α	<i>α</i> -cyano, <i>β</i> -aqua	4.00	6.45	4.08			
2	4_β	<i>α</i> -aqua, <i>β</i> -cyano	4.11	6.52	4.25			
3	2_{on}	<i>α</i> -Dmbz, <i>β</i> -cyano	4.23	6.15	4.16	6.99	6.46	7.24
4a	(2_{on} + 2_α)	<i>α</i> -Dmbz, <i>β</i> -cyano	4.24	6.17	4.18	7.01	6.48	7.25
4b	(2_{on} + 2_α)	<i>α</i> -cyano, <i>β</i> -aqua	4.00	6.46	4.06	9.15	7.57	7.71
5	1_{on}	<i>α</i> -Dmbz, <i>β</i> -cyano	4.22	6.11	4.12	7.12	6.54	7.31

[a] 500 MHz, 300 K, [D₂]D₂O. [b] δ , ppm. [c] $J = 8$ Hz. [d] $J = 11$ Hz.

In a first experiment, dicyano-B12 (**1_{αβ}**) was treated with trifluoroacetic acid at pH 2 (see Supporting Information). Cyanide removal was indicated by a color change from violet to red ($\Delta\lambda_{\text{max}} = 30$ nm), and the reaction products were subsequently isolated by using solid-phase extraction (SPE) techniques as described in the Experimental Section. The UV/Vis spectrum of the reaction solution coincide with that of **1_{on}** (Figure 2, top) and suggests the rapid formation of “base on” B12.

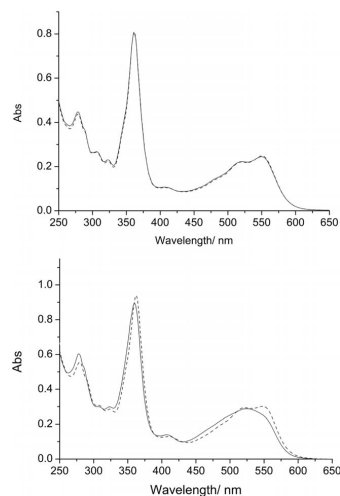


Figure 2. (bottom) UV/Vis spectra of (**2_{on}** + **2_α**) (solid line) derived from **2_{αβ}** (Scheme 1, II) in comparison with **2_{on}** (dashed line); (top) UV/Vis spectra of **1_{on}** (solid line) derived from **1_{αβ}** (see Supporting Information) in comparison with **1_{on}** (dashed line).

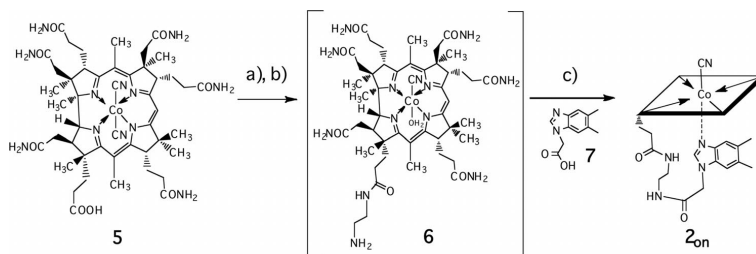
¹H NMR spectroscopy supports this observation and indicates the formation of more than 85% of **1_{on}** after SPE. Additionally, the formation of a minor product (<15%) was observed that further converted to **1_{on}**. The signals of the corrin moiety of this intermediate overlap with the signals of **1_{on}**. These drawbacks impede the analysis of the reaction mixture and preclude potential applications for the identification of diastereomeric Cbi. Apparently, cyanide removal from the lower side (*α* side) of the macrocycle fol-

lowed by simultaneous coordination of the Dmbz base to the cobalt center as well as isomerization to **1_{on}** are strongly favored. This behavior can be explained by the strong intramolecular coordination of the Dmbz base to the metal center, which is expressed by a low $pK_{\text{base-off}}$ value of 0.1^[2] for **1_{on}**. We assumed that the synthesis of “base off” isomers of cyano-aqua Cbl would be more favorable, if intramolecular coordination of the Dmbz base to the metal center would be weaker than that in **1_{on}**. Peptide B12, a recently introduced class of B12 mimics, possesses such tunable coordination properties.^[21] These B12 derivatives with a corrin macrocycle and a peptide backbone instead of the α -ribofuranotide moiety of B12 have the same number of atoms between the metal center and the nitrogen-anchoring group of the Dmbz base.

For this project, we decided to synthesize a novel derivative **2_{on}** with a 3-atom shorter backbone than the linker of the previously described prototype **3_{on}**.^[21] We speculated that this structural deviation would lead to a destabilization of the coordinated “base on” form. A “shortened linker” is also advantageous with regard to ¹H NMR analysis, since it contains fewer protons that potentially interfere with the protons of the corrin ring. The B12 derivative **2_{on}** was synthesized from dicyano-cobyric acid (**5**) through an intermediate **6** and then coupled with **7** as reported earlier for **3_{on}** (Scheme 2).^[21] The high-resolution mass spectrum of **2_{on}** indicates a [M]⁺ ion peak at 1186.57087 ($m/z_{\text{calcd.}} = 1186.57191$), which suggests a molecular formula of C₅₉H₈₁CoN₁₅O₈. The UV/Vis spectrum (Figure 2, bottom in dashed line) and ¹H NMR signals of the corrin ring and the Dmbz base of **2_{on}** were in accordance to those of **1_{on}** (Table 1, Entries 3 vs. 5) and other peptide B12 derivatives in its “base on” forms.^[21] Spectrophotometric pH titration reveals that the “base on” stability of **2_{on}** ($pK_{\text{base-off}} = 2.58$) is indeed 16 and 302 times lower than that of **3_{on}** ($pK_{\text{base-off}} = 1.38$ ^[21]) and **1_{on}** ($pK_{\text{base-off}} = 0.1$ ^[2]), respectively. For the synthesis of axial diastereomers of **2** (Scheme 1, II), we followed the same strategy as that described for the experiments with **1_{αβ}**.

The UV/Vis spectrum of the reaction product differs this time significantly from that of the corresponding “base on” form (**2_{on}**) and suggests rather the existence of a mixture of

“base on” and “base off” compounds (Figure 2, bottom). The ¹H NMR spectrum shows clearly two sets of signals for the characteristic signals of the corrin ring at H3, H10, and H19 [Figure 3, top (**2_{on}** + **2_a**)] and of the aromatic Dmbz base (Table 1, Entries 4a and 4b) in a ratio of approximately 1:1. This information indicates univocally the existence of only two forms of backbone-modified B12 derivatives in solution. The chemical shifts and the coupling constants of one set of signals are identical to those of **2_{on}** (Table 1, Entries 3 vs. 4a). Cobalt-coordinated cyanide at the lower side (α side) of **2_{αβ}** was substituted by the Dmbz base during cyanide removal to form **2_{on}** (Scheme 1, II). The other set of signals in the mixture show an indicative downfield shift for the protonated Dmbz base between 0.46–2.14 ppm (Table 1, Entries 4a vs. 4b).^[22] This suggests the existence of **2_a** with a cyano ligand at the lower side of the macrocycle derived from the abstraction of the β -cyano ligand from **2_{αβ}**. A “complete” cyano-aqua Cbl with a cyano ligand at the α position has not yet been reported under neutral conditions, to the best of our knowledge.^[23] This behavior can be explained by the 300-times higher preference of the “base off” form of **2_{on}** relative to that of **1_{on}**. The mixture of (**2_{on}** + **2_a**) synthesized from **2_{αβ}** with two separated sets of indicative ¹H NMR signals (H3, H10 and H19; Table 1, Entries 4a and 4b) serve now for the identification of **4_a** and **4_b**. Subtraction of the characteristic set of signals of pure **2_{on}** (Table 1, Entry 3) from that of (**2_{on}** + **2_a**) (Table 1, Entries 4a + 4b) leads to signals (almost) that are identical to those of **4_a** (Table 1, Entry 1; Figure 3, top). Friedrich et al. reported earlier on “incomplete” cyano-aqua corrinoids such as cyano-aqua cobinamide and cyano-aqua cobyrinic acid. They assumed that the slower migrating derivatives shared the same configuration at the cobalt center and assigned it to the α - (lower side) cyano form on a tentative basis (Figure 4, inset).^[12,13] Later, Firth et al. showed that a freshly dissolved sample of crystallographically characterized α -cyano, β -aqua cobyrinic acid was indeed the slower migrating derivative.^[24] The UV/Vis spectra of **4_a** was slightly blueshifted relative to that of **4_b** (Figure 4). This is in agreement with earlier reports and confirms now unequivocally Friedrich’s earlier assumptions on the configuration at the metal center.^[11–13]



Scheme 2. Synthesis of **2_{on}** from **5**: (a) NEt₃, ethyl chloroformate, N-Boc-ethylenediamine, DMF, 5 min, 25 °C. (b) HCl (1 M), 1 h, 25 °C. (c) EDC·HCl, DMAP, DMF, 4 h, 0–25 °C.

SHORT COMMUNICATION

K. Zhou, F. Zelder

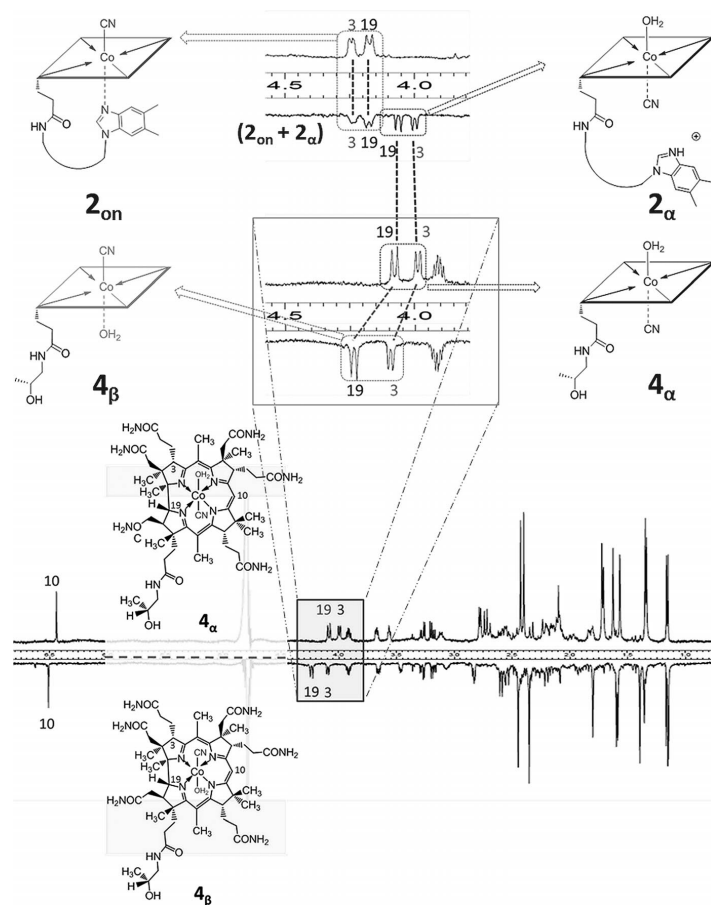


Figure 3. (Bottom) ^1H NMR spectra of 4_α (above) compared to 4_β (below). Characteristic signals are indicated. (Top) Identification of 4_α by analysis of the chemical shifts of H3 and H19: signals (4_α) = signals [$(2_{\text{on}} + 2_\alpha) - 2_{\text{on}}$] (500 MHz, 300 K, D_2O).

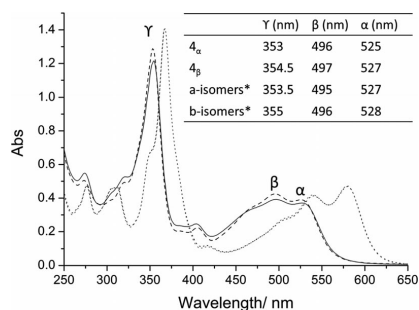


Figure 4. UV/Vis spectra of 4_α (α -cyano, β -aqua-cobinamide; dashed line) and 4_β (α -aqua, β -cyano-cobinamide; solid line). [4_α] = [4_β] = 46 μM . The dotted lines over layer and indicate $4_{\alpha\beta}$ from the reaction of 4_α and 4_β with excess KCN* (ref.^[11–13]).

Conclusions

We present a new backbone-modified vitamin B12 derivative with an unusual configuration at the cobalt center. This compound has been used for the identification of the two axial diastereomers of cyano-aqua cobinamides (Cbi) by using ^1H NMR spectroscopy. The results are in agreement with earlier tentative assignments. We envisage that backbone-modified B12 derivatives with adjustable coordination properties will find further interesting chemical, analytical and biological applications.

Experimental Section

Synthesis of 4_α and 4_β : Compound $4_{\alpha\beta}$ (20.8 mg, 20 mmol) was dissolved in 0.1% aqueous TFA (10 mL), and the reaction solution was stirred for 10 min. Compound 4_α (10.1 mg, 8.8 mmol, 44%) and 4_β (10.3 mg, 9.0 mmol, 45%) were separated by preparative

Identification of Diastereomeric Cyano-Aqua Cobinamides



HPLC as the corresponding TFA salts. ^1H NMR (500 MHz, $[\text{D}_2]-\text{D}_2\text{O}$): see Supporting Information. MS (ESI-MS): m/z (%) = 1015.6 (100) $[\text{M} - \text{H}_2\text{O}]^+$. HPLC-UV/Vis: R_t = 8.8 min (4_α), R_t = 13.5 min (4_β).

Synthesis of 2_{on} : Intermediate **6** was synthesized from dicyanocobyrinic acid (4.9 mg, 5.0 μmol) as described in previous work.^[21] It was dissolved in DMF (1 mL) and cooled to 0 °C, after which DMAP (1.0 mg, 8 μmol) and $7^{[21]}$ (4.5 mg, 15 μmol) were added. After 10 min, EDC-HCl (3.0 mg, 15 μmol) was added. The solution was warmed up to room temperature. After 4 h, the solvent was removed under reduced pressure. The residue was washed with acetone and further purified with preparative HPLC to afford 2_{on} (3.8 mg, 2.9 μmol , 58%) as the corresponding TFA salt. ^1H NMR (500 MHz, $[\text{D}_2]\text{D}_2\text{O}$): see Supporting Information. HR-MS: calcd. for $\text{C}_{59}\text{H}_{81}\text{CoN}_{15}\text{O}_8$ $[\text{M}]^+$ 1186.57191; found 1186.57087. UV/Vis (c = 30 μM , 0.2 M KCl, pH = 5.98): 548 nm (3.96), 521 nm (3.94), 413 nm (3.72), 361 nm (4.43), 279 nm (4.27), HPLC-UV/Vis: R_t = 14.2 min; $\text{p}K_{\text{base-off}} = 2.58$.

Synthesis of ($2_{\text{on}} + 2_\alpha$): Compound 2_{on} (1.3 mg, 1.0 μmol) and KCN (1.3 mg, 20 μmol) were dissolved in water (5 mL) to obtain a violet solution of $2_{\alpha\beta}$. The pH value of the solution was adjusted to 2 with trifluoroacetic acid. After purging the solution with N_2 for 20 min to remove HCN, the reaction solution was adsorbed on a reverse-phase Chromafix® C18ec cartridge. It was washed with water (30 mL) and then eluted with MeOH (3 mL). The solvent was removed under vacuum to yield 2_{on} and 2_α as a mixture of the corresponding TFA salts (1.3 mg, 100%). ESI-MS: m/z (%) = 1186.6 (100) $[\text{M}]^+$ for 2_{on} or $[\text{M} - \text{H}_2\text{O}]^+$ for 2_α .

Synthesis of ($1_{\text{on}} + 1_\alpha$): The synthesis and separation was performed as described for the synthesis of ($2_{\text{on}} + 2_\alpha$) starting from $1_{\alpha\beta}$. The UV/Vis spectrum of ($1_{\text{on}} + 1_\alpha$) is shown in Figure 2 (top).

Supporting Information (see footnote on the first page of this article): Materials and methods, the general atom numbering of B12 derivatives, the synthesis of Cbl_α and Cbl_{on} , and NMR chemical shifts for 2_{on} , 4_α , and 4_β .

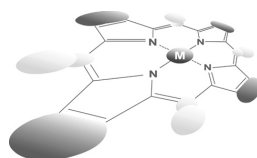
Acknowledgments

The authors thank L. Bigler for the recording of the HR-ESI-MS spectra and R. Alberto for helpful discussions. A generous gift of

vitamin B12 from DSM Nutritional Products AG (Basel/Switzerland) is acknowledged. This work was supported by the Swiss National Science Foundation (Grant No. 200021-117822).

- [1] B. Kräutler, D. Arigoni, B. Golding, *Vitamin B12 and B12-Proteins*, Wiley-VCH, Weinheim, 1998.
- [2] K. L. Brown, *Chem. Rev.* **2005**, *105*, 2075–2149.
- [3] T. Toraya, A. Ishida, *J. Biol. Chem.* **1991**, *266*, 5430–5437.
- [4] P. Butler, M. O. Ebert, A. Lyskowski, K. Gruber, C. Kratky, B. Kräutler, *Angew. Chem. Int. Ed.* **2006**, *45*, 989–993.
- [5] R. Scheffold, *Chimia* **1985**, *39*, 203–211.
- [6] H. Shimakoshi, M. Abiru, S. Izumi, Y. Hisaeda, *Chem. Commun.* **2009**, 6427–6429.
- [7] K. Nakamura, Y. Hisaeda, L. Pan, H. Yamauchi, *J. Organomet. Chem.* **2009**, *694*, 916–921.
- [8] F. H. Zelder, C. Männel-Croise, *Chimia* **2009**, *63*, 58–62.
- [9] Z. Xu, X. Chen, H. N. Kim, J. Yoon, *Chem. Soc. Rev.* **2010**, *39*, 127–137.
- [10] J. A. Ma, P. K. Dasgupta, *Anal. Chim. Acta* **2010**, *673*, 117–125.
- [11] W. Friedrich, H. Ohlms, W. Sandeck, R. Biegnow, *Z. Naturforsch., Teil B* **1967**, *22*, 839–850.
- [12] W. Friedrich, M. Moskopid, *Z. Naturforsch., Teil B* **1968**, *23*, 804–812.
- [13] J. M. Pratt (Ed.) in *Inorganic Chemistry of Vitamin B12*, Academic Press, New York, **1972**, p. 119–124.
- [14] K. L. Brown, X. Zou, *J. Am. Chem. Soc.* **1992**, *114*, 9643–9651.
- [15] K. L. Brown, X. Zou, L. Salmon, *Inorg. Chem.* **1991**, *30*, 1949–1953.
- [16] K. L. Brown, J. M. Hakimi, *Inorg. Chem.* **1984**, *23*, 1756–1764.
- [17] C. Männel-Croise, F. Zelder, *Inorg. Chem.* **2009**, *48*, 1272–1274.
- [18] S. S. M. Hassan, M. S. A. Hamza, A. E. Kelany, *Talanta* **2007**, *71*, 1088–1095.
- [19] M. K. Freeman, L. G. Bachas, *Anal. Chim. Acta* **1990**, *241*, 119–125.
- [20] C. Männel-Croise, B. Probst, F. Zelder, *Anal. Chem.* **2009**, *81*, 9493–9498.
- [21] K. Zhou, F. Zelder, *Angew. Chem. Int. Ed.* **2010**, *49*, 5178–5180.
- [22] F. H. Zelder, C. Buchwalder, R. M. Oetterli, R. Alberto, *Chem. Eur. J.* **2010**, *16*, 6155–6158.
- [23] W. W. Reenstra, W. P. Jencks, *J. Am. Chem. Soc.* **1979**, *101*, 5780–5791.
- [24] R. A. Firth, H. A. O. Hill, J. M. Pratt, R. G. Thorp, *J. Chem. Soc. A* **1968**, 453–456.

Received: October 26, 2010
Published Online: November 26, 2010



One-step synthesis of α/β cyano-aqua cobinamides from vitamin B12 with Zn(II) or Cu(II) salts in methanol

Kai Zhou and Felix Zelder^{*◇}

Institute of Inorganic Chemistry, University of Zürich, Winterthurerstrasse 190, 8057 Zürich, Switzerland

Dedicated to Professor Karl M. Kadish on the occasion of his 65th birthday

Received 28 January 2011

Accepted 18 March 2011

ABSTRACT: This short communication describes the screening of various metal salts for the preparation of cyano-aqua cobinamides from vitamin B12 in methanol. ZnCl_2 and $\text{Cu}(\text{NO}_3)_2 \cdot 3\text{H}_2\text{O}$ have been identified as most active for this purpose and represent useful alternatives to the widely applied Ce(III) method that requires excess cyanide.

KEYWORDS: vitamin B₁₂, cobinamide, screening, phosphodiester cleavage, cyanide, coordination chemistry.

INTRODUCTION

Cobinamides (Cbi), the “incomplete” biological precursors of vitamin B₁₂ (B12) are cobalt complexes with a tetradentate corrin macrocycle at the equatorial positions, while the two axial vacant binding sites can be bound by other ligands [1, 2]. The nature of these ligands influences strongly the electronic properties of the corrin chromophore [3, 4]. This behavior makes this class of compounds useful for analytical applications [5–7]. “Incomplete” corrinoids are among the most promising chemosensors for the rapid, visual detection of μM cyanide in water [8–12]. This class of compounds was also the first that has been successfully applied to visually detect endogenous cyanide in plants [13]. Up to now, only mixtures of “incomplete” diastomeric cyano-aqua corrinoids such as cyano-aqua Cbi have been applied [9, 13]. Different synthetic protocols for the preparation of cyano-aqua Cbi are available. Most widely used for this purpose are Ce(III) salts [14]. Disadvantages of this methodology is the need to generate dicyano-B12 from B12 with additional cyanide prior to the phosphodiester cleavage with the metal salt [14, 15]. Brown and coworkers developed a useful method for the phosphodiester

hydrolysis of alkylcobalamins under strictly anhydrous conditions [16]. Improvements of existing synthetic protocols [17] as well as the development of novel modified B12-derivatives with altered properties are important for further progress and new applications of corrinoids [18–21]. Based on earlier work of Müller and Müller [22], we present a metal-ion mediated one-step synthesis of cyano-aqua Cbi as a useful alternative to existing synthetic protocols.

EXPERIMENTAL

General

Chemicals: B12 was a generous gift from DSM Nutritional Products AG (Basel/Switzerland). All salts were either obtained from Fluka or Aldrich with a purity $\geq 98\%$.

HPLC solvents were 0.1% aqueous trifluoroacetic acid (A, TFA) and methanol (B). HPLC analyses were performed on a Merck-Hitachi L-7000 system equipped with a diode array UV-vis spectrometer and Macherey Nagel Nucleosil C-18ec RP columns (5 μm particle size, 100 Å pore size, 250 \times 3 mm. Flow rate: 0.5 mL min^{-1}). Preparative HPLC separations were performed on a Varian Prostar system equipped with two Prostar 215 pumps, a Prostar 320 UV-vis detector and Macherey Nagel Nucleosil C-18ec RP columns (7 μm particle size,

[◇]SPP full member in good standing

^{*}Correspondence to: Felix Zelder, email: zelder@aci.uzh.ch, fax: +41 44-635-6803

100 Å pore size, 250 × 40 mm. Flow rate: 32 mLmin⁻¹). HPLC-ESI-MS spectra were measured on a Bruker HCT spectrometer equipped with an Aquinity UPLC (Waters) using Nucleosil C-18ec RP columns (5 µm particle size, 100 Å pore size, 250 × 3 mm. Flow rate: 0.3 mLmin⁻¹). HPLC-ESI-MS solvents were 0.1% formic acid (solvent A) and methanol (solvent B). The following gradient was used for all HPLC, HPLC-ESI-MS and preparative HPLC measurements: 25% B for 5 min, then in 25 min to 100% B, then 100% B for 10 min.

UV-vis spectra were recorded on a Cary 50 spectrometer using quartz cells with a path length of 1 cm.

NMR spectra were recorded on a Bruker AV-500 spectrometer (Karlsruhe, Germany). The data processing was carried out with ACD/SpecManager (Advanced Chemistry Development) as described in Ref. 31.

Chromafix C18ec for solid phase extraction (SPE) was obtained from Macherey Nagel. In general the compound was dissolved in little water, transferred to the adsorbent, washed with water and eluted with MeOH.

For safety reasons, the removal of cyano-ligands from the corresponding dicyano-complexes was performed under a well-ventilated fume hood and an HCN-detector from Dräger was used.

For security reasons, reactions with nitrates were performed behind an additional safety shield.

Synthesis

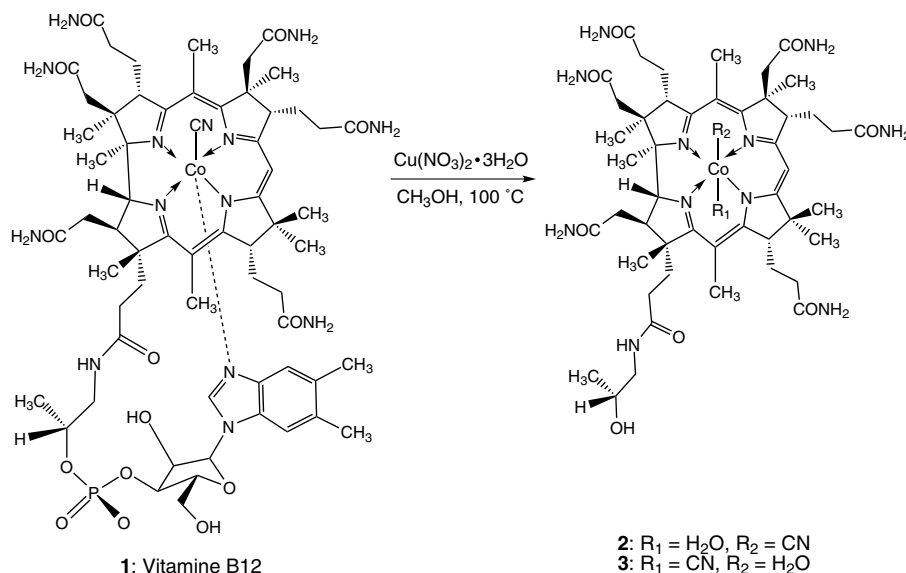
Preparation of α -aqua- β -cyano-cobinamide (2) and α -cyano- β -aqua-cobinamide (3) as the corresponding TFA salts. General procedure: B12 (1, 20 mg, 15 µmol)

and Cu(NO₃)₂·3H₂O (50 mg, 163 µmol) were dissolved in methanol (2 mL) and stirred for 20 min at 100 °C in a Young Tube (1 cm × 15 cm) sealed with a Teflon cap. After cooling the solution to room temperature, the methanol was removed under reduced pressure. The residue was dissolved in water (5 mL) and desalted with the help of SPE. Subsequently, it was separated by preparative reverse phase HPLC to yield α -cyano- β -aqua-cobinamide (3; R₁ = 8.8 min; 6.9 mg, 6.0 µmol, 40%) and α -aqua- β -cyano-cobinamide (2; R₁ = 13.5 min; 3.9 mg, 3.4 µmol, 23%) as their corresponding TFA salts. ¹H NMR, UV-vis, ESI-MS data of 2 and 3 were in agreement with the analytical data of 2 and 3 reported in Ref. 31. For security reasons, the reactions were performed behind an additional safety shield.

RESULTS AND DISCUSSION

Synthesis of 2 and 3 from 1

Müller and Müller applied highly concentrated solutions of ZnCl₂ in MeOH (1 g/mL) at 170 °C for the conversion of vitamin B12 to cyano-aqua cobyrinic acid via a cobinamide intermediate [22, 23]. In contrast to the well-established Ce(III)-method, this procedure did not need to generate dicyano-B12 from B12 with additional cyanide before phosphodiester hydrolysis. Inspired by these important studies, we intended to screen different metal salts for their ability to cleave B12 to cyano-aquo Cbi 2 and 3. For this purpose we selected different metal salts with cations such as Co²⁺, Ni²⁺, Cu²⁺, Mg²⁺ or Zn²⁺



Scheme 1. Conversion of B12 (1) to α -aqua- β -cyano-cobinamide (2) and α -cyano- β -aqua-cobinamide (3) obtained as the corresponding TFA salts. Charges have been omitted

Table 1. Screening of different metal salts for the synthesis of cyano-aqua Cbi (**2**, **3**) from B12 (**1**)

	Zn ²⁺	Co ²⁺	Ni ²⁺	Mg ²⁺	Cu ²⁺
Cl ⁻	√	×	×	×	√/×
NO ₃ ⁻	n.t.	n.t.	n.t.	n.t.	√
SO ₄ ²⁻	×	n.t.	×	×	×

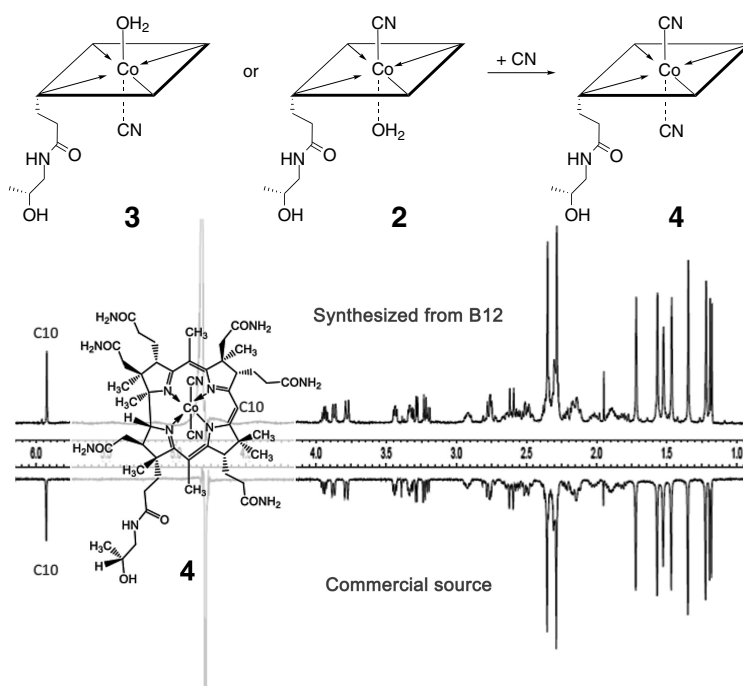
Conditions: B12 (20 mg; 15 μ mol), metal salt concentration (25 mg/mL in MeOH (2 mL)), T = 140 °C, Young Tube (see Experimental section for details). LC-MS-Analysis: √: observation of >90% of **2** and **3**, √/×: **2** and **3** was observed within a complex reaction mixture ×: observation of <5% of **2** and **3**, n.t.: not tested.

as summarized in Table 1. Metal-complexes of some of these cations were already successfully applied towards the hydrolysis of phosphodiester bonds in other molecules than B12 [24–28]. The sulfate and chloride salts of these cations as well as Cu(NO₃)₂·3H₂O were tested. We did not test other nitrates due to their potentially explosive nature [29]. CoSO₄ was not soluble under the reaction conditions. First, the reactions were carried out as described in the Experimental section, but at 140 °C.

The reaction mixtures were analyzed at different time-intervals with HPLC-ESI-MS spectrometry and the

retention times of the molecular ion peaks were compared to those of commercially available B12 (**1**; R_t = 14.9 min; [M + H]⁺, *m/z*: 1355.6) and a mixture of diastereomeric cyano-aqua cobinamide (**2**: R_t = 13.5 min, [M - H₂O]⁺, *m/z*: 1015.6; **3**: R_t = 8.8, [M - H₂O]⁺, *m/z*: 1015.6). The latter compounds have been obtained from the non-selective abstraction of one cyano-ligand from commercially available dicyano-cobinamide (**4**) under acidic conditions [4, 9]. Cobalt(II), nickel(II), and magnesium(II) salts did not convert B12 to **2** and **3** (Table 1). In contrast, the formation of **2** and **3** was observed within a complex reaction mixture using CuCl₂. Substituting CuCl₂ with Cu(NO₃)₂·3H₂O led to more than 90% conversion of B12 to cyano-aqua Cbi (**2**, **3**). Similar results were obtained with ZnCl₂ (Table 1). Under these reaction conditions, the formation of less than 5% of side-products has been observed with HPLC-ESI-MS.

We assume that amide side-chains of the corrin ring have been unselectively transformed to the corresponding methyl-esters as suggested by molecular ion peaks with a 15 units higher *m/z* ratio. Isomerization of the β -(upper) cyano ligand to the α -(lower) position of the macrocycle occurred during conversion of **1** to a mixture of **2** and **3**. This behavior has been observed earlier for “incomplete” cyano-aqua corrinoids at elevated temperatures [3, 30]. The most promising two candidates, Cu(NO₃)₂·3H₂O and



Scheme 2. Top: Synthesis of dicyano-cobinamide (**4**) from cyano-aqua cobinamide (**2** or **3**). Bottom: Comparison of the ¹H NMR spectra of **4** from a commercial source (down) and from the reaction of cyanide with a mixture of **2** and **3** (up). The latter compounds have been obtained from the Cu(NO₃)₂·3H₂O mediated cleavage of B12. Charges have been omitted

Table 2. Optimized reaction condition for the preparation of cyano-aqua Cbi (**2**, **3**) from B12 (**1**) with $\text{Cu}(\text{NO}_3)_2 \cdot 3\text{H}_2\text{O}$ and ZnCl_2

Entry	Metal salt	Temperature, °C	Time, min	Conversion ^a , %
1	$\text{Cu}(\text{NO}_3)_2 \cdot 3\text{H}_2\text{O}$	100	20	>98%
2	ZnCl_2	120	60	>98%

Conditions: B12 (20 mg; 15 μmol), metal salt (50 mg: 163 μmol of $\text{Cu}(\text{NO}_3)_2 \cdot 3\text{H}_2\text{O}$ or 370 μmol of ZnCl_2), MeOH (2 mL), Young Tube (see Experimental section for details).

^a Determined by HPLC-MS-Analysis, based on **1**.

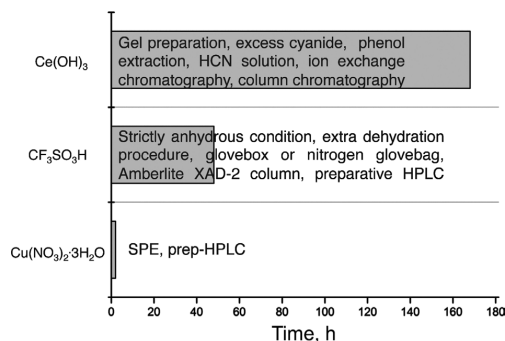
ZnCl_2 (Table 1), were selected for further optimization. Lower temperature and metal salt loading as well as shorter reaction time were aimed to reduce the formation of the undesired side-products.

We identified $\text{Cu}(\text{NO}_3)_2 \cdot 3\text{H}_2\text{O}$ (25 mg mL^{-1}) as the most efficient metal salt for the formation of **2** and **3** at 100 °C in 20 min. With ZnCl_2 higher reaction temperature and longer reaction time were necessary (Table 2). Compound **2** and **3** were isolated with preparative C18-reverse phase HPLC in a total yield of 63%. The isolated yield of **2** (23%) was lower than that of **3** (40%) since it could not be completely separated from B12 and the α -ribazole moiety by preparative HPLC. It is possible to improve the isolated yield of **2** to 41% with an additional Amberlite XAD-2 column prior to separation by preparative HPLC [16]. The products were analyzed with ^1H NMR, UV-vis spectroscopy and ESI-MS spectrometry and the analytical data were in agreement with earlier reports [31]. Coordination of cyanide to a mixture of **2** and **3** obtained from the Cu(II) mediated cleavage of B12 led to the formation of the corresponding dicyano-species **4**.

The corresponding ^1H NMR spectra were identical to those of commercially available **4** (Scheme 2). This behavior suggests that undesired isomerization at the periphery of the corrin ring did not occur.

CONCLUSION

We identified $\text{Cu}(\text{NO}_3)_2 \cdot 3\text{H}_2\text{O}$ and ZnCl_2 in MeOH as a useful one-step alternative for the preparation of cyano-aqua cobinamides from B12. Advantages of these reagents compared to the well-established $\text{Ce}(\text{OH})_3$ [14, 15] and $\text{CF}_3\text{SO}_3\text{H}$ [16] methods seem to be the shorter reaction time and the simplified work-up procedure. In contrast to the application of Ce(III) salts, there is no need to use additional cyanide (Fig. 1), but large excess of metal salts, high temperatures and separation with preparative HPLC are still required. The practicability of this method for the preparation of large quantities (e.g. in gram scale) of the products still has to be demonstrated. On the basis of these experiments, we intend to identify the underlying cleavage mechanism and develop

**Fig. 1.** Comparison of the estimated time for synthesis and isolation as well as the synthetic requirements and work-up procedures for the preparation of Cbi with the $\text{Ce}(\text{OH})_3$ [14], $\text{CF}_3\text{SO}_3\text{H}$ [16] and $\text{Cu}(\text{NO}_3)_2 \cdot 3\text{H}_2\text{O}$ methods

metal-complexes for the catalytic phosphodiester hydrolysis of B12 in the near future.

Acknowledgements

The authors thank R. Alberto and B. Spingler for helpful discussions. A generous gift of vitamin B12 from DSM Nutritional Products AG (Basel/Switzerland) is acknowledged. This work was supported by the Swiss National Science Foundation (Grants No. 200021-117822, 200020-129479).

REFERENCES

- Kräutler B, Arigoni D and Golding B. *Vitamin B12 and B12-Proteins*, Wiley-VCH: Weinheim, 1998.
- Brown KL. *Chem. Rev.* 2005; **105**: 2075–2149.
- Inorganic Chemistry of Vitamin B12*, Pratt JM. (Ed.) Academic Press: New York, 1972.
- Werthemann L. ETHZ (Switzerland), 1968; Vol. PhD.
- Zelder FH and Männel-Croise C. *Chimia* 2009; **63**: 58–62.
- Xu Z, Chen X, Kim HN and Yoon J. *Chem. Soc. Rev.* 2010; **39**: 127–137.
- Ma JA and Dasgupta PK. *Anal. Chim. Acta* 2010; **673**: 117–125.
- Zelder FH. *Inorg. Chem.* 2008; **47**: 1264–1266.
- Männel-Croise C and Zelder F. *Inorg. Chem.* 2009; **48**: 1272–1274.
- Touceda-Varela A, Stevenson EI, Galve-Gasion JA, Dryden DTF and Mareque-Rivas JC. *Chem. Comm.* 2008; 1998–2000.
- Kim Y, Zhao H and Gabbai FP. *Angew. Chem. Int. Edit.* 2009; **48**: 4957–4960.
- Cho D-G, Kim JH and Sessler JL. *J. Am. Chem. Soc.* 2008; **130**: 12163–12167.
- Männel-Croise C, Probst B and Zelder F. *Anal. Chem.* 2009; **81**: 9493–9498.

14. Renz P. *Methods Enzymol.* 1971; **18**: 212.
15. Friedrich W and Bernhauer K. *Chem. Ber.* 1956; **89**: 2507–2512.
16. Zou XA, Evans DR and Brown KL. *Inorg. Chem.* 1995; **34**: 1634–1635.
17. Butler PA, Murtaza S and Kräutler B. *Monatsh. Chem.* 2006; **137**: 1579–1589.
18. Butler P, Ebert MO, Lyskowski A, Gruber K, Kratky C and Kräutler B. *Angew. Chem. Int. Edit.* 2006; **45**: 989–993.
19. Zhou K and Zelder F. *Angew. Chem. Int. Edit.* 2010; **49**: 5178–5180.
20. Zelder FH, Buchwalder C, Oetterli RM and Alberto R. *Chem. Eur. J.* 2010; **16**: 6155–6158.
21. Proinsias KO, Sessler JL, Kurcon S and Gryko D. *Org. Lett.* 2010; **12**: 4674–4677.
22. Müller G and Müller O. *Z Naturforsch.* 1966; **B21**: 1159.
23. Renz P. *Methods Enzymol.* 1971; **18**: 82.
24. Krämer R. *Coord. Chem. Rev.* 1999; **182**: 243–261.
25. Feng GQ, Natale D, Prabakaran R, Mareque-Rivas JC and Williams NH. *Angew. Chem. Int. Ed.* 2006; **45**: 7056–7059.
26. Wall M, Linkletter B, Williams D, Hynes RC and Chin J. *J. Am. Chem. Soc.* 1999; **121**: 4710–4711.
27. Chin J, Chung S and Kim DH. *J. Am. Chem. Soc.* 2002; **124**: 10948–10949.
28. Muller JG, Chen X, Dadiz AC, Rokita SE and Burrows CJ. *J. Am. Chem. Soc.* 1992; **114**: 6407–6411.
29. Check the Risk and Safety Statements of the compounds.
30. Friedrich W, Ohlms H, Sandeck W and Bieganow R. *Z Naturforsch.* 1967; **B 22**: 839–850.
31. Zhou K and Zelder F. *Eur. J. Inorg. Chem.* 2011; 53–57.

Cite this: *Chem. Commun.*, 2011, **47**, 11999–12001

www.rsc.org/chemcomm

COMMUNICATION

“Intra base off/inter base on” coordination: self-assembly of a dimeric vitamin B12 derivative with a versatile tail†

Kai Zhou and Felix Zelder*

Received 11th August 2011, Accepted 20th September 2011

DOI: 10.1039/c1cc14996b

A self-complementary, artificial vitamin B12 derivative dimerises in an unprecedented “intra base off/inter base on” coordination mode.

Coordination chemistry is fundamental for understanding the form, function and reactivity of many protein-cofactor complexes.^{1–3} The three dimensional structure of these biological assemblies is controlled by multiple intermolecular interactions. Binding of a cofactor to a protein side chain through non-covalent coordinative bonds is often observed.^{4–7} These principles have inspired chemists to develop artificial porphyrin assemblies.^{8–12}

Supramolecular complexes of “complete” corrinoids are rare. Examples include a rotaxane cobalamin (Cbl)-dimer that is bridged by a metallorganic linker¹³ and a Cbl with a dissociated, encapsulated dimethylbenzimidazole (Dmbz) base.¹⁴

Herein, we describe a new structural motif for “complete” corrinoids: self-assembly of a dimeric B12 derivative in an “intra base off/inter base on” mode (Fig. 1, *right*). The design of the self-complementary building block was based on our understanding of the structure and function of natural Cbls.^{15,16} In the latter, the accessibility of the Co(III) centre at the α -face of the macrocycle combined with connection of the u-turn shaped nucleotide loop to the α -directing f-side chain defines intramolecular coordination of the Dmbz base to this face of the macrocycle (Fig. 1 *left*).¹⁷

To overcome this limitation and render self-assembly possible, we envisaged a modified Cbl having a flexible loop at the f-side chain, a free coordination site at the β -, but denied access at the opposite face of the octahedral complex (Fig. 1 *right*). Coordination of cyanide to the α -face is ideal for prevention of intramolecular coordination. The binding of cyanide to diaqua-corrinoids with formation constants of 10^{14} M^{-1} is much higher compared to those with other ligands.^{3,18} Coordination can therefore only occur at the β -face of the corrin macrocycle (Fig. 1 *right*). Compound **1-H** with a deamino-histidine linker as well as the desired β -aqua, α -cyano

constitution at the Co(III) centre seemed to be a good choice to be tested as self-complementary building block and was synthesized from dicyano cobyric acid (Cby-CN) in 38% yield as outlined in Scheme 1^{19,20}

The constitution of the axially bound ligands of **1-H** was verified with ¹H-NMR spectroscopy and comparison to characteristic signals of the corrin macrocycle of β -aqua, α -cyanocobinamide.^{20,21} Deprotonation of the imidazole base of **1-H** under neutral conditions (pH 7.0, “Britton-Robinson buffer”) led to a red shift in the UV-vis spectrum suggesting the formation of a base on Cbl species.^{3,20} Coordination of imidazole to the cobalt(III) centre of **1-H** was also observed with ¹H-NMR spectroscopy. The signals of the imidazole ligand are characteristically upfield shifted ($\Delta\delta = 1.48 \text{ ppm}$ for $\text{H}_{2\text{N}}$ and 1.82 ppm for $\text{H}_{4\text{N}}$; $\text{H}_{2\text{N}}$ and $\text{H}_{4\text{N}}$ are indicated in Fig. 2) because of shielding from the ring current of the macrocycle. ¹H-ROESY spectroscopy has been used to investigate the coordination sites of the imidazole groups in **1-I**. NOEs between imidazole ($\text{H}_{2\text{N}}$ and $\text{H}_{4\text{N}}$) and side chains of the corrin macrocycle directing to the β -face confirm Co(III)-imidazole coordination at this site of the macrocycle (Fig. 2). The proton $\text{H}_{2\text{N}}$ is oriented toward the northern and $\text{H}_{4\text{N}}$ to the southern part of the corrinoid suggesting that the base is positioned parallel to the C_{51} - C_{151} axis.

Dimerisation of **1** to **1-I** was also indicated by concentration dependent UV-vis spectroscopy at pH 8.0. At high total “cobalt concentration”²² ($[\text{Co}]_{\text{total}} = 174 \text{ }\mu\text{M}$), the spectrum is similar to those of Cbls in the base on form.

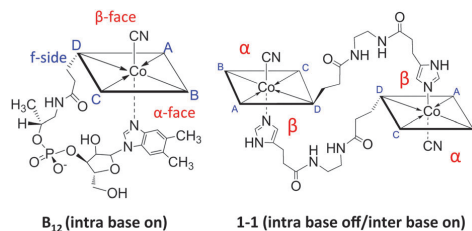


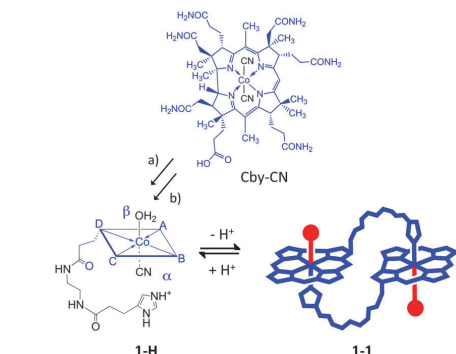
Fig. 1 Left: Intramolecular coordination of vitamin B12 (**B12**; “intra base on”). Right: Intermolecular coordination of an artificial B12 derivative to the “intra base off/inter base on” dimer **1-I** (The corrin ring is simplified for clarity. Charges of the macrocycle and counterions (CF_3COO^-) have been omitted. The same principles have been applied in the following Schemes and Figures).

Institute of Inorganic Chemistry, University of Zürich, Winterthurerstrasse 190, 8057 Zürich, Switzerland.

E-mail: zelder@aci.uzh.ch, www.zelder.ch.vu; Fax: + 41 44 635 6803

† Electronic supplementary information (ESI) available: Experimental details and additional schemes, tables and figures. See DOI: 10.1039/c1cc14996b

View Online



Scheme 1 Synthesis of **1-H** from dicyano cobyric acid (Cby-CN): (a) EDC-HCl, DMAP, BocNHCH₂CH₂NH₂, DMF, and then HCl 1M; (b) EDC-HCl, DMAP, deamino histidine (for details see ESI†). Self-assembly of the self-complementary building block **1-H** to the dimer **1-1** (Red dots indicate the coordination sites of the cyano ligand and **1-1** is shown as a schematic structure).

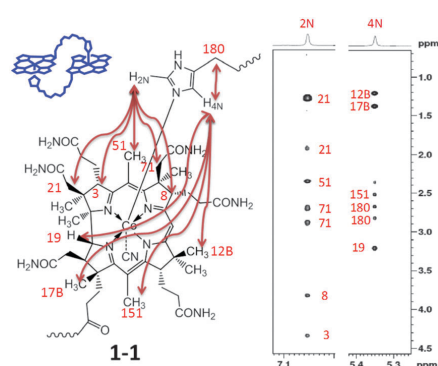


Fig. 2 ROESY spectra (500 MHz, 300 K) of **1-1**. NOEs between the imidazole moiety (H_{2N}, H_{4N}) and hydrogen atoms at the periphery of the corrin ring of **1-1** are indicated.

Stepwise dilution leads to a blue shift and a change of the intensity ratio of the α -, and β -bands. This behaviour is shown in Fig. 3, in which the spectra have been normalized to the intersection at 508 nm. This wavelength represents an isosbestic point of the spectra of the base on (pH 8.0) and base off (pH 4) forms, respectively (Fig. 3, red line: “intra base off/inter base on” dimer **1-1**, dashed line: base off monomer **1-H**). The spectral changes observed during dilution are consistent with the partial formation of a base off species having an aqua, cyano-, instead of a cyanoimidazolyl constitution (base on) at the metal centre.^{23,24}

The concentration dependence excludes intramolecular coordination of the imidazole ligand to the β -face of a hypothetical monomer **1-M** (Scheme 2) and rather suggests the “intra base off/inter base on” dimer **1-1** (Scheme 1, 2). A dissociation constant of 1.29×10^{-6} M was determined for the equilibrium between dimer **1-1** and the two monomers of **1** from the corresponding UV-vis spectra as described in

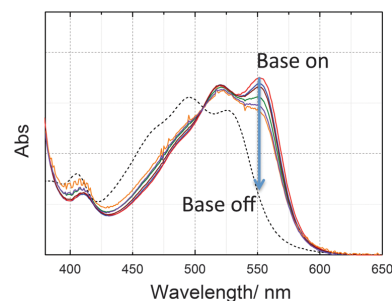
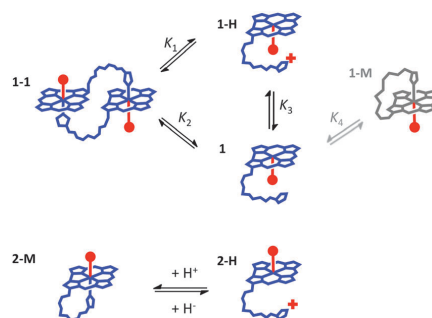


Fig. 3 Normalized UV-vis spectra (to the intersection at 508 nm) of **1-1** ([Co]_{total}: 174 μ M, (red)) and mixtures of **1-1** and **1** ([Co]_{total}: 49.3 μ M (blue), 35.1 μ M (brown), 17.4 μ M (green), 9.79 μ M (violet), 4.44 μ M (yellow)). Black dashed line indicates the spectrum of **1-H** as a reference for the “base off” constitution.



Scheme 2 Summary of potential equilibria in solution (Red dots indicate the coordination sites of the cyano ligand, while cobalt coordinated water has been omitted. Red “+” symbols indicate protonation of the imidazole moiety (Hypothetical **1-M** and K_4 are depicted in grey color).

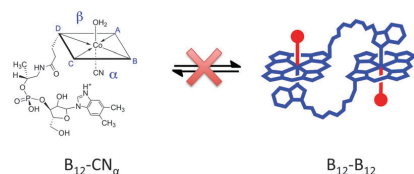
the ESI† (Scheme 2; Table 1: K_2).²⁰ Acid induced dissociation of dimer **1-1** to the monomeric subunits **1-H** has been identified with pH-dependent spectrophotometric titrations (Scheme 2; Table 1: K_1). A concentrated solution of **1-1** (87 μ M) was applied to suppress undesired self-dissociation. An inflection point at 5.83 was obtained from the Boltzmann fit of an absorbance *versus* pH plot.²⁰ At this pH value half of dimer **1-1** is dissociated to the protonated, base off monomers **1-H**. A dissociation constant K_1 of 7.95×10^7 M⁻¹ was calculated based on this consideration.²⁰ Further strong evidence for the existence of dimer **1-1** was obtained from calculations of the thermodynamic cycle between **1-1**, **1** and

Table 1 Binding constants

Constant	Terms	Equilibrium constant
K_1	$[1-H]^2/[1-1][H]^2$	7.95×10^7 M ^{-1a}
K_2	$[1]^2/[1-1]$	1.29×10^{-6} M ^{a,b}
K_3	$[1][H]/[1-H]$	1.27×10^{-7} M ^c
K_4	$[1]/[1-M]$	/

^a Experimentally determined. ^b ESI.† ^c Calculated *via* the thermodynamic cycle depicted in Scheme 2.

View Online



Scheme 3 Base off β -aqua, α -cyano B_{12} ($B_{12}\text{-CN}_\alpha$) does not dimerise in an “intra base off/ inter base on” fashion.

1-H (Scheme 2 *top*) using the experimentally determined equilibrium constants K_1 and K_2 . The calculated pK_a of the dissociated, protonated imidazole moiety of **1-H** ($pK_a = pK_3 = p(K_2/K_1)^{1/2} = 6.89$) is in excellent agreement with the acidity constant of protonated imidazole ($pK_a = 6.95^{25}$), which further supports our assumptions.

After the existence of dimer **1-I** with an intra base off/inter base on coordination mode was shown with different spectroscopic methods and thermodynamic calculations, we investigated the configuration at the metal centre as well as the artificial loop structure as a structural prerequisite for self-assembly in more detail. The importance of the β -aqua, α -cyano configuration at the Co(III) centre for dimerisation was demonstrated with monomer **2-H** (Scheme 2 *bottom*). This compound is identical to **1-H**, but has the opposite constitution of the axially bound ligands (α -aqua, β -cyano).²⁰ Concentration as well as pH dependent UV-vis studies demonstrated *as expected* intramolecular coordination in **2-M** as the only structural motif (Scheme 2 *bottom*).²⁰ Size exclusion-, and ion exchange chromatography of a mixture of **1-I** and **2-M** gave further evidence for the existence of both species as described in the ESI.^{†20}

The necessity of the artificial loop structure for dimerisation was demonstrated by comparison of **1-H** to base off B_{12} having the same β -aqua, α -cyano constitution at the metal centre ($B_{12}\text{-CN}_\alpha$, Scheme 3).²⁰ In contrast to dimerisation of **1** to **1-I**, $B_{12}\text{-CN}_\alpha$ has no trend of self-assembly even up to 1 mM at pH 8. We assume that this behaviour is due to the more bulky Dmbz base as well as the less flexible loop structure compared to **1**. In natural Cbls, the nucleotide loop seems to be preorganized for intramolecular coordination to the metal centre from the lower face of the corrin ring.¹⁶ Until today, “complete” corrinooids are considered to coordinate exclusively in an intramolecular fashion. Recently, Gruber, Kräutler and coworkers reported about an “incomplete” corrinooid that dimerises in the solid-state.²⁶

We developed a self-complementary, artificial B12 derivative that dimerises in an unprecedented “intra base off/inter base on” mode. It was demonstrated that this novel coordination motif depends on both, the configuration at the metal centre as

well as the flexibility of the artificial, connecting linker. On the basis of these findings, we envisage constructing even more complex assemblies.

This work was supported by the Swiss National Science Foundation (Grant No. 200021-117822). A generous gift of vitamin B12 from DSM Nutritional Products AG (Basel/Switzerland) and support by R. Alberto are acknowledged. The authors thank E. Freisinger and K. Tarasava for help with the size exclusion chromatography experiment.

Notes and references

- J. P. Collman and L. Fu, *Acc. Chem. Res.*, 1999, **32**, 455–463.
- G. N. Schrauzer, *Acc. Chem. Res.*, 1968, **1**, 97–103.
- Inorganic Chemistry of Vitamin B12*, ed. J. M. Pratt, Academic Press, New York, 1972.
- U. Ermler, W. Grabarse, S. Shima, M. Goubeaud and R. K. Thauer, *Science*, 1997, **278**, 1457–1462.
- C. L. Drennan, S. Huang, J. T. Drummond, R. G. Matthews and M. L. Ludwig, *Science*, 1994, **266**, 1669–1674.
- J. C. Kendrew, R. E. Dickerson, B. E. Strandberg, R. G. Hart, D. R. Davies, D. C. Phillips and V. C. Shore, *Nature*, 1960, **185**, 422–427.
- M. F. Perutz, H. Muirhead, J. M. Cox and L. C. G. Goaman, *Nature*, 1968, **219**, 131–139.
- C. A. Hunter and L. D. Sarson, *Angew. Chem., Int. Ed. Engl.*, 1994, **33**, 2313–2316.
- C. A. Hunter, C. M. R. Low, M. J. Packer, S. E. Spey, J. G. Vinter, M. O. Vysotsky and C. Zonta, *Angew. Chem., Int. Ed.*, 2001, **40**, 2678–2682.
- T. S. Balaban, *Acc. Chem. Res.*, 2005, **38**, 612–623.
- T. S. Balaban, M. Linke-Schaetzel, A. D. Bhise, N. Vanthuyne, C. Roussel, C. E. Anson, G. Buth, A. Eichhofer, K. Foster, G. Garab, H. Gliemann, R. Goddard, T. Javorfi, A. K. Powell, H. Rosner and T. Schimmel, *Chem.-Eur. J.*, 2005, **11**, 2268–2275.
- J. E. Redman, N. Feeder, S. J. Teat and J. K. M. Sanders, *Inorg. Chem.*, 2001, **40**, 2486–2499.
- R. B. Hannak, G. Farber, R. Konrat and B. Kräutler, *J. Am. Chem. Soc.*, 1997, **119**, 2313–2314.
- R. Wang, B. C. MacGillivray and D. H. MacCartney, *Dalton Trans.*, 2009, 3584–3589.
- B. Kräutler, D. Arigoni and B. Golding, *Vitamin B12 and B12-Proteins*, Wiley-VCH, Weinheim, 1998.
- A. Eschenmoser, *Angew. Chem., Int. Ed. Engl.*, 1988, **27**, 5–39.
- K. L. Brown, *Chem. Rev.*, 2005, **105**, 2075–2149.
- G. C. Hayward, H. A. O. Hill, J. M. Pratt, N. J. Vanston and R. J. P. Williams, *J. Chem. Soc.*, 1965, 6485–6493.
- K. Zhou and F. Zelder, *Angew. Chem., Int. Ed.*, 2010, **49**, 5178–5180.
- Supporting Information.
- K. Zhou and F. Zelder, *Eur. J. Inorg. Chem.*, 2011, 53–57.
- [Co]_{total} was determined from the absorption of [1-CN] after conversion with excess cyanide as described in the Supporting Information.
- M. S. A. Hamza, X. Zou, R. Banka, K. L. Brown and R. van Eldik, *Dalton Trans.*, 2005, 782–787.
- K. L. Brown, X. Zou, R. R. Banka, C. B. Perry and H. M. Marques, *Inorg. Chem.*, 2004, **43**, 8130–8142.
- T. C. Bruice and G. L. Schmir, *J. Am. Chem. Soc.*, 1958, **80**, 148–156.
- K. Gruber, S. Murtaza, P. Butler, C. Kratky and B. Kräutler, *Chem.-Eur. J.*, 2008, **14**, 7521–7524.